**Center for Air Environment Studies**

**The Pennsylvania State University**

PB 204 356

APTD-0796

# A STUDY OF THE EFFECTS OF AEROSOL PROPERTIES ON SCATTERING OF LASER LIGHT

Contract # CPA [illegible]

Sponsor: Environmental Protection Agency

Reproduced by
NATIONAL TECHNICAL
INFORMATION SERVICE
Springfield, Va. 22151

Final Report

July 1, [illegible]

CAES

A

139

# A STUDY OF THE EFFECTS OF AEROSOL PROPERTIES ON SCATTERING OF LASER LIGHT

Contract #CPA 70-103

Sponsor: Environmental Protection Agency

July 1, 1971

Prepared by: R. Lee Byers
Douglas W. Cooper
John W. Davis

FINAL REPORT

# THE CENTER FOR AIR ENVIRONMENT STUDIES

The Center for Air Environment Studies at The Pennsylvania State University was established in 1963 to coordinate research and instruction concerning the interaction of man and his air environment. A unit of the interdisciplinary Institute for Science and Engineering, the Center has a staff with backgrounds in many of the physical, biological, social, and allied sciences.

A broad, flexible research program, dependent on faculty and student interest, is maintained by the Center. Some of the current research topics are:

The operation of an air pollution information service utilizing computers and other mechanized systems for the collection, retrieval, and dissemination of air environment literature. "Air Pollution Titles" and "Index to Air Pollution Research," information retrieval periodicals, are produced using computers. (See inside back cover).

Effects of air pollutants on trees, food, and fiber crops, predisposition to attack by other pathogens, and economic loss through damage to plants.

Studies of small particle behavior.

Development of high accuracy, low cost mobile analysis equipment for routine sampling of ambient air.

Biological effects of air pollutants on animals and natural ecologies.

Studies of basic combustion processes leading to lower contaminant emissions.

A statewide survey of vegetation damage due to air pollution.

Development of rapid response, specialized instrumentation for the quantitative measurement of contaminant concentration.

Controlled atmosphere air quality studies for a life-support system.

Fundamental research on the chemistry of airborne contaminants.

Basis facilities and services are maintained and provided by the Center. In addition, through the direct participation of all University Departments, departmental laboratories and facilities are utilized whenever possible. Collectively, these provide an extensive resource for research at The Pennsylvania State University.

The Center has also developed a unique set of educational programs supported by grants from the National Air Pollution Control Administration. In the Graduate Study Program, students conduct thesis work on an air pollution problem in their major field and take a minor course sequence in air pollution topics. In cooperation with the Graduate School and the academic departments, the Center manages the program and organizes the course sequence.

Potential air pollution administrators are prepared in the Introduction to Air Pollution and Control Administration Program, which involves one term of fulltime work on campus. This program is offered in the Summer for graduate students and advanced undergraduates of many disciplines and representatives of air pollution control agencies at the local, state, and federal level.

The Air Pollution Specialist Training Program is an intensive course designed to provide specialized knowledge and skills necessary for work in air pollution control instrumentation for field monitoring and sampling. The program involves one term of full time work on campus for students who have

continued on inside back cover

| | | | |
|---|---|---|---|
| **BIBLIOGRAPHIC DATA SHEET** | 1. Report No.<br>APTD-0796 | 2. | 3. Recipient's Accession No. |

4. Title and Subtitle
A Study of the Effects of Aerosol Properties on Scattering of Laser Light

5. Report Date
July 1, 1971

6.

7. Author(s) R. Lee Byers, Douglas W. Cooper and John W. Davis

8. Performing Organization Rept. No.

9. Performing Organization Name and Address
The Pennsylvania State University
1307 Old Main Building
University Park, Pennsylvania 16802

10. Project/Task/Work Unit No.

11. Contract/Grant No.
CPA 70-103

12. Sponsoring Organization Name and Address
Environmental Protection Agency
Office of Air Programs
Research Triangle Park, North Carolina 27711

13. Type of Report & Period Covered
Final

14.

15. Supplementary Notes DISCLAIMER - This report was furnished to the Office of Air Programs by The Pennsylvania State University, 1307 Old Main Building, University Park, Pennsylvania 16802 in fulfillment of CPA 70-103

16. Abstracts The influence of several variables on the backscattering of laser light by aerosols was studied. He-Ne laser light was used to illuminate aerosol particles generated by a Collison atomizer. The backscattering of light by the particles (effective angle: 173.5 ) was measured as a function of relative humidity. Depolarization and field studies were also made. Potassium chloride, sodium chloride, and sodium bromide particles all scattered more than twice as much light after becoming droplets. The change in phase occurred at lower humidities than those appropriate for the bulk material. These salt particles depolarized 13 to 25% of the incident polarized light intensity when dry particles and 6 to 12% of the incident light when droplets. The effect of changing ambient relative humidity was also studied for methylene blue dye and uranine dye particles. Depolarization measurements were also made for polystyrene latex and dioctyl phthalate aerosols. These gave depolarizations of 6% and 4% respectively. The laboratory device which measured the backscattering from the aerosols was used in a field test along with a LIDAR device. The field test, while not conclusive, indicated that relative humidity did affect LIDAR measurements.

17. Key Words and Document Analysis. 17a. Descriptors

Lasers
Laser beams
Backscattering
Aerosols
Humidity
Depolarization
Field tests

17b. Identifiers/Open-Ended Terms

17c. COSATI Field/Group 13B, 4A

| | | |
|---|---|---|
| 18. Availability Statement Unlimited | 19. Security Class (This Report)<br>UNCLASSIFIED | 21. No. of Pages<br>152 |
| | 20. Security Class (This Page<br>UNCLASSIFIED | 22. Price |

C

# ABSTRACT

The influence of several variables on the backscattering of laser light by aerosols was studied. He-Ne laser light was used to illuminate aerosol particles generated by a Collison atomizer. The backscattering of light by the particles (effective angle: 173.5°) was measured as a function of relative humidity. Depolarization and field studies were also made. Potassium chloride, sodium chloride, and sodium bromide particles all scattered more than twice as much light after becoming droplets. The change in phase occurred at lower humidities than those appropriate for the bulk material. These salt particles depolarized 13 to 25% of the incident polarized light intensity when dry particles and 6 to 12% of the incident light when droplets. The effect of changing ambient relative humidity was also studied for methylene blue dye and uranine dye particles. Depolarization measurements were also made for polystyrene latex and dioctyl phthalate aerosols. These gave depolarizations of 6% and 4% respectively. The laboratory device which measured the backscattering from the aerosols was used in a field test along with a LIDAR device. The field test, while not conclusive, indicated that relative humidity did affect LIDAR measurements.

## TABLE OF CONTENTS

Page No.

Abstract------------------------------------------------ iii

List of Figures----------------------------------------- ix

List of Tables------------------------------------------ xiii

General Introduction------------------------------------ 1

Section 1. The Effects of Humidity on Laser Light Backscattering from Laboratory Aerosols------- 3

- I. Introduction---------------------------------------- 3
- II. Equipment------------------------------------------ 3
  - A. Aerosol Generation------------------------------ 3
  - B. Aerosol Transport------------------------------- 8
  - C. Humidity Control-------------------------------- 10
  - D. Humidity Measurement---------------------------- 13
  - E. Light Scattering Measurement-------------------- 14
- III. General Procedure--------------------------------- 29
- IV. Results and Analysis------------------------------ 31
  - A. Size Distributions------------------------------ 31
  - B. Dependence of Backscattering on Particle Volume---------------------------------------- 44
  - C. Results of Subsidiary Tests--------------------- 49
  - D. Backscattering versus Relative Humidity------- 57
- V. Discussion----------------------------------------- 64
- VI. Conclusions--------------------------------------- 72

Section 2. Depolarization of Laser Light by Laboratory Aerosols-------------------------- 79

- I. Introduction---------------------------------------- 79
- II. Experimental System------------------------------- 79
- III. Procedure----------------------------------------- 86
- IV. Results------------------------------------------- 89
- V. Discussion----------------------------------------- 93
- VI. Conclusions--------------------------------------- 100

Section 3. Field Experiment------------------------------ 101

- I. Introduction---------------------------------------- 101
- II. Equipment----------------------------------------- 101
- III. Sampling Plan and Instrument Description---------- 102
- IV. Results and Analysis------------------------------ 105
- V. Conclusions---------------------------------------- 113

References---------------------------------------------- 115

TABLE OF CONTENTS (Continued)

Page No.

Appendix 1. Correction Factor Relative Humidity versus Temperature---------------------------- 119

Appendix 2. Pressure Correction for Humidity--------------- 121

Appendix 3. Relative Humidities at which some Salts Change Phase---------------------------------- 123

Appendix 4. Estimate of Weighing Errors-------------------- 125

Appendix 5. Atmospheric Lidar Measurements----------------- 127

## LIST OF FIGURES

Figure No. Page No.

1.1 Aerosol Generation Set-up------------------------- 4

1.2 Schematic of Collison Atomizer--------------------- 5

1.3 Aerosol Modification and Scattering Measurement System---------------------------- 9

1.4 Scattering Chamber, Model 1----------------------- 11

1.5 Humidifier---------------------------------------- 12

1.6 Angular Distribution of Scattered Intensity Polarized Vertical (1) and Parallel (2) to Observation Plane for Spheres of m = 1.60.---------------------------------- 26

1.7 Angular Distribution of Scattered Intensity Polarized Vertical (1) and Parallel (2) to Observation Plane for Spheres of = 2.2.-------------------------------------- 27

1.8 Schematic of Bendix Electrostatic Sampler--------- 33

1.9 Cumulative Size Distribution for Aerosols Generated from 1% v/v NaCl, 1% v/v KCl, 8% v/v NaCl Aqueous Solutions.---------------- 38

1.10 Backscattering versus Relative Humidity for 1% v/v Methylene Blue Aerosol----------------- 73

1.11 Backscattering versus Relative Humidity for 1% v/v Uranine Aerosol------------------------ 74

1.12 Backscattering versus Relative Humidity for 1% v/v NaBr Aerosol--------------------------- 75

1.13 Backscattering versus Relative Humidity for 1% v/v KCl Aerosol---------------------------- 76

1.14 Backscattering versus Relative Humidity for 1% v/v NaCl Aerosol--------------------------- 77

1.15 Backscattering versus Relative Humidity for 8% v/v NaCl Aerosol--------------------------- 78

2.1 Polarization Modification------------------------- 81

2.2 Scattering Chamber, Model 2, with Polarizer-------- 82

LIST OF FIGURES (Continued)

Figure No. Page No.

3.1 Equipment Configuration for Field Test------------ 103

3.2 Laboratory Laser Backscattering Device (Model 2, without polarizing filter).--------- 104

3.3 Temperature, Humidity, and Light Scattering on May 11, 1971-------------------------------- 107

3.4 Temperature, Humidity, and Light Scattering on May 12, 1971-------------------------------- 108

3.5 Product of aerosol mass concentration times aerosol backscattering cross section versus relative humidity for May 11, 1971----- 109

3.6 Backscatter and Relative Humidity versus Time of Day, May 11, 1971-------------------------- 111

3.7 Backscatter and Relative Humidity versus Time of Day, May 12, 1971-------------------------- 112

A.1 Product of aerosol mass concentration times a aerosol backscatter cross section versus time of day for May 11, 1971 and May 12, 1971.----- 138

## LIST OF TABLES

Table No. Page No.

1.1 Model 1 Optical Response as a Function of Perpendicular Distance from Optical Receiver Plane and as Function of Scattering Angle.------------------------ 17

1.2 Size Distributions for 1% v/v KCl Aerosol----------- 35

1.3 Size Distributions for 1% v/v NaCl Aerosol---------- 36

1.4 Size Distributions for 8% v/v NaCl Aerosol---------- 37

1.5 Size Parameters of Particles Formed by Nebulizing Salt Solutions with a Collison Atomizer------------- 40

1.6 Net Scattering Per Unit Particle Volume for Several Aerosols at Low Humidities (less 40% RH)----- 45

1.7 Average Dry Scattering per Average of the First, Second and Third Powers of the Diameters------------ 46

1.8 Backscattering and Forward Scattering for Several Aerosols at Different Humidities-------------------- 55

1.9 Sedimentation Losses for NaCl Particles in Scattering Chamber---------------------------------- 70

1.10 Estimated Sedimentation Losses for NaCl Particles in Chamber------------------------------------------ 70

1.11 NaCl Particle Stopping Distance for Velocity of 700 cm/sec.------------------------------------------ 71

2.1 Optical Response as a Function of Scatterer Distance from Plane of Light Pipe Face-------------- 84

2.2 Net Scattering Received as a Function of the Angle of the Receiver Polarizer-------------------------- 88

2.3 Ratios of the 90° Polarization Components to the 0° Polarization Components of the Net Scattering Received------------------------------------------------ 91

2.4 Results of Secondary Scattering Tests---------------- 94

3.1 High Volume Sampler Results------------------------- 106

A.1 Atmospheric and Lidar Data for May 11, 1971--------- 136

A.2 Atmospheric and Lidar Data for May 12, 1971--------- 137

# FINAL REPORT

## A Study of the Effects of Aerosol Properties on Scattering of Laser Light

Contract #CPA 70-103

General Introduction:

The objective of this work was the study of the influence of several variables on the backward scattering of laser light by aerosol particles. Suspended particles are an important air pollution problem in many locations. Devices which illuminate these particles and measure the light scattered by them are widely used to measure their concentrations. One promising method of obtaining information on the spatial distribution of aerosol particles uses pulses of laser light as "lidar" ("light direction and ranging"), which is analogous to radar (Ligda, 1965; Clemesha, et al., 1967; Johnson, 1969).

Hygroscopic particles are present in the air (Twomey, 1954) and so are droplets formed by a variety of chemical interactions, so that one of the areas of study in this work was an investigation of the relationship between changes in humidity and resultant changes in backscattering for some hygroscopic as well as for some nonhygroscopic particulates. Such changes could lead to erroneous concentration measurements.

It has been suggested that light scattered from aerosol particles could be distinguished from that scattered by gas molecules by the degree to which the particles depolarized the light they scattered (Clemesha, et al., 1967). Another phase of this work was a study of the depolarization of the laser light by different particles.

# Section 1. The Effects of Humidity on Laser Light Backscattering from Laboratory Aerosols

## I. Introduction

This section of the report concerns the effects of changing the humidity of several laboratory aerosols on their backscattering of laser light. This work was done using a scattering chamber designated "Model 1" which was later altered (into "Model 2") for the depolarization studies.

## II. Equipment

The experimental set-up had to make provisions for the following: generation of the aerosol, transport of the aerosol, control of the aerosol humidity, measurement of the humidity, illumination of the aerosol, measurement of the scattering of light by the aerosol, and measurement of the aerosol size distribution.

### A. Aerosol Generation

The overall schematic of the aerosol generation system is given in Figure 1.1. Compressed air was piped through glass fiber filters and a drying column (silica gel) so that when it reached the pressure regulator it was clean and dry. The pressure regulator was set at 30 lb/in$^2$ (30 p.s.i.g.) or two atmospheres above atmospheric. The air was then divided between a Collison atomizer, which is shown in Figure 1.2, and a tube containing a critical orifice. The orifice maintained a dilution flow into the mixing chamber of 63 x 10$^3$ cm$^3$/min (2.2 ft$^3$/min). The only exception to this flow

Because humidity changes could induce changes in shape and composition for some aerosols, depolarization was measured for humidities above and below the "critical" humidities, the relative humidities at which phase changes occurred.

To do the experimental work, a device was designed and built which approximated the geometry used in lidar and yet could be used in the confines of an indoor laboratory. If lidar were to become a major means for monitoring pollution, a relatively inexpensive laser backscattering device might be useful in applications where the use of the more expensive lidar would not be justified. It would be desirable that the less expensive device, the one used in this work, give readings easily related to those of lidar, and it would be desirable that such readings be simply related to the commonly used gravimetric analysis of air samples pulled through high volume filter samplers. The third section of this report describes a limited field comparison of the laboratory device, a lidar installation, and a high volume sampler all run at the same time and same location.

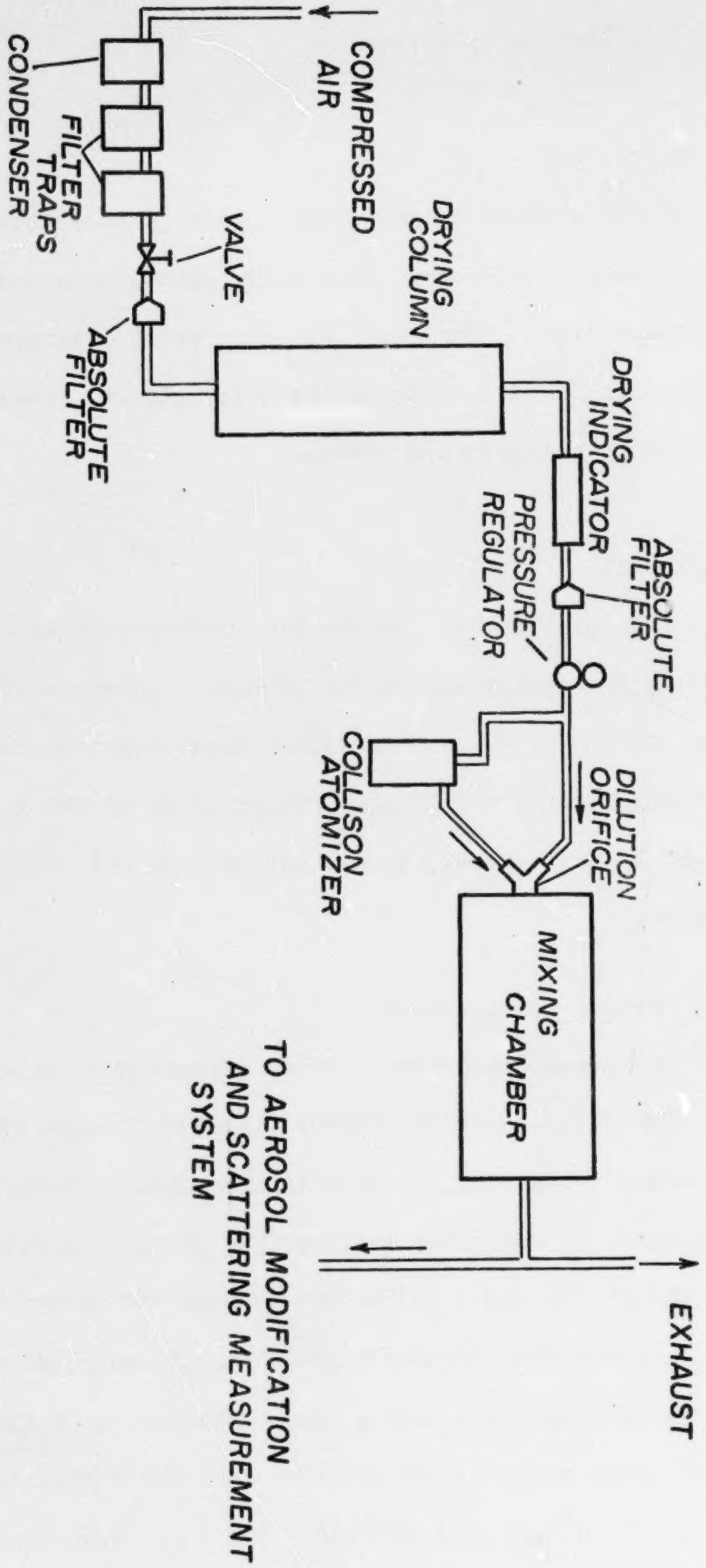
COMPRESSED AIR
FILTER TRAPS
CONDENSER
VALVE
ABSOLUTE FILTER
DRYING COLUMN
DRYING INDICATOR
ABSOLUTE FILTER
PRESSURE REGULATOR
DILUTION ORIFICE
COLLISON ATOMIZER
MIXING CHAMBER
EXHAUST
TO AEROSOL MODIFICATION AND SCATTERING MEASUREMENT SYSTEM

Figure 1.1. Aerosol Generation Set-up

BLANK PAGE

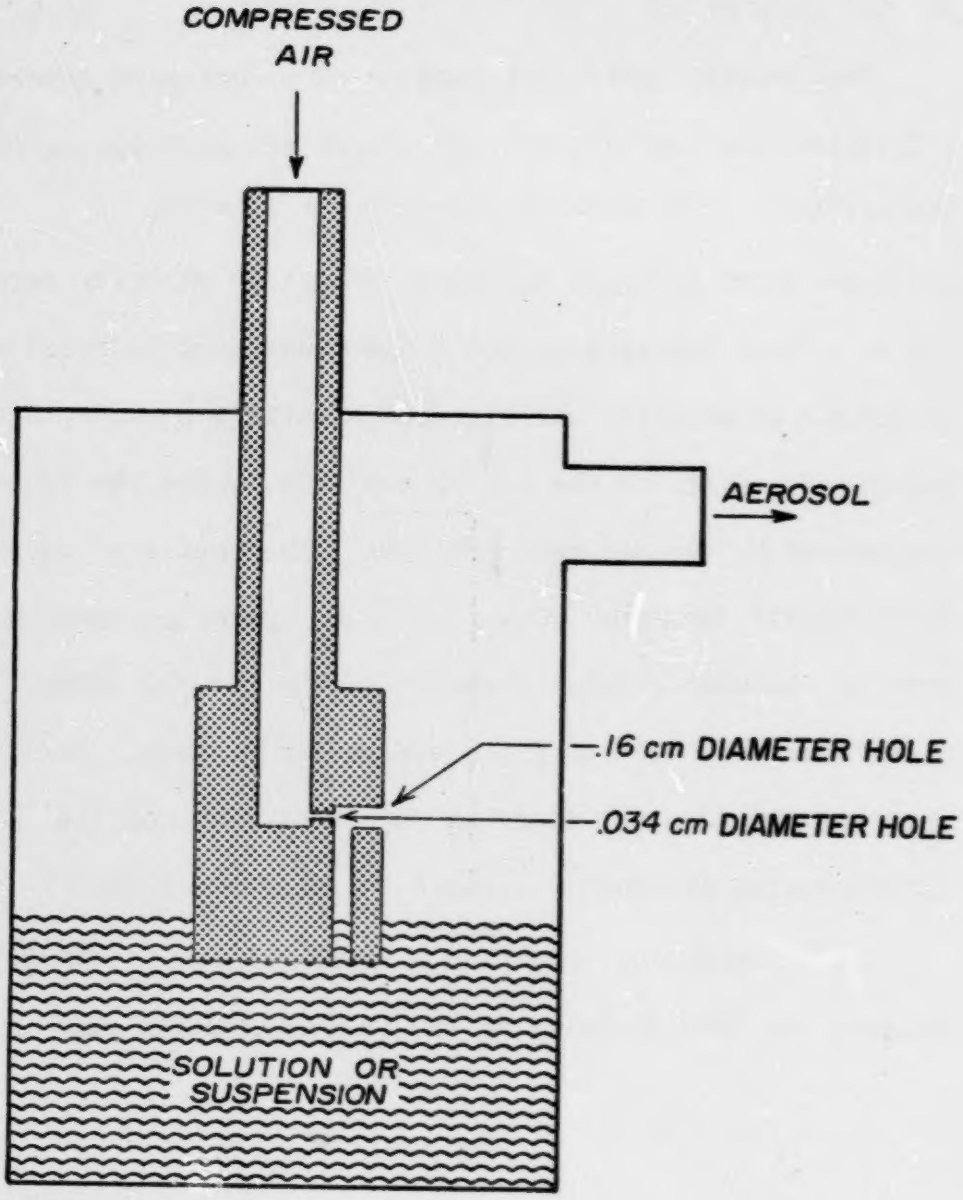
COMPRESSED
AIR
AEROSOL
.16 cm DIAMETER HOLE
.034 cm DIAMETER HOLE
SOLUTION OR
SUSPENSION

Figure 1.2. Schematic of Collison Atomizer

rate occurred in tests run with polystyrene latex particles, as described below. The dilution air and the output from the atomizer mixed in the mixing chamber (baffled) which had a volume of 71 x $10^3$ $cm^3$ (2.5 $ft^3$).

The aerosol particles used in this work were generated by a Collison atomizer (Figure 1.2), which was modified by removing the baffle. Compressed air was forced into the Collison inlet and made to travel at a high velocity across the top of a tube immersed in the fluid containing material which was to become an aerosol; the air flow created a pressure drop which brought the fluid to the top of the tube, where the fluid was fragmented by the air into droplets. The empirical equations of Nukiyama and Tanasawa (Green and Lane, 1964) are available to predict the mean droplet diameter of the aerosol formed by this air-blast atomizer. The droplets emerged in a spray. Sufficient distance was provided to allow settling out of course droplets. Only fine droplets were discharged through the atomizer outlet.

If the droplets contained a dissolved solute, then upon evaporation, the diameter of the solid particles was

$$(\pi/6)D_p^3 = C(\pi/6)D_d^3 ,$$

which becomes

$$D_p = C^{1/3}D_d ,$$

where

$D_p$ = diameter of the solid particle, cm,

C = ratio of solute volume to volume of solvent plus solute

$D_d$ = original droplet diameter, cm.

Thus an 8% v/v (i.e. 8% by volume) solution nebulized with a mean droplet diameter of one micron ($10^{-4}$ cm) would produce a mean dry particle size of 0.43 micron.

Because particles having diameters of about one-half micron make the major contribution to light scattering in the atmosphere (Pueschel and Noll, 1966), and because the particles generated by a Collison atomizer in an earlier work (Cooper and Byers, 1970) were generally smaller than this, attempts were made to increase the mean particle diameter in several ways. One way was to remove the baffle which was originally in the Collison atomizer, thus lengthening the distance the particles had to travel before impaction. Some larger droplets would thus have a lower probability of impacting. Early in this work it was noticed that aerosols generated from 8% v/v solutions formed heavy deposits downstream from the dilution orifice in the tee where the two air streams met. Subsequently, for 8% v/v aerosols, the aerosol from the atomizer was routed past the jet issuing from the dilution orifice before releasing the aerosol into the mixing chamber.

The result of removing the Collison atomizer baffle was an increase of about 20% in particle diameter as measured by an aerosol photometer (Royco Instruments, Model No. 202) in the aerosol generated from a 1% v/v NaCl solution. Avoiding impaction by the dilution orifice jet resulted in an increase of 30% in the backscattering from the aerosols generated by 8% v/v NaCl solution, but only 10% increase in backscattering from 1% v/v NaCl solution. The rerouting of the aerosol stream was done only with 8% v/v solutions.

## B. Aerosol Transport

The flow path of the aerosol after it left the mixing chamber is diagrammed in Figure 1.3. After the aerosol left the mixing chamber, it flowed a horizontal distance of 3 meters in plastic tubing having a diameter of 5.1 cm, from which it was sampled by means of a vertical 1.5 meter length of 2.5 cm diameter plastic tubing and a horizontal 0.3 meter length of 0.64 cm diameter rubber tubing. The aerosol then passed through 10 cm of 0.15 cm diameter glass capillary tubing into a plastic container having a volume of $8.5 \times 10^3$ $cm^3$. From this holding chamber, used to reduce concentration fluctuations, the aerosol flowed through 15 cm of 0.64 cm diameter rubber tubing into a mixing tee where it was mixed with filtered air of controlled humidity. The diluted aerosol then went through 45 cm of 0.64 cm diameter tubing to the relative humidity (RH) chamber, where its humidity was measured. The total flow rate at the RH chamber was $13 \times 10^3$ $cm^3$ per minute (0.46 $ft^3$/min) and the RH chamber volume was $17 \times 10^3$ $cm^3$, so that the average residence time of a particle was 1.3 minutes or 78 seconds. The diluted, humidity-controlled aerosol flowed to the tee containing a thermometer through 15 cm of 0.64 cm diameter rubber tubing. From the tee with the thermometer, the

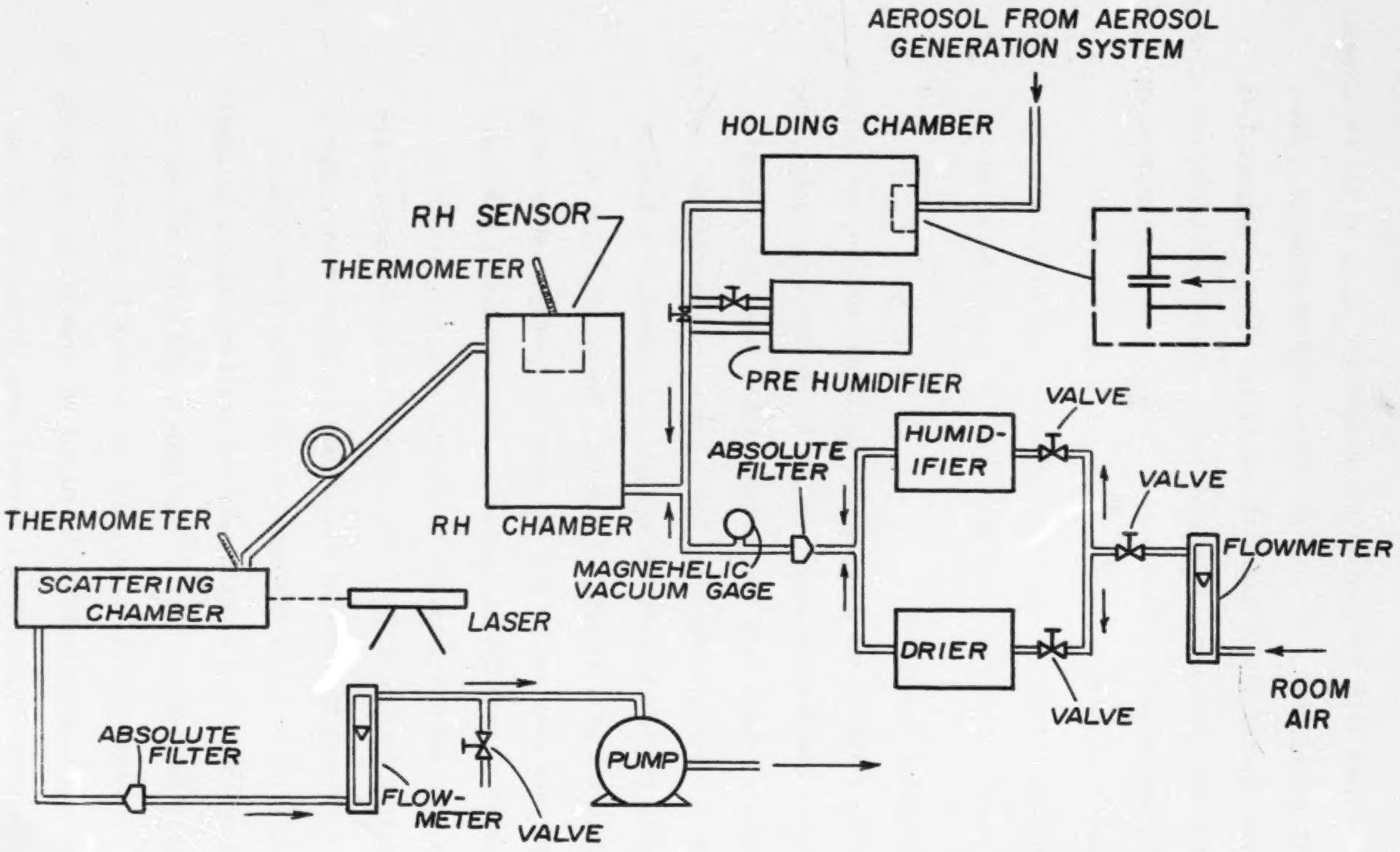
AEROSOL FROM AEROSOL GENERATION SYSTEM
HOLDING CHAMBER
RH SENSOR
THERMOMETER
PRE HUMIDIFIER
VALVE
HUMID-IFIER
ABSOLUTE FILTER
VALVE
FLOWMETER
THERMOMETER
RH CHAMBER
MAGNEHELIC VACUUM GAGE
SCATTERING CHAMBER
LASER
DRIER
VALVE
ROOM AIR
ABSOLUTE FILTER
PUMP
FLOW-METER
VALVE

Figure 1.3. Aerosol Modification and Scattering Measurement System

aerosol went into the scattering chamber via 15 cm of 1.3 cm diameter rubber tubing bent into a single loop of 10 cm diameter. The aerosol entered the cylindrical scattering chamber (Figure 1.4) through the side; turbulence resulted in mixing which appeared thorough to the eye in a test using a dense smoke and a clear plastic end piece on the scattering chamber. After the aerosol left the scattering chamber it was caught on a filter, except when its size distribution was being determined as described below.

## C. Humidity Control

The filtered air going to the Collison atomizer and dilution jet had a humidity of less than 10% RH (relative humidity), and the aerosol which left the mixing chamber (with the exception of the polystyrene aerosols) had a humidity under 20% RH. Before going to the RH chamber, the aerosol was joined by a flow of filtered air of controlled humidity. The dry fraction of the air was obtained by pulling room air through a dessicator (containing Linde Type 5A molecular seive material) and the moist fraction was obtained by drawing room air through the humidifier (Figure 1.5). The combination of wet and dry air passed through an absolute filter (Gelman glass fiber, Type E) before being added to the aerosol. The total flow of the humidity-controlled dilution air was monitored with a rotameter and kept constant at 11 x $10^3$ $cm^3$/min (0.183 x $10^3$ $cm^3$/sec or 0.38 $ft^3$/min). As described, the set-up gave final aerosol humidities ranging from 10% RH to 85% RH. Humidities above 85% RH were obtained by passing the aerosol over the surface of the water in a one-pint (0.5 x $10^3$ $cm^3$) Mason jar one-quarter filled with water, which served as the "pre-humidifier".

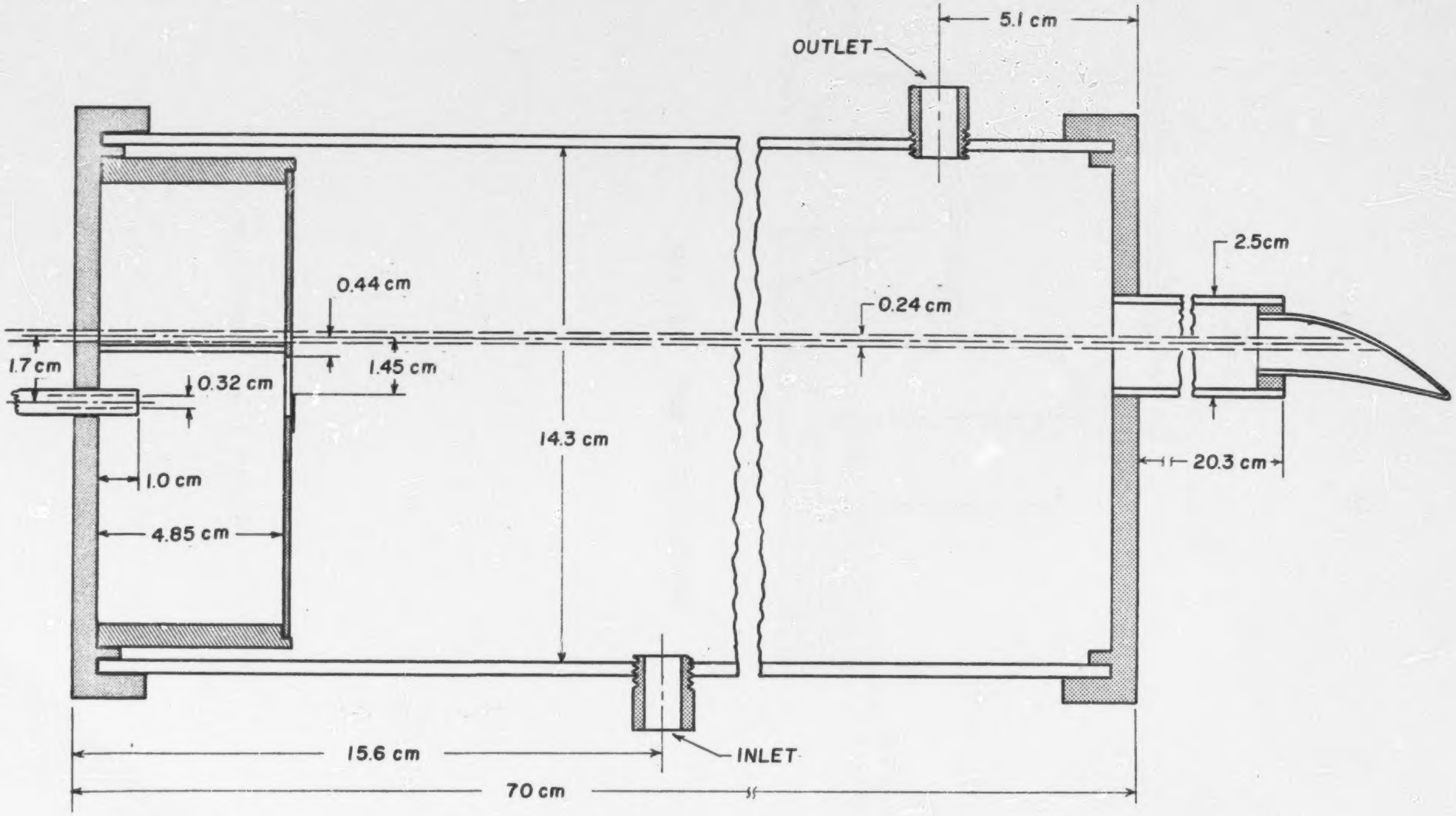
5.1 cm
OUTLET
2.5cm
0.44 cm
0.24 cm
1.7 cm
0.32 cm
1.45 cm
14.3 cm
1.0 cm
20.3 cm
4.85 cm
15.6 cm
INLET
70 cm

Figure 1.4. Scattering Chamber, Model 1.

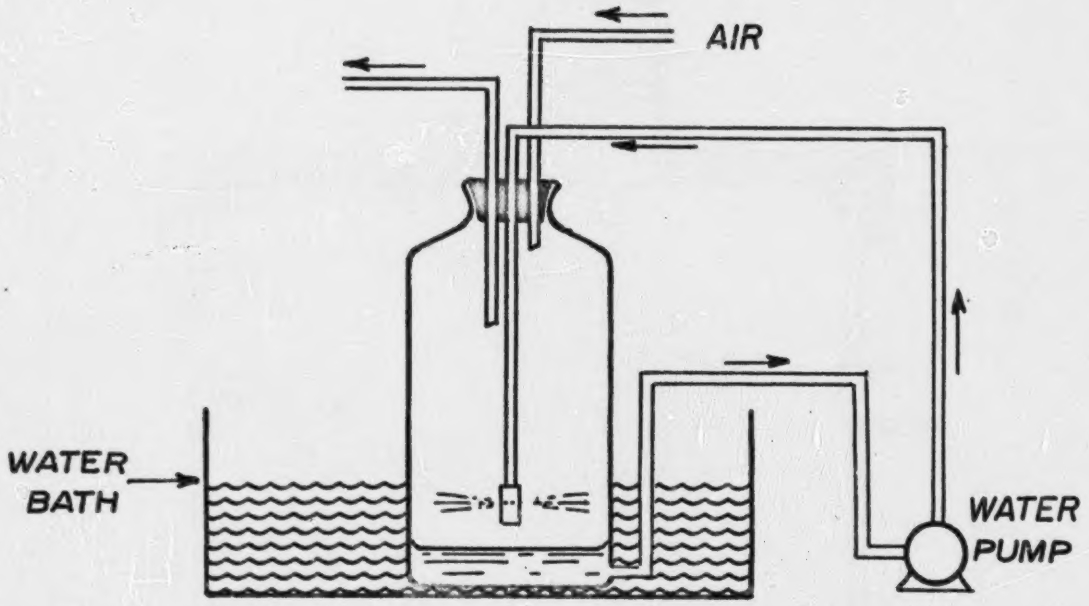
AIR
WATER BATH
WATER PUMP

HUMIDIFICATION SET-UP

Figure 1.5. Humidifier

### D. Humidity Measurement

The humidity of the diluted aerosol was measured in the RH chamber, which was made from a metal canister about 30 cm in diameter and 30 cm high. The aerosol entered the RH chamber from the bottom, mixed in the chamber for an average of 1.3 minutes and exited from the chamber near the top, at measured and controlled temperature and humidity. The humidity sensors were glass coils impregnated with various hygroscopic salts; the conductivities of the coils are functions of relative humidity (the system was a Model 15-3001 Hygrometer Indicator and Model 4-4824 Hygrosensors from Hygrodynamics, Inc., Silver Springs, Maryland). The sensors are rated to respond to 65% of an instantaneous change in humidity within 3 seconds and are accurate to within ±1.5% RH according to the manufacturer. Sensors were intercompared at the limits of their ranges and no discrepancy with the claimed accuracy was found; the same was true (to within the psychrometer accuracy available) for comparisons with a sling psychrometer for several of the sensors; all were not tested against the psychrometer. The sensors' accuracy was not dependent on air flow rate, according to the manufacturer, which is a major advantage in comparison with the wet-bulb/dry-bulb thermometry method of determining relative humidities.

The amount of water vapor air will hold when saturated is a function of temperature; the relative humidity, the ratio of the water vapor present to the saturation amount, is also temperature-dependent. The use of two thermometers, one in the RH chamber and one in the inlet to the scattering chamber, allowed for a correction for temperature change in the fashion suggested by the material in Appendix 1. Usually the temperature differences were around a few tenths of a degree centigrade. Appendix 2 demonstrates that pressure corrections to the humdity were negligible.

## E. Light Scattering Measurement

The illumination of the aerosol and the measurement of its scattering of the incident light was done with the scattering chamber (Model 1) shown in Figure 1.4.

The Model 1 scattering chamber is a long cylinder lined throughout with black velvety material to absorb light. It is light-tight and air-tight. The laser beam enters through a window made from a microscope slide cover glass, and the beam ends in a light horn made of bent glass tubing painted outside with optical black paint. Optical stops determine how much of the beam can be viewed by the light pipe, which transmits light to the photomultiplier tube (RCA 7265, with 2000 volts applied). The details of the optical geometry are given in Figure 1.4, and, in a latter part of the manuscript, a description is included of a test which was made to determine the response of the optical system to a target placed at various positions along the beam.

The light was provided by a He-Ne laser (Quantum Physics Model LS-32). The laser light was polarized with its electric vector vertical, i.e., being perpendicular to the scattering plane. The nominal rating of this laser is 3 milliwatts. The laser is in continuous-wave, multimode operation at the wavelength 6328 Å ($10^{-10}$m). The constancy of the laser output was monitored with a General Electric X-6 Photoconductive Cell, preceded by a translucent light diffuser: the response of this cell, in the range used ($10 \times 10^3$ ohm), is related to the laser power output to an exponent between 1/2 and 1 (estimated from the calibration curves supplied). The measurements reported here were made for a laser output range of 10.3 to $11.6 \times 10^3$ ohms, with the usual value near $11.0 \times 10^3$ and with changes rarely as much as $0.1 \times 10^3$ between wet and dry scattering measurement. Corrections were not made for these changes, which were a few percent or less. Because the transmittances of the front and rear mirrors of the He-Ne laser were 99% and 99.9% respectively, the photoconductive cell located at the rear should have received one-tenth the output of the laser constantly; in other words, any major changes in output power other than those due to contamination of the mirrors would have been noticed. The laser drew its power from a constant voltage transformer (Sola Model CVS).

The light pipe is 0.32 cm (1/8 inch) in diameter and 30 cm (12 inches) long. The manufacturers (American Optical Co.) state that it will accept 70% of the light incident upon it and transmit wavelengths from 4,000 to 20,000 Å, with a loss of 50% every 210 cm (7 feet). A fairly large chamber was used to reduce the amount of light reflected from the walls into the light pipe, which was shielded from the light reflected from the spot at the termination of the laser beam.

The light which reaches the light pipe is transmitted to the RCA 7265 photomultiplier tube, which is in use in at least one commercial lidar. The tube is housed in a light-tight case. The light pipe touches the center of the sensitive face of the photomultiplier tube. The photomultiplier tube was chosen for low dark current ($<0.3 \times 10^{-7}$ amps at our operating conditions). The power was supplied to the tube by a voltage supply (Keithley Model 246) which allowed adjustment to the precision of 1 volt. The resulting current was read by an electrometer (Keithley Model 610 CR), which had a range that extended down to $10^{-14}$ amps. The output of the electrometer was recorded on a strip chart recorder.

Since light scattering from particles varies with the angle between the directions of incidence and scattering, it is useful to know the response of the scattering chamber to scattering from various positions (thus various angles) along the laser beam. This response was measured and the measurements used to compute the effective scattering angle of the scattering chamber geometry. To obtain the response of the receiving optics as a function of scatterer distance from the light pipe face, and thus as a function of scattering angle, a diffuse reflector (0.45 micron white Millipore membrane filter) was moved along the path of the laser beam, with its face perpendicular to the beam. The laser light was attenuated by two filters having a total attenuation of about $2 \times 10^{-5}$. Table 1.1 gives results of these measurements.

Table 1.1

Model 1 Optical Response as a Function of Perpendicular Distance From Optical Receiver Plane and as Function of Scattering Angle.

| Perpendicular Distance from Light Pipe Face Plane (cm) | Scattering Angle (Degrees) | Net Scattering ($10^{-5}$ A) |
|---|---|---|
| 5.0 | 161.2 | 0.00 |
| 5.25 | 162.0 | 0.255 |
| 5.5 | 162.8 | 0.288 |
| 5.6 | 163.1 | 0.592 |
| 5.7 | 163.4 | 0.97 |
| 5.8 | 163.7 | 1.25 |
| 5.9 | 163.9 | 1.40 |
| 6.0 | 164.2 | 1.50 |
| 6.25 | 164.8 | 1.46 |
| 6.5 | 165.3 | 1.33 |
| 6.75 | 165.8 | 1.25 |
| 7.0 | 166.3 | 1.19 |
| 7.5 | 167.2 | 1.04 |
| 8.0 | 168.0 | 0.932 |
| 8.5 | 168.7 | 0.847 |
| 9.0 | 169.3 | 0.763 |
| 10.0 | 170.4 | 0.624 |
| 11.0 | 171.2 | 0.522 |
| 12.0 | 171.9 | 0.452 |
| 13.0 | 172.5 | 0.382 |
| 14.0 | 173.1 | 0.327 |
| 16.0 | 173.9 | 0.262 |
| 18.0 | 174.6 | 0.203 |
| 20.0 | 175.1 | 0.151 |
| 22.0 | 175.6 | 0.116 |
| 24.0 | 175.9 | 0.084 |
| 26.0 | 176.2 | 0.057 |
| 28.0 | 176.5 | 0.044 |
| 34.0 | 177.1 | 0.017 |
| 39.0 | 177.5 | 0.008 |
| 44.0 | 177.8 | 0.006 |
| 49.4 | 178.0 | 0.003 |

The calculation of the effective scattering angle gives the result that if the particles scattered diffusely (Lambert's law) near 180°, the amount of light measured in the scattering chamber would be equal to what would have been measured if all the particles had been placed 15.0 cm (perpendicular distance) from the light pipe face. This corresponds to an effective scattering angle of 173.5°. Half the light scattered by diffusely scattering particles would have come from positions corresponding to angles greater than the median scattering angle of 170°. As noted below, the difficulty of making exact calculations for expected scattering lessens the theoretical importance of having measured at an angle less than 180°. It is also shown that the experimental scattering angle may be greater than 173.5°, because of the angular distribution of scattering from particles similar to these.

The "effective scattering angle" is the angle corresponding to the position along the beam at which, if all particles were placed there, the received scattering intensity would equal the total intensity received from the same number of diffusely scattering particles when spread out homogeneously along the beam path.

For this analysis, the following definitions hold:

$$I_1(\theta) = \frac{\text{(flux scattered per unit solid angle in direction } \theta)}{\text{(flux geometrically incident on object)}}$$

$\pi a^2$ = projected area of particle in beam direction

$Q(z)$ = solid angle subtended by optical receiver as a function of scatterer position along beam

$F$ = flux incident on object

$f$ = flux incident on optical receiver

$A(z)$ = cross-sectional area of laser beam

$n(z)$ = particle concentration (number/volume)

$N$ = total number of illuminated particles viewed

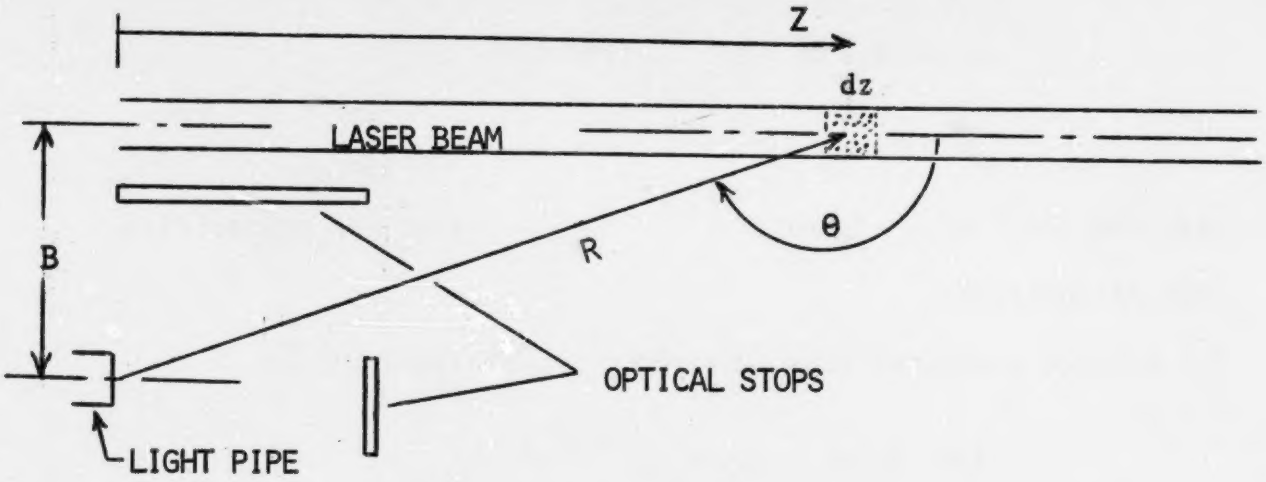

$$\tan\theta = (B/z)$$

$$\theta = \tan^{-1}(B/z)$$

Actually, a ray diagram for the light reaching the light pipe would be more complicated, but these complications are included in the experimental evaluation of $Q(z)$.

Note that if

$dN$ = differential number of illuminated particles viewed, then

$dN = n(z)\ \ A(z)\ \ dz$.

In what follows, $n(z)$ and $A(z)$ are assumed constant--that is, homogeneous mixing and negligible beam divergence are assumed.

The total flux reaching the receiver is

$$f = \int_{z_o}^{z_f} F\ \ I_1(z)\ \ Q(z)\ \ dN$$

where $z_o$ and $z_f$ are the limits of the viewed portion of the beam.

Then,

$$f = \int_{z_o}^{z_f} F \; I_1(z) \; Q(z) \; n(z) \; A(z) \; dz$$

$$f = F \, n \, A \int_{z_o}^{z_f} I_1(z) \; Q(z) \; dz$$

with the additional assumption that F is constant (no appreciable beam attenuation).

The average scattered flux received per particle would be

$$f/N = [n \; A \; (z_f - z_o)]^{-1} \; f$$

$$= F \; (z_f - z_o)^{-1} \int_{z_o}^{z_f} I_1(z) \; Q(z) \; dz$$

The same scattering would result from the N particles if they were placed so that

$$FN \; \overline{I_1 Q} = F \; N \; (z_f - z_o)^{-1} \int_{z_o}^{z_f} I_1(z) \; Q(z) \; dz$$

It is important to note that we are working with an average over the particles, which is an average with respect to dN and thus dz, rather than with averages weighted by dθ. $\overline{I_1 Q}$ is the ensemble average of $I_1 Q$.

$$\overline{I_1 Q} = (z_f - z_o)^{-1} \int_{z_o}^{z_f} I_1(z) \; Q(z) \; dz$$

For a monodisperse aerosol we would expect to find some position z* along the beam for which

$$I_1(z^*) \; Q(z^*) = \overline{I_1 Q} \quad ,$$

and this would define the effective scattering angle, $\theta^* = \tan^{-1}(B/z^*)$. Because the function $I_1(z)$ is a complicated funciton of position (that is, of scattering angle) as well as particle index of refraction and the ratio of particle circumference to the light's wavelength, the approximation is made which would hold if the sum of the $I_1(z)$ contributions from the polydisperse particles changes much less rapidly than does the function $Q(z)$, that is, we assume

$$\overline{I_1 Q} \doteq \overline{I_1}\ \overline{Q} = \overline{I_1}\,(z_f - z_o)^{-1} \int_{z_o}^{z_f} Q(z)\,dz$$

and get the effective position $z_e$ from

$$\overline{Q} = Q(z_e) = (z_f - z_o)^{-1} \int_{z_o}^{z_f} Q(z)\,dz$$

This defines $z_e$, which in turn gives the estimated effective scattering angle $\theta_e$,

$$\theta_e = \tan^{-1}(B/z_e)$$

The data in Table 1.1 come from measurements made with a Lambert's law ($I_1(\theta) \sim \cos\theta$) reflector whose $I_1(z)$ is a much more nearly constant function of z than is $Q(z)$, which varies roughly as the inverse square of the distance from the position of dz to the center of the light pipe. Equal dz correspond to equal dN, thus the data in Table 1.1 as weighted by distance along beam (not by angle) give $\theta_e = 173.5°$.

The flux received from the reflector is $f = FI_1Q(z)$ which is integrated to give

$$\int_{z_o}^{z_f} f\,dz = \int_{z_o}^{z_f} F\,I_1 Q(z)\,dz = (z_f - z_o)\,\bar{f}\,(z),$$

so that

$$\bar{f}\ (z_e) = F\ I_1\bar{Q}(z_e) \quad .$$

Therefore, the $z_e$ corresponding to $\bar{f}$ is that corresponding to $\bar{Q}$. The computation for f consists of taking f(z) at each interval times the width of that interval and dividing the sum of these contributions by the effective beam length, because $\Delta z$ is proportional to $\Delta N$.

The light scattered back from a particular volume of aerosol will be proportional to the number of particles illuminated and related in some way to the size of the particles and to their composition. Particles which contribute most significantly to natural light scattering in the atmosphere are those of about one-half micron ($0.5 \times 10^{-4}$cm) in diameter (Pueschel and Noll, 1966). Unfortunately, in this size region, where the particle diameter is of the same order of magnitude as the wavelength of the incident light, the theoretical analysis of light scattering is quite complicated, involving the use of the Mie scattering equations, whose solutions are infinite sums of Riccatti-Bessel functions. Although there are tabulated solutions of the Mie equations for many combinations of index of refraction and ratio of particle diameter to light wavelength (Davies, 1966), theoretical solutions for practical situations are difficult to calculate for a number of reasons.

One complication in the use of Mie functions is that natural aerosols are not one size but "polydisperse", i.e.,composed of particles of many sizes. Estimates based upon approximations of the size distribution as a sum of many monodisperse (single-size) contributions are required.

Another problem in applying the exact theory is that the Mie solutions have been tabulated almost exclusively for spherical particles, but cannot be computed practically for irregular particles. There is some disagreement about how different the results are for particles which are only roughly spherical (Davies, 1964; Huffman et al., 1969).

Finally, although much experience and data have been accumulated about light scattering in the forward direction or at right angles to the incident beam, very little work has been done on backscattering, which in this size range is roughly 1 or 2 orders of magnitude less than forward scattering.

The behavior of light which impinges on a particle is determined by the ratio of the particle circumference to the wavelength of the light ( $\alpha = \pi D_p/\lambda$), by the complex index of refraction of the particle, which takes into account refractive index and absorptivity, and by the polarization of light. When the wavelength of the light is either quite large or quite small compared to the particle circumference, several simplifying assumptions can be made. In the intermediate regime, the full "Mie" theory must be used. Long-intermediate- and short-wavelength regimes are now examined.

Rayleigh regime, for $\alpha<0.3$: In the Rayleigh regime, the amount of light scattered is proportional to the sixth power of the diameter and inversely proportional to the fourth power of the wavelength. This regime includes gas molecules and Aitken nuclei ($D_p$ <0.04 microns) and is responsible for the blue of the sky and the red of sunsets. The portion of light which is polarized perpendicular to the plane of incidence and observation ($I_1$) has no angular dependent Rayleigh scattering; that which is polarized parallel to the plane of incidence and observation ($I_2$) has a cosine squared dependence; their sum for unpolarized incident light is (Kerker, 1969):

$$I = \frac{\pi^4 D_p^6}{8R^2\lambda^4}\left[\frac{m^2 - 1}{m^2 + 2}\right]^2 (1 + \cos^2 \theta) = (I_1 + I_2)/2$$

where:

$I$ = intensity of light received in direction $\theta$/unit illumination

$D_p$ = particle diameter

$m$ = index of refraction of particle

$\lambda$ = wavelength of light

$R$ = distance from particle to observer

Mie regime, for $0.3<\alpha<3/(m-1)$: In this regime the scattering pattern loses its symmetry and becomes quite complicated. Scattering theory computations must be used, somewhat simplified by the use of tables which are available for a variety of indices of refraction and circumference-to-wavelength ratios. The Mie function does not increase or decrease monotonically with increasing particle size for a given wavelength, making monochromatic light-scattering measurements of a variety of particle sizes very difficult to interpret.

Mie equations for irregular particles would seem hopelessly difficult to solve. Although the detailed angular pattern may be considerably different from that of spheres, the total scattering from particles having some measure of size (e.g.; area, volume) in common with a sphere of a given diameter of the same index of refraction should be of the same order of magnitude as that of the sphere (Davies, 1966).

It is instructive at this point to examine some scattering diagrams, Figures 1.6 and 1.7 extracted from the work of Pueschel and Rossano (1966). The mass mean diameter of the aerosols generated from 1% v/v solutions was 0.2 microns; the mass median diameter was 0.6 microns; the mass mean diameter for the 8% v/v NaCl aerosol was 0.43 microns and the mass median diameter was 1.5 microns (see size distribution data and analysis in the Results part of this section); These diameters correspond to scattering parameters (α) of approximately 1, 3, 2, and 7.5 respectively. The index of refraction of KCl is 1.49 and for NaCl, 1.54. It is seen from Figures 1.6 and 1.7 that for monodisperse spherical aerosols near these sizes, and having an index of refraction near these (m = 1.6), the scattering generally does increase toward 180°; thus it is likely that the experimental scattering angle is greater than 173.5°, because scattering from particles near the back end of the chamber should be weighted more heavily than is shown above.

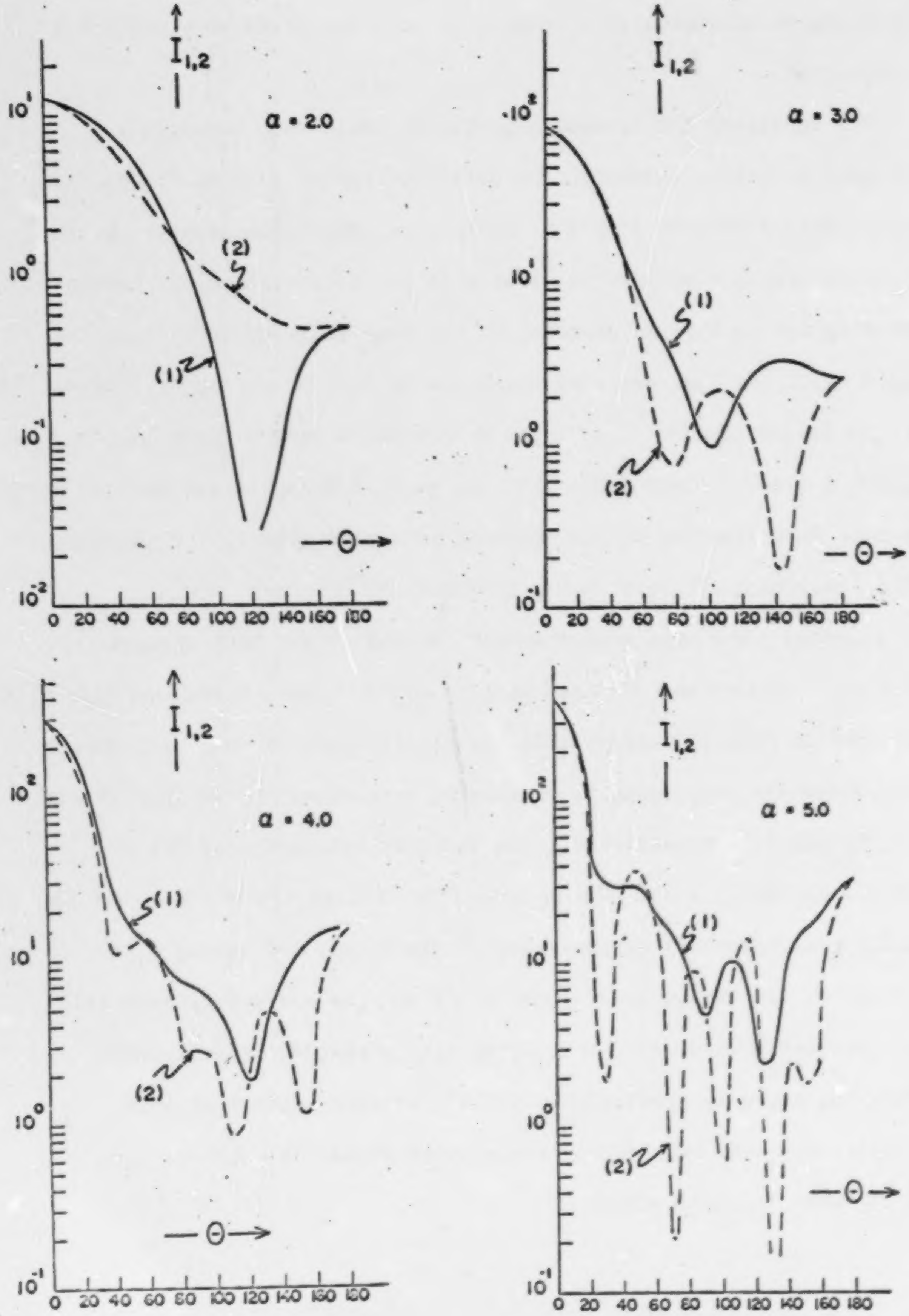

Figure 1.6. Angular Distribution of Scattered Intensity Polarized Vertical (1) and Parallel (2) to Observation Plane for Spheres of m = 1.60. (Pueschel and Rossano, 1966)

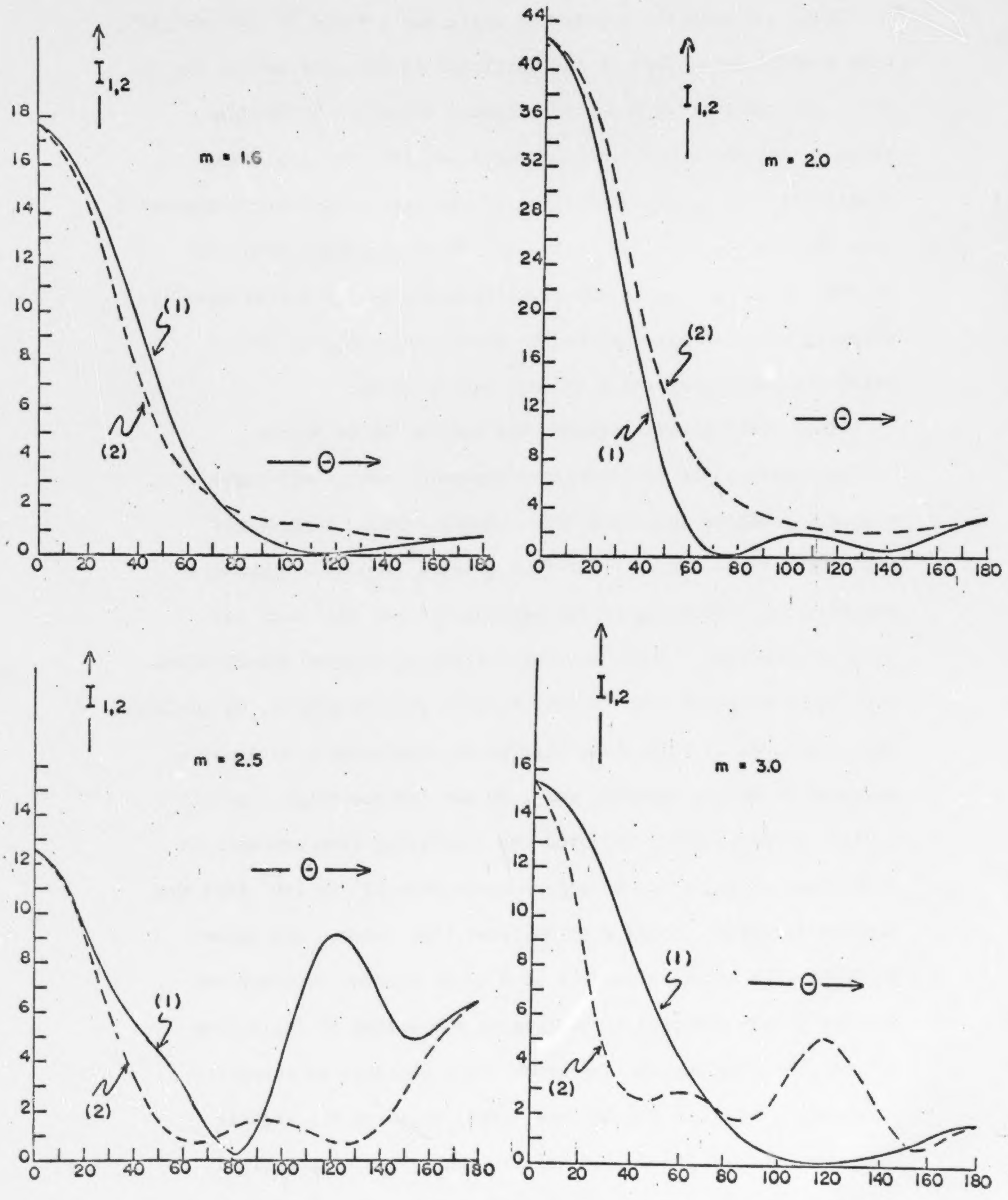

Figure 1.7. Angular Distribution of Scattered Intensity Polarized Vertical (1) and Parallel (2) to Observation Plane for Spheres of $\alpha = 2.2$. (Pueschel and Rossano, 1966)

Thus, although the scattering angle has a range of 161° to 178°, only a small percentage of the particles in the beam are in the first few centimeters and the estimated effective scattering angle is 173.5°, and the median angle is 170°, for isotropic scatterers. If $I_1$ (flux of light of vertical polarization scattered into angle $\theta$ per unit incident light flux) increases from 160° to 180° (see Figures 1.6 and 1.7), then the larger angles are weighted more heavily than in the above estimate, and the effective scattering angle is even closer to 180°.

Other workers have measured the scattering of nearly monochromatic light by laboratory aerosols, but at effective scattering angles less than 170°. Eiden (1966) measured the scattering of polarized light from a xenon lamp by atmospheric aerosols for scattering angles between 50° and 160° from the forward direction. (Matching the scattering angular distribution with those computed from several natural aerosol models, he concluded that the index of refraction for the dry atmospheric aerosols he measured in Mainz, Germany, was 1.50 and for the moist aerosols 1.44.) Setlzer (1969) measured the scattering from aerosols as a function of angle in one-degree steps from 12° to 146° from the forward direction, using a He-Ne laser light source and water aerosols with median diameters of 5 to 10 micron. Huffman and Thursby (1969) measured scattering as a function of angle from 10° to 150° with unpolarized green light incident on irregular particles. Pueschel and Rossano (1966) measured the angular distribution from 20° to 130° of the scattering of polarized monochromatic light from monodisperse polystyrene latex aerosols having diameters from 0.26 to 2.02 microns for many wavelengths.

They found discrepancies between the measurements and Mie scattering theory which they suggest could be due to anisotropy in the latex particles, suggested also by Maron, et al.(1963). Phillips, et al. (1970) measured the scattering of polarized light (argon laser at 0.514 microns) from a single polystyrene latex sphere for angles from about 10° to about 160° and found that they got excellent agreement with the Mie theory predictions for polystyrene latex by using an index of refraction of 1.59 ± 0.01 and a diameter of $1.200 \pm 0.01 \times 10^{-4}$ cm instead of the diameter given by the manufacturer ($1.099 \pm 0.006 \times 10^{-4}$ cm).

## III. General Procedure

Aerosol generation: A volume of 550-600 $cm^3$ of solution to be nebulized was placed in the Collison atomizer jar, and the atomizer head was screwed into place. The clean, dry air was turned on. The magnetic stirrer was turned on and adjusted so that there was turbulent mixing in the atomizer jar, but only a shallow vortex formed, so as not to pull the free surface below the liquid intake of the nebulizing head. A filter was placed in the filter holder following the scattering chamber; the filter was a 0.45 micron membrane filter (Millipore) for the microscope counts of the polystyrene or a glass fiber absolute filter (Gelman Type E) for the weight determinations (for which determinations the filter was desiccated for at least 12 hours and preweighed). Then the pump at the end of the flow train was turned on and sampling begun, with the flows adjusted to give 9.5"$H_2O$ pressure drop across the capillary tube--this corresponded to a volumetric flow of 42 $cm^3$/sec (0.09 $ft^3$/min) from the mixing chamber aerosol and a flow of 170 $cm^3$/sec (0.36 $ft^3$/min) of dilution air.

Humidity control and measurement: By changing the ratio of wet air to dry air in the filtered air used to dilute the aerosol before entering the RH chamber, the humidity in the resulting mixture could be controlled. Humidity readings were considered stabilized after the rate of change in humidity was below about 1/2% RH per minute. The temperature in the RH chamber was measured with a thermometer (Thomas Model 9534) which extended into the chamber to the level of the middle of the RH sensors. The temperature of the mixture immediately preceding the scattering chamber was measured with the same kind of thermometer, which had found to read identically with the first to less than 0.1°C difference. Corrections for the temperature dependence of relative humidity were made, although these temperature differences were usually 0.2°C or less. To improve the ability to reset the correct dilution ratio, reference marks were made which lowered parallax errors involved in reading the flow meter and pressure gauge.

Light scattering measurement: Before taking any readings, the photomultiplier tube and the laser were given at least an hour's warm-up by which time the photomultiplier dark current had stabilized, as had the laser output. Initial readings would be made on the "dry" conditions, that is at a relative humidity of less than 20%. Then the humidity was raised in steps and the light scattering measured, the net scattering being the difference between these readings and the readings given by filtered air (which showed a generally negligible increase in scattering with increased humidity). Ten to fifteen minutes elapsed between readings for the humidity to stabilize and generally two such "wet readings were taken and then a "dry" reading was made to re-establish the baseline. If the humidity dependence showed it was warranted, the tests were accelerated by taking "dry" as being less than 40% RH rather than 20% RH. For the highest humidity tests, up to half an hour was required to take the final humidity readings, in order to extend the upper range of relative humidities studied. If no changes (such as adding more fluid to the Collison) had been made in the test set-up during the run, the "dry" measurements before and after the "wet" measurements were used and interpolations were made to obtain the best estimate of the "dry" scattering; otherwise, the "dry" test nearest in time to the "wet" test was used. The ratios of wet to dry scattering are listed as "Scattering Ratios," meaning the ratio of the scattering at an elevated humidity to that at a low humidity.

## IV. Results and Analysis

### A. Size Distributions

The properties of aerosol particles are strongly size-dependent, in general, so that it is useful to characterize the size of the aerosols produced by the Collison atomizer. Usually such characterization is done by presenting size distribution data such as the number distribution, which shows the percentages of the total number of aerosol's particles having diameters which fall in a series of size intervals. Another way of presenting size data is through the mass distribution, the percentages of the total mass of the aerosol due to particles having diameters falling within a series of size ranges. Quite often it is useful to work with the cumulative mass distribution, the percentage of the total aerosol mass due to particles of a certain diameter or smaller, plotted against diameter. To ascertain the size distribution of the aerosol produced, the particles were collected on aluminum foil using a Bendix electrostatic sampler. Parts of the foil were then cut out and photographed in an electron microscope.

The Bendix sampler is shown schematically in Figure 1.8. It was modified so that it could be used in the flow series; normally, a small blower in the sampler pulls air samples through the instrument at atmospheric pressure, but in this case the sampler was made air tight and a pump and flow meter were connected to the exhaust so that air flowed into the sampler through its inlet. The aerosol was drawn into the sampling cylinder, which has a wire along its axis raised to a potential of ten thousand volts. The unipolar corona discharge from the central wire charged the particles as they passed and the voltage gradient forced the charged particles onto the foil which lined the inside of the cylinder. Half-hour samples of the 1% v/v aerosols and ten-minute samples of the 8% v/v aerosols gave a clearly visible deposit, which ran in a band from 2 1/2 to 10 or 12 cm from the inlet edge. Samples for the electron microscope were taken from positions 2, 4, 6, 8, 10 and 12 cm from the leading edge of the foil for the 1% v/v aerosol (also 14 cm for the 8% NaCl).

A sample of the aerosol (at humidity less than 30% RH) was collected on aluminum foil. Electron microscope pictures of the samples on the foil were taken at a 10,000x magnification and sizing was done by comparing the area of the particles to the areas of circles having the diameters given as $D_p$ in the tables;

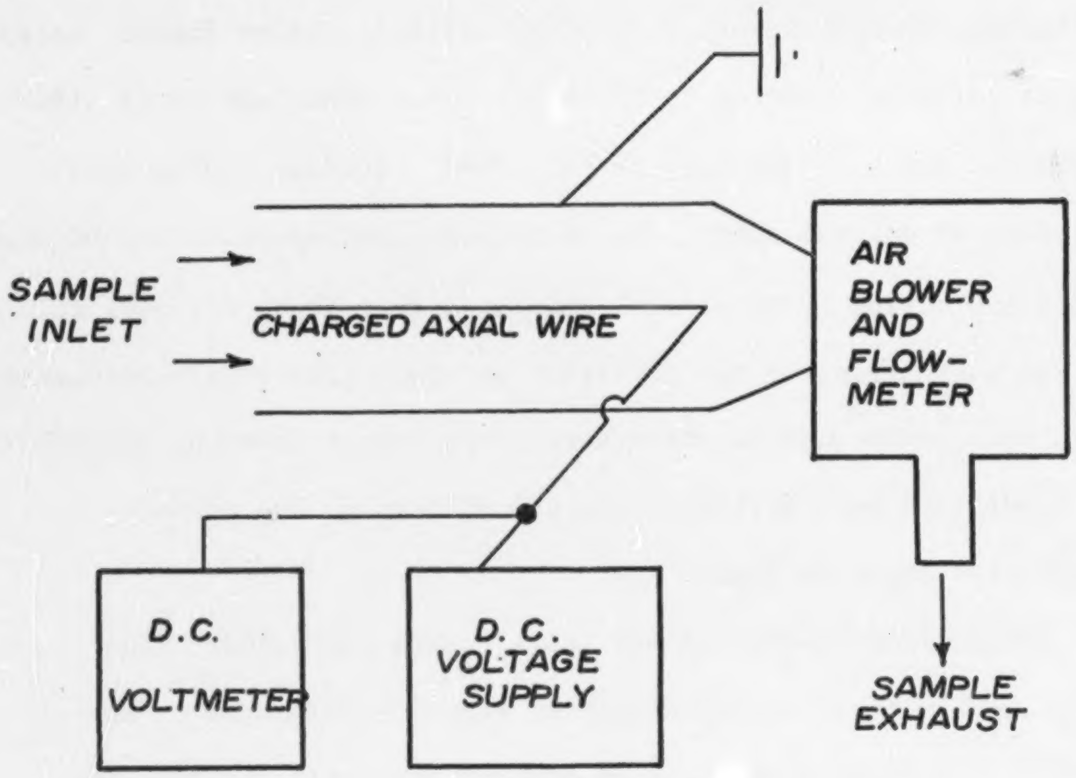
SAMPLE INLET
CHARGED AXIAL WIRE
AIR BLOWER AND FLOW-METER
D.C. VOLTMETER
D. C. VOLTAGE SUPPLY
SAMPLE EXHAUST

Figure 1.8. Schematic of Bendix Electrostatic Sampler

the essential size information is given in Tables 1.2 to 1.4. The size distributions given in these tables were obtained by counting techniques, rather than by weighing techniques, but these have been converted to mass distributions for the graphical presentation, since light scattering is more closely related to particle volume (hence, mass) than to particle diameter to the first power (Charlson et al.,1967; Cooper and Byers, 1970; Noll et al., 1968). Because sizing small particles by optical comparison is tedious and expensive, we decided to use one sizing of an aerosol generated from an 8% v/v NaCl solution and one each sizing of two different aerosols from 1% v/v solutions (KCl, NaCl) were used to characterize the output from the nebulizer. The cumulative mass distributions are plotted on log-normal probability paper in Figure 1.9.

The smallest particles are least accurately sized. Those particles listed as having diameters around 0.05 microns are actually all those that small or smaller and still visible; more particles were not seen when the magnification was doubled so that the total number count is believed to be nearly correct. The number mean diameters, heavily influenced by the size inaccuracies for the smallest particles, are likely to be less accurate than the mass mean and mass median diameters, which are more strongly influenced by the larger particles (whose sizes were determined more accurately).

Two sets of size distributions are listed in Table 1.5. The first set is the result of this work, the second set is derived from the work of Cooper and Byers (1970). Although both investigations used Collison atomizers, in this work the atomizer was not baffled; also the 8% v/v NaCl aerosol of the earlier work was

| Particle Diameter $D_p$ ($10^{-4}$ cm) | Number of Particles in Size Interval Centered on $D_p$ | Fraction by Number in Interval | Cumulative Number Fraction | Cumulative Mass Fraction |
|---|---|---|---|---|
| 0.050 | 7682. | 0.5613 | 0.5613 | 0.0032 |
| 0.100 | 1612. | 0.1178 | 0.6791 | 0.0085 |
| 0.140 | 1340. | 0.0979 | 0.7770 | 0.0208 |
| 0.200 | 962. | 0.0703 | 0.8473 | 0.0463 |
| 0.280 | 865. | 0.0632 | 0.9105 | 0.1094 |
| 0.400 | 722. | 0.0528 | 0.9632 | 0.2630 |
| 0.560 | 339. | 0.0248 | 0.9880 | 0.4608 |
| 0.760 | 106. | 0.0077 | 0.9958 | 0.6154 |
| 1.100 | 47. | 0.0034 | 0.9992 | 0.8232 |
| 1.540 | 9. | 0.0007 | 0.9999 | 0.9324 |
| 2.160 | 2. | 0.0001 | 1.0000 | 0.9994 |
| Total: | 13686. | | | |

Table 1.2. Size Distributions for 1% v/v KCl Aerosol

| Particle Diameter $D_p$ ($10^{-4}$ cm) | Number of Particles in Size Interval Centered on $D_p$ | Fraction by Number in Interval | Cumulative Number Fraction | Cumulative Mass Fraction |
|---|---|---|---|---|
| 0.050 | 8611. | 0.8158 | 0.8158 | 0.0171 |
| 0.100 | 817. | 0.0774 | 0.8932 | 0.0301 |
| 0.140 | 393. | 0.0372 | 0.9305 | 0.0472 |
| 0.200 | 247. | 0.0234 | 0.9539 | 0.0786 |
| 0.280 | 216. | 0.0205 | 0.9743 | 0.1539 |
| 0.400 | 155. | 0.0147 | 0.9890 | 0.3115 |
| 0.560 | 73. | 0.0069 | 0.9959 | 0.5152 |
| 0.760 | 30. | 0.0028 | 0.9988 | 0.7244 |
| 1.100 | 13. | 0.0012 | 1.0000 | 0.9993 |
| Total: | 10555. | | | |

Table 1.3. Size Distributions for 1% v/v NaCl Aerosol

| Particle Diameter $D_p$ ($10^{-4}$ cm) | Number of Particles in Size Interval Centered on $D_p$ | Fraction by Number in Interval | Cumulative Number Fraction | Cumulative Mass Fraction |
|---|---|---|---|---|
| 0.050 | 7486. | 0.6146 | 0.6146 | 0.0010 |
| 0.100 | 1194. | 0.0980 | 0.7126 | 0.0022 |
| 0.140 | 1126. | 0.0924 | 0.8051 | 0.0054 |
| 0.200 | 527. | 0.0433 | 0.8484 | 0.0098 |
| 0.280 | 646. | 0.0530 | 0.9014 | 0.0245 |
| 0.400 | 579. | 0.0475 | 0.9490 | 0.0628 |
| 0.560 | 301. | 0.0247 | 0.9736 | 0.1176 |
| 0.760 | 155. | 0.0127 | 0.9864 | 0.1881 |
| 1.110 | 81. | 0.0066 | 0.9930 | 0.2998 |
| 1.540 | 65. | 0.0053 | 0.9984 | 0.5457 |
| 2.160 | 15. | 0.0012 | 0.9996 | 0.7022 |
| 3.020 | 2. | 0.0002 | 0.9998 | 0.7593 |
| 4.260 | 3. | 0.0002 | 1.0000 | 0.9995 |

Total: 12180.

Table 1.4. Size Distributions for 8% v/v NaCl Aerosol

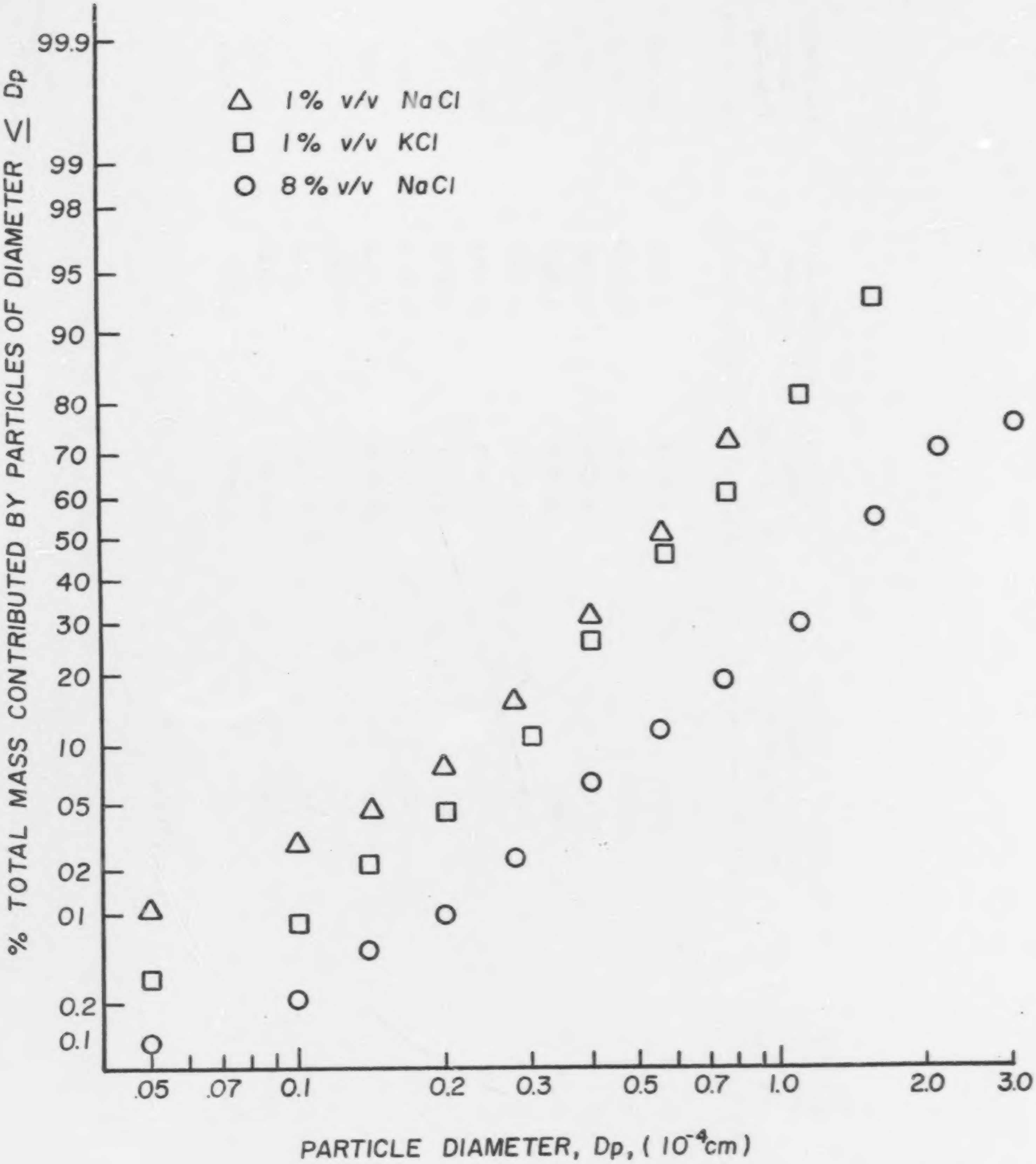

Figure 1.9. Cumulative Size Distribution for Aerosols Generated from 1% v/v NaCl, 1% v/v KCl, 8% v/v NaCl Aqueous Solutions.

not routed past the dilution orifice jet, which may have led to a preferential loss of the larger particles; finally, the flow paths in the two experiments were different. Comparison of the size of the aerosols in Table 1.5 leads to the following conclusions:

1. The particle sizes increased in the order: 1% v/v NaCl, 1% v/v KCl, 8% v/v NaCl.
2. The number mean diameters in the Cooper and Byers (1970) aerosols were consistently larger.
3. The mass mean diameters in the Cooper and Byers (1970) aerosols were larger for the 1% v/v aerosols and smaller for the 8% v/v NaCl aerosol.
4. The geometric standard deviation of the Cooper and Byers (1970) aerosols were larger in two of three cases.
5. The mass median diameters of the 1% v/v NaCl and 8% v/v NaCl aerosols were approximately 0.5 microns and 1.5 microns respectively in both experiments.

The aerosols sizing done in Cooper and Byers (1970) used 0.1 microns as the smallest size classification; this work used 0.05 microns thus, it is not surprising that the number means reported here are smaller, and they are probably more accurate. Also, more than 10,000 particles were counted for each size determination in this work in contrast to the approximately 2,000 counted per aerosol in the former. Since the percentage uncertainty of the count is inversely proportional to the square root of the number counted (Poisson statistics), the random error in the size

| | Aerosols Used in This Work | | | | Aerosols Used in Cooper and Byers (1970) | | | |
|---|---|---|---|---|---|---|---|---|
| Solution Nebulized | Number Mean Diameter (microns) | Mass Mean Diameter (microns) | Mass Median Diameter (microns) | Geometric Standard Deviation | Number Mean Diameter (microns) | Mass Mean Diameter (microns) | Mass Median Diameter (microns) | Geometric Standard Deviation |
| 8% v/v NaCl | 0.14 | 0.43 | 1.5 | 2.3 | 0.21 | 0.36 | 1.54 | 2.6 |
| 1% v/v NaCl | 0.08 | 0.18 | 0.55 | 2.2 | 0.16 | 0.22 | 0.45 | 2.0 |
| 1% v/v KCl | 0.13 | 0.28 | 0.62 | 2.1 | 0.20 | 0.32 | 1.26 | 2.6 |

Table 1.5. Size Parameters of Particles Formed By Nebulizing Salt Solutions with a Collison Atomizer.

determination herein should be less. All other things being equal, the particle diameters should vary with the cube root of the dissolved solids' volume fraction. Thus, the particles from the two 1% solutions should have equal size distributions upon being nebulized. The difference in size of the 1% v/v NaCl and KCl aerosols is unexpected.

Whitby and Peterson (1965) also produced aerosols from aqueous solutions in a Collison atomizer operated at a pressure of 40 $lb/in^2$, with an impactor which removed original droplets having diameters larger than 2 microns. Their measurements for 1% w/w (one percent by weight) uranine dye aerosol as analyzed by electron microscopy gave a number median diameter of 0.054 microns, a mass median of 0.103 microns and a geometric standard deviation of 1.41. Their impactor would have eliminated droplets which would have become dry particles 0.43 microns and larger and their concentration corresponds to 0.7% v/v uranine for uranine particles having a density about 1.3 to 1.5 $gm/cm^3$ (Sehmel, 1967), which would lead to a particle size $(0.7)^{1/3}$ = 90% of the 1% v/v aerosol size. From the number median of Whitby and Peterson and their geometric standard deviation one can, assuming a log-normal distribution, compute the number mean and mass mean diameters of their aerosol, using equations available in the literature (Herdan, 1960; Lapple, 1968). The concentration difference will contribute $(0.7)^{1/3}$ to the number mean and (0.7) to the mass mean differences.

Calculations from the data of Whitby and Peterson (1965), using formulas for relationships between log-normal parameters from Lapple (1968), show an inconsistency between the number median diameter ($D_{mo}$ in Lapple's notation), the mass median diameter ($D_{m3}$) and the geometrical standard deviation ($\sigma$), which should be related as:

$$D_{mx} = D_{my} \exp \, [(x-y) \ln^2 \sigma ],$$

giving

$$D_{m3} = D_{mo} \exp \, [(3-0)(\ln 1.41)^2]$$

Their measured mass median was 0.103 microns; that from the equation above is 0.076 microns. This deviation may be caused by approximating as log-normal a distribution which is not quite log-normal. Their number mean (based on $D_{mo}$ and $\sigma$) is computed to have been 0.057 microns. Their mass mean (based on $D_{m3}$ and $\sigma$) is 0.097 microns (which should be raised by factor $1/(0.7)^{1/3}$ to be compared with 1% v/v case). Adjusted for concentration of 1% v/v, the size distribution measured by Whitby and Peterson corresponded to number mean diameter of 0.06 microns, mass mean diameter of 0.14 microns, mass median diameter of 0.15 microns and geometric standard deviation of 1.41. They sized particles as small as 0.02 microns. An impactor which removed 0.4 micron diameter particles as theirs did would have removed 74% and 69% by mass of our 1% v/v KCl, 1% v/v NaCl respectively. Thus it is not surprising that the concentration-adjusted mass mean and mass median diameters of their aerosol were smaller than those here. (The "mass median diameter" for our 1% v/v aerosols KCl, NaCl would be 0.28 microns if only the aerosol particles smaller than 0.4 microns are considered.) Incidentally, Whitby and Peterson found their un-neutralized 1% v/v uranine aerosol to have an average of 0.75 electronic charges (±) per particle, which serves as an estimate for the charges on the aerosols in this work.

In all size intervals but the smallest, the 1% v/v NaCl has a smaller percentage of its total number present than does the 1% v/v KCl and in all intervals the difference is statistically significant, so that the difference in their size distributions is not due to random counting errors.

Green and Lane (1964) gave a formula for the "mean volume/surface diameter" of particles generated by atomization, which they attribute to Nukiyama and Tanasawa. The formula indicates that the fluid density, surface tension and viscosity affect particle size; the dependence of droplet size on these variables is to powers of absolute value of 1/2 or less. We do not know how different these properties are for the KCl and NaCl solutions, though differences greater than a few percent seem unlikely. Inertial impaction and gravitational settling would be dependent on particle density (see Fuchs 1964 for more detail) so that these loss mechanisms might be significantly different for KCl (density of 1.98 gm/cm$^3$) and NaCl (density of 2.16 gm/cm$^3$). The density difference is 9% and the density dependence is approximately linear for both mechanisms. Brownian diffusion, another loss mechanism, is not density dependent. Surface properties of the two salts may play a part in electrostatic loss mechanisms.

From the scatter in the data for the cumulative mass distribution curves in Figure 1.9,the difference in size between the two 1% aerosols seems real, and the two 1% v/v aerosols are more like each other in size than either is similar to the 8% v/v NaCl aerosol. Hence, the aerosols produced from 1% v/v solutions are estimated to have mass mean diameters of 0.23 microns, mass median diameters of 0.58 microns and geometric standard deviations of 2.2.

## B. Dependence of Backscattering on Particle Volume

Some recent work has maintained that total scattering by atmospheric aerosols is proportional to their volume concentrations (Charlson et al., 1967; Noll et al., 1968); other workers have found it related to the ratio of the mean volume diameter to the mean surface diameter, the third and second moments of the size distribution (Dobbins and Jizmagian, 1966). Cooper and Byers (1970) found that aerosols similar to those used here had backscattering which was nearly proportional to the volume of particles per volume of air, for non-absorbing particles with indices of refraction near 1.5.

The data in Tables 1.6 and 1.7 allow us to make some comparison between size dependence relationships. The average net dry scattering is the time average of the scattering at humidities below the change of phase, and is in terms of photomultiplier current. The averages were done by taking the areas under strip chart recordings of scattering versus time, and are probably accurate to within ±10%. The weighing errors are discussed in Appendix 4. They are about $0.15 \times 10^{-3}$ gm, or less than 5%. There were some variations in flow rate, and we estimate the error in net flow volume to be 10 to 20%, so that the accuracy to be expected for the dry scattering per unit aerosol volume is about ±20%. The results are consistent with the hypothesis that the laser light backscattering for these aerosols is proportional to the volume fraction of the aerosol doing the backscattering; the results do not seem consistent with an extension of the third-to-second moment hypothesis. This ratio changed little (1.41 to 1.68 range) but the scattering changed greatly (1.0 to 9.2 range). If it is

Table 1.6. Net Scattering Per Unit Particle Volume for Several Aerosols at Low Humidities (less than 40% RH).

| Aerosol | Net Mass ($10^{-3}$ gm) | Total Flow Volume ($m^3$) | Mass Concentration ($10^{-6}$ gm/$m^3$) | Material Density (gm/$cm^3$) | Average Dry Scattering ($10^{-7}$ A) | Average Dry Scattering Per Particle Volume ($10^{-3}$ A/$cm^3$) | Ratio of Third to Second Moment of Size Distribution ($d_o$, $10^{-4}$ cm) |
|---|---|---|---|---|---|---|---|
| 1% v/v KCl | 6.8 | 15 | 450 | 1.98 | 1.0 | 0.44 | 1.41 |
| 1% v/v NaCl | 9.0 | 11.3 | 800 | 2.16 | 2.2 | 0.61 | 1.55 |
| 1% v/v Methylene Blue | 3.6 | 6.8 | 540 | 1.3[a] | 2.8 | 0.67 | ---- |
| 8% v/v NaCl | 47.4 | 13.8 | 3400 | 2.16 | 9.2 | 0.57 | 1.68 |

[a] Based on work of Sehmel (1967).

Table 1.7. Average Dry Scattering per Average of the First, Second and Third Powers of the Diameters.

| Aerosol | $\overline{D_p}$ ($10^{-4}$ cm) | $\overline{D_p^2}$ [a] ($10^{-10}$ cm$^2$) | $\overline{D_p^3}$ [a] ($10^{-14}$ cm$^3$) | $d_o$ [b] | Average Dry Scattering (A.D.S.) ($10^{-7}$ A) | Ratio of A.D.S. to $\overline{D_p}$ ($10^{-3}$A/cm) | Ratio of A.D.S. to $\overline{D_p^2}$ ($10^{3}$A/cm$^2$) | Ratio of A.D.S. to $\overline{D_p^3}$ ($10^{7}$A/cm$^3$) | Ratio of A.D.S. to $d_o$ ($10^{-7}$A) |
|---|---|---|---|---|---|---|---|---|---|
| 1% v/v NaCl | 0.077 | 1.37 | 0.59 | 1.55 | 2.2 | 2.8 | 1.6 | 3.7 | 1.4 |
| 1% v/v KCl | 0.131 | 3.9 | 2.2 | 1.41 | 1.0 | 7.6 | 0.26 | 0.45 | 0.71 |
| 8% v/v NaCl | 0.139 | 6.5 | 7.9 | 1.68 | 9.2 | 66. | 1.4 | 1.16 | 5.5 |

[a] $$\overline{D_p^n} = \sum_{i=1}^{N} (D_p^n)_i / N$$

[b] $$d_o = \left(\overline{D_p^3}\right)^{1/3} \Big/ \left(\overline{D_p^2}\right)^{1/2}$$

assumed that the Collison atomizer output was roughly constant in number for the various aerosols, then differences in scattering for aerosols of the same composition (e.g. NaCl) would be due to differences in size.

Although not within the estimated experimental error,the values of scattering of light per unit volume of particle as shown in the next to the last column on Table 1.6 are quite similar. This similarity is striking especially when one considers both the 1% v/v aerosols and the difference in chemical composition and optical properties between the colorless, cubic NaCl and KCl crystals and the spherical, methylene blue particles.

What do Tables 1.6 and 1.7 indicate? If the number of particles per second generated by the atomizer in these tests were constant, then the differences in scattering would be due to particle size, shape, and composition. If the generation rate were constant, the size dependence of backscattering could be tested by dividing the net scattering by the various means--mean diameter, mean surface area diameter $\left(\overline{D_p^{\,2}}\right)^{1/2}$, mean volume diameter $\left(\overline{D_p^{\,3}}\right)^{1/3}$, and ratio of volume mean to surface mean ($d_o$)--and determining which mean gave a ratio which was least dependent on the aerosol studied. This is done in Table 1.7. The results of these calculations make it difficult to choose which of the last three of the four means mentioned is more fitting. Recall that this table is based on the assumption of constant particle number from the atomizer. If the particle generation rate were constant and if particle losses were negligible, the mass concentrations divided by particle material density (in other words, the volume concentrations) should be proportional to the original volume concentrations in the atomizer. Such a calculation gives volume concentrations of 230, 370, 420 x $10^{-6}$ for the 1% v/v KCl, NaCl, and methylene blue aerosols respectively and 1570 x $10^{-6}$ for the 8% v/v NaCl. The KCl aerosol is lower than the other two 1% v/v aerosols, which may explain the consistently low values for the KCl scattering in Table 1.2. The volume concentration of the 8% v/v NaCl is not 8 times greater than that of the 1% NaCl. This indicates that the number concentration of the 8% v/v NaCl was lower than that of the 1% v/v NaCl by about a factor of two by the time its scattering was measured at the scattering chamber. Assuming that the number concentration of both the 1% KCl and 8% NaCl was not the same as that of the 1% v/v NaCl, as indicated by the weight determinations in Table 1.6, then the ratios in the last three columns for these two aerosols should be doubled. The numbers which result have the least extreme ratios for the comparison based on the mean volume. On the other hand, the data in Table 1.7 support the hypothesis that the scattering for these sizes was proportional to volume fraction of aerosol without relying on assumptions about constant generation or negligible losses.

## C. Results of Subsidiary Tests

A variety of tests were made to check for possible problems; other tests were made to serve as controls. Both types are described here in brief.

At the experimental flow rates, the scattering chamber responded to a step change in concentration at its inlet by reaching greater than 90% of the ultimate scattering value in less than two minutes.

Measurements with a Sinclair-Phoenix (forward-scattering) Aerosol Photometer showed that less than 5% of the particles (as measured by their dry forward scattering) at low relative humidity and less than 15% of the particles (also as measured by their dry scattering) at 85% RH were lost traversing the scattering chamber for an 8% v/v NaCl aerosol which was generated in such a way that it did intercept the jet of air from the dilution orifice; this aerosol had size parameters between those of the 1% v/v NaCl and those of the 8% v/v NaCl aerosols which bypassed the dilution orifice.

The intent of this work was to measure the backscattering from the specific aerosol particles, not scattering from molecules in the carrier gas, nor from contaminants, nor scattering from the walls of the scattering chamber. The control test deemed most appropriate as the baseline was the measurement of the scattering from the carrier gas (air) after it had been filtered by an absolute filter (Gelman Type E glass fiber filter). Near the beginning of this work room air was sampled, humidified, or dried as with an aerosol and drawn through a filter into the scattering chamber (it had been ascertained that there were no leaks and that the chamber was not sensitive to the small change in pressure involved). With a dark current (laser beam blocked from chamber) of 0.31 ±0.01 x $10^{-7}$ A, the following net current was observed:

0.23 x $10^{-7}$ A at 13% RH,

0.25 x $10^{-7}$ A at 80% RH,

0.25 x $10^{-7}$ A at 85% RH.

This same test was repeated midway through this section's work, and with a dark current of 0.25 x $10^{-7}$ A the following net current was recorded:

0.10 x $10^{-7}$ A at 8% RH,

0.10 x $10^{-7}$ A at 49% RH,

0.13 x $10^{-7}$ A at 78% RH,

0.11 x $10^{-7}$ A at 14% RH.

Finally, the same test was repeated near the end of this section's work. The net current (0.35 x $10^{-7}$ A dark current subtracted) was:

0.06 x $10^{-7}$ A at 28% RH,

0.09 x $10^{-7}$ A at 79% RH,

0.09 x $10^{-7}$ A at 14% RH,

for tests done in that order. Experience indicated that the greatest source of change in the net current for such control tests came from minor imperfections in optical alignment and from the use of different glass covers on the laser inlet hole, a microscope slide early in the work and microscope cover glasses later. The ten control tests above were specifically designed to test for humidity dependence of the baseline, and they indicate that changes in the second decimal place ($10^{-9}$ A) could be expected. Except for the control tests, the "net scattering" reported in this work is the scattering above that which was found for filtered air; the filtered air scattering was measured several times for each aerosol (usually at a low relative humidity) during the scattering versus humidity tests of the various aerosols. The air in the laboratory gave net current of about $0.15 \times 10^{-7}$ A when it was sampled (undiluted, thus at its ambient humidity, about 50% RH) and the salt aerosols averaged from $1 \times 10^{-7}$ A to $9 \times 10^{-7}$ A net current at low relative humidities, making the above changes with humidity of the filtered air readings negligible (i.e., a few percent or less).

The light scattering from polystyrene latex aerosols was not expected to change appreciably with changes in relative humidity (Lundgren and Cooper, 1969). The following readings were obtained from nebulizing a suspension (0.1 $cm^3$ solids in 200 $cm^3$ water) of 0.71 micron diameter polystyrene latex spheres (prepared and sized by Dow Chemical, Midland, Michigan). Their net current was $0.69 \times 10^{-7}$ A and the scattering ratios (scattering at specified relative humidity divided by scattering at less than 25% RH) were:

| Relative Humidity | Scattering Ratio |
|---|---|
| 21% RH | 1.00 ± 0.02 |
| 32% RH | 1.00 |
| 34% RH | 1.02 |
| 43% RH | 1.00 |
| 52% RH | 1.03 |
| 75% RH | 1.02 |
| 75% RH | 1.03 |
| 80% RH | 1.05 |
| 84% RH | 1.06 |
| 84.5% RH | 1.08 |

The slight increase at higher humidities could be due to the humidification of a small amount of scattering impurities, either from the emulsifier in the polystyrene latex suspension or from leakage or from contamination of the system from other tests.

The response of our equipment was tested with an aerosol of 0.80 micron diameter polystyrene beads. The beads were atomized by a Collison atomizer, with one orifice, at 30 $lb/in^2$. They were nebulized from a solution which was less than 1 part per thousand polystyrene beads in water, which gave <5% doublets and <1% triplets, by computation from Poisson statistics. They were diluted with clean, dry air. The results of this test were:

| | |
|---|---|
| Photomultiplier dark current | $0.32 \times 10^{-7}$ A |
| Filtered air sample | $0.41 \times 10^{-7}$ A |
| Collison atomizer (filtered) air supply | $0.41 \times 10^{-7}$ A |
| Filtered water nebulized | $(0.44 \pm .01) \times 10^{-7}$ A |
| 0.80 micron Polystyrene latex nebulized | $(0.87 \pm .02) \times 10^{-7}$ A |
| Net Scattering: | $(0.46 \pm .02) \times 10^{-7}$ A |
| Estimated number of particles per $cm^3$: | $0.6 \times 10^2$, by filter change in weight;<br>$0.9 \times 10^2$, by filter count |

The estimated random error in the weight determination is ±25% (see Appendix 4), that of the count, ±10%.

For tests with the 0.71 and 0.80 micron monodisperse polystyrene latex particles, the dilution flow rate in the mixing chamber was reduced to $0.23 \times 10^3 cm^3$/sec($0.5\ ft^3$/min). The test for the relative humidity dependence (0.71 micron) required dilution and humidification of the aerosol; the other test (0.80 micron) did not.

To raise the final relative humidity of the aerosols to 85% RH and above, two steps were required. In the first step, the aerosols were passed through the prehumidifier (see Figure 1.3) after leaving the holding chamber. Possible increases in aerosol losses due to the prehumidifier were tested with both the 1% v/v NaCl aerosol and the 8% v/v NaCl aerosol. The 1% v/v NaCl aerosol was passed through the prehumidifier, then its scattering was measured at less than 30% RH. Differences of 0%, 1%, 3%, 2% in scattering were found by alternately passing through and by-passing the prehumidifier. It was concluded that the prehumidifier did not contribute significantly to losses for the 1% v/v aerosols. The same tests for 8% v/v NaCl aerosol, however, gave scattering losses of 15% and 16%, so that the experimental values for the scattering for 8% v/v aerosols were increased by 16% before being plotted as the "prehumidified" data points in Figure 1.15 (p. 78), for those measurements for which the pre-humidifier was used.

The possibility was considered that at increased humidity some of the scattered light would be absorbed by water molecules. Although there is a water vapor absorption line near the wavelength of the pulsed ruby laser (6943Å), water vapor absorption was not found to be a problem for the continuous wave He-Ne laser, which operates at a shorter wavelength (6329Å). Experimental evidence for this is that for polystyrene aerosols there was no decrease in light back-scattering with increasing humidity nor was there for the salt aerosols below their phase change humidities, which would be expected if increasing the humidity resulted in increasing the concentration of an absorbing species. Using filtered air, no decreases were observed in the backscattering (presumably partly from the chamber walls) when the humidity was increased. It is concluded that absorption of light by water vapor was negligible.

As an experimental measure of the greater deposition (loss) of particles at high humidities than at low humidities, the particles were dried after exiting from the scattering chamber and the dry, forward-direction, white-light scattering was measured with a Sinclair-Phoenix Aerosol Photometer. Connected to the scattering chamber outlet was 3 meters of 0.64 cm I.D. rubber tubing, which was followed by a two-quart (about $2 \times 10^3$ $cm^3$) metal can wrapped with heating tape, then a thermometer and finally the Sinclair-Phoenix Aerosol Photometer. The relative humidity in the room was about 50%. The flow through the scattering chamber was the usual 220 $cm^3$/sec.

Table 1.8 lists the aerosols tested, their humidities and scattering in both the scattering chamber and aerosol photometer, the scattering ratios (wet to dry scattering), and the ratios of the forward scattering (aerosol photometer) measurements to the backscattering measurements. The object of the experiment whose results are in Table 1.8 was to get an experimental estimate of the increase in particle losses at high relative humidities.

Table 1.8. Backscattering and Forward Scattering for Several Aerosols at Different Humidities.

| Aerosol | Scattering Chamber Relative Humidity | Net Back-Scattering ($10^{-7}$ A) | Aerosol Photometer Relative Humidity[a] | Forward Scattering (Arbitrary Aerosol Photometer Units) | Scattering Ratio[b] | | Ratio of Measurements of Dry Forward Scattering to Dry Backscattering (Arbitrary Units) |
|---|---|---|---|---|---|---|---|
| | | | | | Back-Scattering | Forward Scattering | |
| 1% v/v Uranine Dye | 7% RH | 10.2 | ~10% RH | 37.0 ± 0.3 | - | - | 3.6 |
| | 82% RH | 8.7 | 43% RH | 44.0 | 0.85 | 1.27 | - |
| | 8% RH | 10.2 | ~10% RH | 34.5 | - | - | 3.4 |
| 1% v/v NaCl | 6% RH | 1.04 | ~10% RH | 35.0 | - | - | 34 |
| | 84% RH | 4.4 | 45% RH | 32.2 | 4.0 | 0.92 | - |
| | 12% RH | 1.14 | ~10% RH | 35.0 | - | - | 31 |
| 1% v/v Methylene Blue | 5% RH | 1.25 | ~10% RH | 19.0 | - | - | 15 |
| | 84% RH | 1.30 | 43% RH | 25.5 | 1.06 | 1.28 | - |
| | 10% RH | 1.20 | ~10% RH | 21.0 | - | - | 18 |

[a] Estimated from the temperature difference between the temperature at the inlets of the scattering chamber and of the Sinclair-Phoenix photometer, which difference was usually 11°C.

[b] Scattering at the higher humidity divided by the averages of the scattering at the lower humidities.

If the NaCl particles actually dried in the heated metal can (the 45% RH is near the change-of-phase humidity for decreasing humidity, as can be seen from Figure 1.14 (p.77 )), then the value 0.92 is a measure of the fraction of the humidified aerosol which reached the aerosol photometer compared with the originally dry aerosol which reached the photometer. The losses (in terms of light scattering) were on the order of 8%. From an earlier study of the dependence of forward scattering on humidity using the aerosol photometer (Lundgren and Cooper, 1969) no increase in scattering was expected for the methylene blue aerosol at 45% RH when its humidity has been raised to that value, but that work gave no information about the behavior of methylene blue aerosols whose humidity decreased to that value. Similarly, the same study indicated that the uranine forward scattering at 45% RH would be 1.5 times that at low relative humidity for increasing humidity, in which case (if it is the same for decreasing humidity) only (1.28/1.5) or 85% of the change has been measured, and 15% lost. This loss may partially explain the surprising decrease in backscattering with increasing relative humidity shown in Figure 1.11 (p. 74 ) for the uranine aerosol.

Although the ratios of forward, white-light scattering to backward, red-light scattering as shown in Table 1.8 do not tell the actual ratio of the scattered intensities because the forward and backward scattering measurements were in different units, the variations of the ratio from aerosol to aerosol are illuminating. The ratio for the methylene blue aerosol was half that for the NaCl aerosol and the ratio for the uranine aerosol was a tenth of that for the NaCl. The dry uranine aerosol scattered much more red light backward (it is orange-red in appearance when dry) than did the NaCl and methylene blue aerosols. The number concentrations and size distributions of these aerosols should have been similar to that of the uranine and the forward scattering of white light from them was not nearly so different from uranine's as was their backscattering.

### D. Backscattering vs Relative Humidity

The results of the experimental determinations of backscattering as a function of relative humidity are contained in the graphs in this section, Figures 1.10 to 1.15 (p. 73-78). "Backscattering ratio" is the ratio of the scattering of the aerosol at the indicated relative humidity to the scattering at a very low humidity (~10% RH) and is used to allow comparisons between aerosols scattering different amounts of light.

The backscattering ratio for 0.71 micron polystyrene latex beads test aerosol was less than 1.10 at 84% RH.

Other test aerosols commonly used are the dyes uranine and methylene blue; their responses to change in humidity are given in Figures 1.10 (p. 73) and 1.11 (p. 74). Earlier work (Lundgren and Cooper, 1969) done on the forward scattering of white light by similar uranine dye and methylene blue dye aerosols showed a linear increase in scattering versus RH for the uranine from 1.0 at 10% RH to 1.8 at 80% RH, whereas under the present conditions there was a decrease in backscattering of monochromatic light. The earlier work also showed an increase in scattering for methylene blue from 1.0 at 60% RH and below to 1.3 at 80% RH; under the present conditions, the backscattering from methylene blue remained constant up to 65% RH, increased to 1.26 at 76% RH, then decreased to 1.07 at 85%. Some aerosols become more compact due to capillary forces as humidity increases (Fuchs, 1964) and thus smaller. The behavior of the uranine and methylene blue aerosols is unexplainable although an increase in particle loss at higher humidities could account for decreased scattering from that which would be expected from the forward scattering observations. Microscopic observations of uranine particles have shown that they do increase in size with increasing relative humidity.

The behavior of the hygroscopic salt aerosols NaBr, NaCl and KCl is illustrated in the graphs of Figures 1.12 to 1.15 (p. 75-78 ). The theory of the growth of hygroscopic particles was presented quite clearly in the work of Orr, et al. (1958). Their description is paraphrased in the following paragraph.

At low humidities, hygroscopic particles adsorb on their surfaces a thin layer of water a few molecules thick or less. As the humidity is increased, the humidity is reached at which the particles become droplets of a concentration which is such as to be in equilibrium with the water vapor (relative humidity) present; these droplets continue to grow as the relative humidity is increased. They contract if the humidity is decreased. If the humidity continues to decrease, the droplets become solids again, this change of phase taking place at a lower humidity than that at which they changed phase when the humidity was increasing. Additionally, the change of phase humidity depends on particle size, smaller particles changing phase at lower relative humidities.

In Appendix 3 the humidities at which the change of phase occurs for increasing humidity for salt particles so large that the size dependence is negligible are listed.

Although the thin film of water on a particle exists even at low humidities, no significant changes were measured in the scattering from the KCl and NaCl aerosols for humidities from 10% RH to 60% RH when they were undergoing increasing humidity. A condition of increasing humidity occurred when the aerosols were not "pre-humidified" (this involved passing them through a 1/2-liter jar one-quarter filled with water). The theory for scattering from concentric spheres of different refractive indices has been worked out (Aden and Kerker, 1951) and some computations have been made (Kerker et al., 1962). No change in scattering occurred at these lower humidities. Since the exact scattering computations are rather difficult, we will merely demonstrate how small a size change is involved in the formation of this water film and use this as the explanation for the observation of no appreciable change in scattering for different low humidities.

Orr et al. (1958) gave the following equation for the thickness of an adsorbed molecular film at a given vapor pressure of the films' constituent:

$$V/V_m = C'(P/P_o)/(1-P/P_o)\ (1+(C'-1)P/P_o)$$

V = volume of gas adsorbed at P, T

P = partial pressure of adsorbed gas

$P_o$ = saturation vapor pressure of adsorbed gas

T = temperature of system

$V_m$ = volume occupied by shell one molecule thick,

$C' = \exp((E_1 - E_L)/RT)$

$E_1$ = heat of adsorption of gas in first layer

$E_L$ = heat of liquification of gas

R = gas constant, $8.31 \times 10^7$ erg/mole-°K.

Each water molecule occupies about 10.8 $\mathring{A}^2$ (Orr et al., 1958) and $E_1 - E_L$ can be estimated by the surface energy of NaCl, 276 ergs/cm$^2$. From this point, the following estimate can be made

$$C' = \exp[(6.02 \times 10^{23} \text{ molecules/mole}) \times (10.8 \times 10^{-16} \text{ cm}^2/\text{molecule}) \times (276 \text{ ergs/cm}^2)/(8.31 \times 10^7 \text{ ergs/mole-}^\circ\text{K}) \times (298^\circ\text{K})]$$

$$C' = 1.38 \times 10^3.$$

Thus $C' \gg 1$, and for RH = $P/P_o > 10\%$, $(C'-1)\,P/P_o \gg 1$; therefore,

$$V/V_m \doteq 1/(1-RH)$$

where RH is the relative humidity.

For relative humidity of 30%, this predicts a water shell 1.4 molecules thick or about $5 \times 10^{-8}$ cm thick, for NaCl. This would be an increase of only one part in three hundred in diameter for a particle with a diameter of 0.3 microns.

From the graphs (Figures 1.12 to 1.15, p.73-78) of backscattering ratio versus relative humidity for the four salt aerosols tested (1% v/v NaBr, KCl, NaCl, and 8% v/v NaCl) the following--under conditions in which the humidity was increasing (not pre-humidified) or decreasing (pre-humidified)--are noted:

1. Each aerosol exhibited increased backscattering for humidities exceeding a critical humidity.
2. This critical humidity, which is associated with a change of phase from solid particle to liquid droplet, was different for each salt species, was lower in each case than the values given in Appendix 3 and was in the same order as given there.

3. Using the arbitrary criterion for the "critical humidity" for these aerosols being that humidity at which, for increasing humidity, their scattering ratio equals 2.0 (twice as much scattering at that humidity than at 10% RH), we get the following critical humidities:

| | |
|---|---|
| 1% v/v KCl | 75 ± 3% RH |
| 1% v/v NaCl | 68 ± 3% RH |
| 1% v/v NaBr | 53 ± 3% RH |
| 8% v/v NaCl | 71 ± 3% RH |

   At these critical humidities, enough of the aerosol particles had changed phase (and had thus grown in size) to double the backscattering. The error estimates are based on combining the uncertainty of the accuracy of the humidity measurements (±1.5% RH) with the uncertainty from the scatter of the data (about± 2.5% RH) by taking square root of the sum of their squares.

4. The backscattering ratio for 1% v/v NaCl was greater than that for 1% v/v NaBr at all humidities above the change of phase humidity for NaCl.

5. The backscattering ratio for 8% v/v NaCl was indistinquishable from that of 1% v/v NaCl for all relative humidities tested above 75%, the change of phase humidity for bulk NaCl. Thus the difference in particle size of these two aerosols was reflected by different critical humidities, as expected, but it did not measurably change their scattering behavior above the critical humidity.

6. Some fraction of the KCl and NaCl aerosols which passed through the pre-humidifier became droplets, displaying the hysteresis

noted in Orr et al. (1958); they stayed droplets below the critical humidity. This is an interesting result, because the test aerosols were run through the pre-humidifier alone at the usual flow rate (0.09 $ft^3$/min or 2.5 x $10^3$ $cm^3$/min) and humidities of 62% RH for 8% NaCl and 59% RH for 1% v/v NaCl were measured. These humidities are below the phase change humidities, so that phase changes were not expected. A test at 20% RH with 8% v/v NaCl indicated that a loss of 16% of the aerosol dry scattering was incurred by adding the pre-humidifier. Therefore the "prehumidifier" values were raised by 16% in Figure 1.15 (p. 78 ).

7. Neither the 1% nor 8% NaCl aerosol displayed the small decrease (about 10%) in light scattering noticed in the forward direction for white light in previous work (Lundgren and Cooper, 1968).
8. In comparison with the results of Lundgren and Cooper (1968), who also used aerosols generated from 1% v/v solutions in a Collison atomizer, the laser light backscattering ratio for the NaCl aerosols at 80% RH (a ratio of 3.6), is considerably less than that for forward scattering of white light at 80% RH (a ratio of 9), suggesting that under some circumstances lidar measurements will be less affected by humidity interference than would measurements by devices using the forward scattering of white light.

9. From the graphs presented in Orr et al.(1958), the following change-of-phase humidities for particles having the indicated diameters are expected:

   83% RH for KCl particles of diameter 0.1 microns
   82% RH for KCl particles of diameter 0.06 microns
   73% RH for NaCl particles of diameter 0.1 microns
   68.5% RH for NaCl particles of diameter 0.06 microns

   At the change of phase, the volume of a hygroscopic particle increases to approximately 1/(1-RH) times its original volume (Neiburger and Wurtele, 1949). These particles would, therefore, have volume increases of three to six times their original volume, or diameter increases proportional to the cube roots of three to six times the original diameters. That is, this indicates that at change of phase to droplets they would have diameter increases of 50 to 80%, making the 0.1 micron particles nearly as large as the mass mean diameters of the dry 1% v/v aerosols. KCl particles having diameters of 0.03 microns would change phase at 78% RH. It is concluded that the numerous particles smaller than the mass mean diameter and smaller still than the mass median diameter make a significant contribution to the backscattering versus relative humidity of these aerosols.

10. Those NaCl particles which changed phase in the prehumidifier changed back to solid particles at relative humidities below 40% RH and those KCl particles which had changed to droplets changed back at relative humidities below 55% RH.

## V. Discussion

The history of the aerosol particles was as follows: droplets were generated by the atomizer and dried in the mixing chamber when mixed with clean, dry air. Some particles deposited in the mixing chamber; more were lost going to and passing through the holding chamber. The remainder were then humidified or kept in a dry state by the addition of air of controlled humidity. When the particles reached the RH chamber, they had on the average 1.3 minutes to come into equilibrium with the water vapor present, which was almost always at a higher relative humidity than was the air in the mixing chamber. In coming to equilibrium with the humidity, the particles would either adsorb a surface layer of water a few molecules or less thick, or they would change phase, becoming droplets, based on the analysis and experimental work of Orr et al. (1958). The exceptions to this description were those aerosols which went through the pre-humidifier. Although the relative humidity of these aerosols was measured to be 55-60% RH in two tests, these aerosols behaved as though at least some of the particles had changed to droplets, even though for NaCl and KCl the resulting humidity (55-60% RH) was below the critical humidity for change of phase with increasing humidity. Two explanations are possible: 1) Only the smallest particles change phase, in keeping with the fact that small particles change phase at somewhat lower humidities than the critical change of phase humidity for the bulk material. A 0.04 micron NaCl cube would change phase at 68% RH, but a 1 micron NaCl cube changes at 75% RH, the bulk critical relative humidity. 2) There are humidity gradients in the pre-humidifier, and some or all of the particles experience humidities high enough to cause them to change phase.

If only some of the particles changed into droplets in the pre-humidifier, it should be reflected in an abrupt change in the scattering for the pre-humidified aerosols near the critical humidity as the dry particles changed phase; this is not apparent from the data.

Finally, the dry particles or the droplets flowed to the scattering chamber, where the amount of backscattering they caused was measured. While traversing the chamber, some would be deposited, and the rest would leave through the exhaust where they were caught for weight analysis or for size distribution analysis.

In terms of light scattering, the hygroscopic particles were observed in one of three possible states: 1) the very dry condition, in which the scattering was that from crystals (colorless, cubic) of NaCl, NaBr, KCl, or dry dyestuff (roughly spherical); 2) an intermediate condition for the salts in which they had adsorbed a few molecular layers or less of water on their surfaces, which condition might have led to perceptible changes in scattering (Aden and Kerker, 1951), and in fact these changes may have been observed before for NaCl and forward light scattering (Lundgren and Cooper, 1969), but were not apparent in the present work; and 3) the droplet condition, in which the particle has become a droplet a suspension or solution, having a different index of refraction (between that of the salt or dye and that of water) and a different density. In going from dry particle to droplet, the change in size, shape and index of refraction would alter its light-scattering behavior. The change in size, shape and density would also alter its aerodynamic behavior.

Although the change in scattering due to changes in size, shape and index of refraction cannot be computed, the growth of the aerosol particles on change of phase is calculated and the effect on their aerodynamic behavior is shown.

Once the dry particle has changed phase and become a droplet, its volume is inversely proportional to (1-RH) where RH is the relative humidity. Any NaCl particle changing phase at 70% RH would thus have a volume 3.3 times the original volume. A NaCl particle changing phase at 75% RH would have a volume 4 times the original.

Let a prime denote characteristics of the droplet; unprimed characteristics are those of the dry particle. The subscript s refers to the salt (or dye). The subscript w refers to water.

The droplet diameter is

$$D_p' = D_p/(1-RH)^{1/3}.$$

If the scattering depended only on the particle diameter to the power n, it would depend on the relative humidity as $[1/(1-RH)^{1/3}]^n$. For changes of phase at 75% RH and 80% RH, this would mean a change by the following factors:

| | 75% RH | 80% RH |
|---|---|---|
| n | $(D_p'/D_p)^n$ | $(D_p'/D_p)^n$ |
| 1 | 1.59 | 1.71 |
| 2 | 2.53 | 2.93 |
| 3 | 4.00 | 5.00 |
| 4 | 6.37 | 8.6 |
| 5 | 10.1 | 14.6 |
| 6 | 16.0 | 25.0 |

Work done by Pueschell et al. (1969) with artificial aerosols generated from an aqueous solution of 3% w/w NaCl by vigorous bubbling gave a scattering increase of 3.1 at 75% RH in comparison to the dry (40% RH) scattering as measured by their "integrating nephelometer." The integrating nephelometer sums the scattering over the angular range from 8° to 170° from the forward direction. Lundgren and Cooper (1969), using NaCl aerosols similar to the 1% v/v NaCl used here, found an increase in forward scattering of about 7 at 75% RH, for white light. The backscattering ratio for the 1% v/v NaCl aerosol used here was 3.5 at 75% RH. Scattering is dependent on angle and wavelength. It is quite sensitive to the humidity and small humidity errors can lead to larger percentage errors in the ratio of wet to dry scattering.

When the dry salt particle of density $\rho_s$ changes phase, the droplet density becomes:

$$\rho_p' = \rho_s\ (1-RH)+\rho_w(RH)$$

A particle's aerodynamic properties are conveniently characterized by the particle "relaxation time" ($\tau$) in the medium. For spherical particles moving with Stokes law resistance in a fluid, $\tau$ is given by Fuchs (1964) as

$$\tau = C(1/18)\ \rho_p\ D_p^2/\mu$$

where $C \doteq 1 + (0.16 \times 10^{-4})/D_p$, at STP, and is the Cunningham correction factor in air. The terminal velocity of a particle under gravitational acceleration (g) is $g\tau$ and the distance a particle having initial velocity $V_o$ will go in a stationary medium before stopping is $V_o\tau$. After a change of phase from solid to droplet, the relaxation time changes from $\tau$ to $\tau'$, where $\tau'$is given by

$$\frac{\tau'}{\tau} = \left[\frac{(1-RH)\rho_s + H\rho_w}{\rho_s}\right] \frac{C'}{C} \left(\frac{D_p'}{D_p}\right)^2$$

or

$$\frac{\tau'}{\tau} = \left[\frac{(1-RH)\rho_s + H\rho_w}{\rho_s}\right] \frac{(D_p' + 0.16\ \mu m)}{(D_p + 0.16\ \mu m)} \qquad \left(\frac{D_p'}{D_p}\right)$$

For NaCl with dry $D_p$ = 0.4 microns, at 80% RH, $D_p'$ = 0.68 microns and the ratio in brackets becomes 0.57. For this case, $\tau'/\tau$ = (0.57)(1.71)(0.84/0.56) = 1.5. The decrease in density has somewhat offset the increase in size.

There are several reasons why the deposition of the particles (and thus their relaxation times) is of concern. Deposition which occurred in the scattering chamber or in the tubing preceding the filter which caught the weight samples or preceding the sampler which captured the particles for electron microscope, would result in a sample size distribution different from the size distribution which scattered the light. Since the tubing to the filter and the tubing to the sampler were kept short and any bends made gradual, the sedimentation losses in the scattering chamber are assumed to predominate. If losses of the humidified aerosols were significantly greater than those of the dry aerosols, then the ratio of their scattering would be biased. The losses could also make the size distributions different from those which other experimenters using the same atomizer but having different losses have observed.

The ratio of the final number concentration (n) to the initial number concentration ($n_o$) due to losses by sedimentation of particles in horizontal turbulent flow through a cylindrical pipe over a distance L is (Fuchs, 1964):

$$(n/n_o) = \exp\ [-2g\tau L/\pi\bar{U}R]$$

where g = gravitational acceleration, 980 cm/sec$^2$

$\bar{U}$ = average flow velocity, cm/sec

R = radius of cylinder, cm.

This can also be written

$$(n/n_o) = \exp\ [-2g\tau LR/Q]$$

where

Q = volume rate of flow, cm$^3$/sec.

For the flow in the scattering chamber, Q = 220 cm$^3$/sec, L = 65 cm and R = 7.1 cm. Using this last formula and $\tau$ and $\tau'$ for NaCl at low relative humidity and at 80% RH, respectively, the fractional losses ($1-n/n_o$) due to the sedimentation in the scattering chamber have been calculated and are given in Table 1.9. The difference in the losses at high (80% RH) and low humidities from settling out in the scattering chamber is less than 10% for NaCl particles with original diameters smaller than 2.0 microns

A similar loss estimate can be made for the losses in the RH chamber for which $n/n_o \doteq \exp[-L'/h]$ in which L' is the distance the particle would fall in the 78 seconds it is in the RH chamber and h is the height (30 cm) of the RH chamber (Table 1.10).

Table 1.9. Sedimentation Losses for NaCl Particles in Scattering Chamber.

| Diameter of Particle When Dry (microns) | Dry Relaxation Time, τ ($10^{-6}$ sec) | Relaxation Time[b], τ' at 80% RH ($10^{-6}$ sec) | Fractional Loss $(1-n/n_o)$ Dry | Fractional Loss $(1-n/n_o)$ at 80% RH |
|---|---|---|---|---|
| 0.1 | 0.19 | 0.24 | 0.00 | 0.00 |
| 0.2 | 0.49 | 0.67 | 0.00 | 0.00 |
| 0.4 | 1.49 | 2.2 | 0.01 | 0.01 |
| 1.0 | 7.7 | 12. | 0.03 | 0.05 |
| 2.0 | 28. | 45. | 0.11 | 0.17 |
| 4.0 | 109. | 177. | 0.36 | 0.51 |

a) Based on Fuchs (1964) table on page xiv, including Cunningham correction factors.

b) $\tau' = \tau(0.57)(1.71)(D_p' + 0.16 \times 10^{-4}\ \text{cm})/(D_p + 0.16 \times 10^{-4}\ \text{cm})$

Table 1.10. Estimated Sedimentation Losses for NaCl Particles in RH Chamber.

| Particle Diameter When Dry (microns) | Fractional Loss $(1-n/n_o)$ Dry | Fractional Loss $(1-n/n_o)$ at 80% RH |
|---|---|---|
| 0.1 | 0.00 | 0.00 |
| 0.2 | 0.00 | 0.00 |
| 0.4 | 0.00 | 0.00 |
| 1.0 | 0.02 | 0.03 |
| 2.0 | 0.07 | 0.11 |
| 4.0 | 0.24 | 0.36 |

The difference in the losses due to settling in the RH chamber is less than 4% for NaCl particles with original (dry) diameters less than 2.0 microns.

Another possible source of losses of particles is impaction. A rough estimate of the importance of this effect can be obtained by comparing the particle stopping distance (the product, here, of the flow velocity and the particle characteristic time) with the scale of the dimensions of changes in the flow field, for example the 0.64 cm I.D. of the tubing. The flow velocity through this tubing was the largest velocity in the system (excluding the capillary tube in the holding chamber inlet) and was $6.9 \times 10^2$ cm/sec. Impaction losses are on the order of 50% when the particle stopping distance is the same order of magnitude as the length characteristic of major changes in the flow field. Such losses to a first approximation seem insignificant for NaCl particles with initial dry diameters of 2.0 microns or smaller (Table 1.11). In all calculations of $\tau$, the non-sphericity of the particles was ignored because the difference in $\tau$ is less than 10% even for a cube compared to a sphere.

Table 1.11. NaCl Particle Stopping Distance for Velocity of 700 cm/sec.

| Particle Diameter When Dry (microns) | Stopping Distance (S.D.) Dry[a] ($10^{-3}$ cm) | Stopping Distance (S.D.)' at 80% RH[b] ($10^{-3}$ cm) |
|---|---|---|
| 0.1 | 0.13 | 0.17 |
| 0.2 | 0.34 | 0.47 |
| 0.4 | 1.04 | 1.53 |
| 1.0 | 5.4 | 8.4 |
| 2.0 | 19.5 | 31.0 |
| 4.0 | 76.0 | 124.0 |

a) Based on $(S.D.) = V_o\tau = (700 \text{ cm/sec})\ \tau$

b) Based on $(S.D.)' = V_o\tau' = (700 \text{ cm/sec})\ \tau'$

## VI. Conclusions

The backscattering of light from a He-Ne laser by hygroscopic aerosols was considerably altered by changes in humidity. The results presented here should be useful in estimating the influence of humidity on aerosol particles present in the atmosphere (NaCl) as well as aerosols often used in laboratory work. If humidity is ignored as an interference, serious errors of measurement can occur.

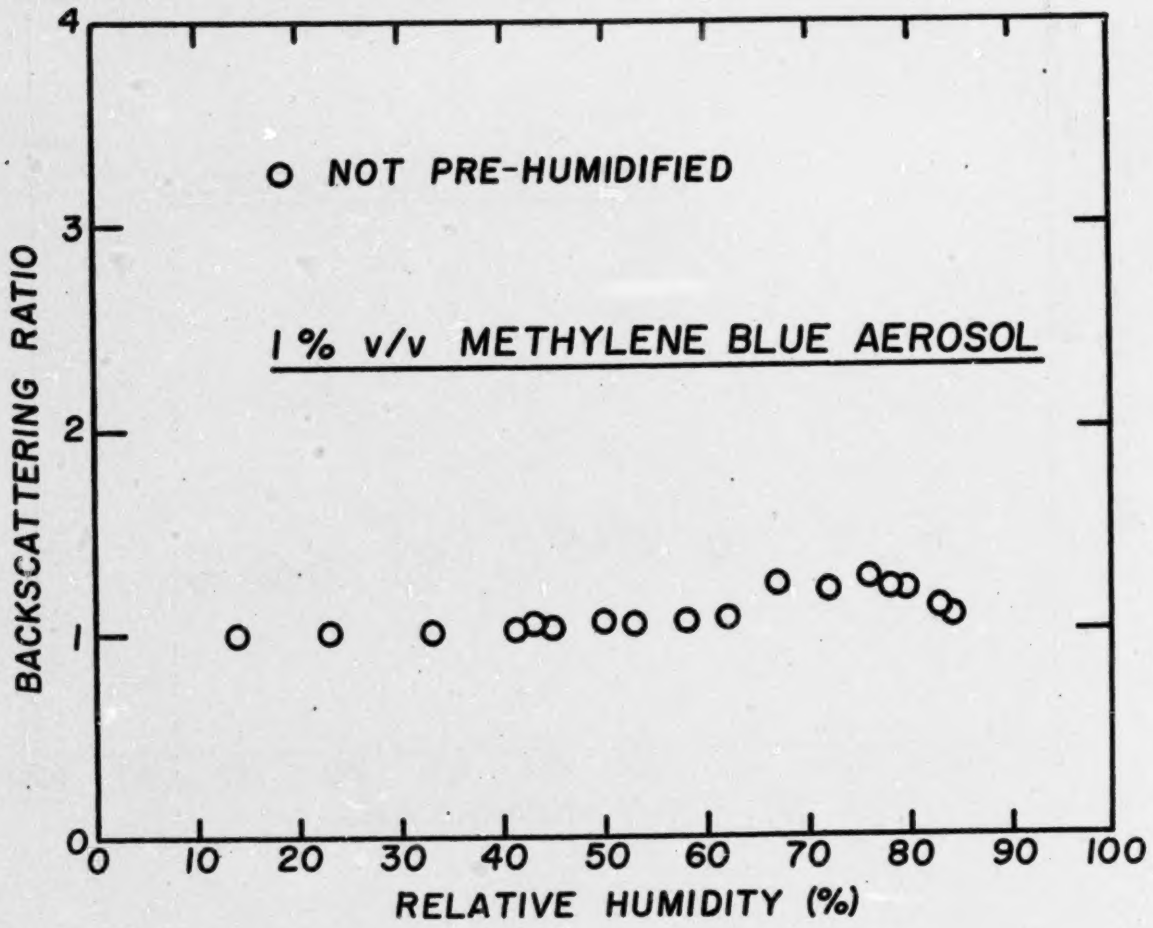

Figure 1.10. Backscattering vs. Relative Humidity for 1% v/v Methylene Blue Aerosol

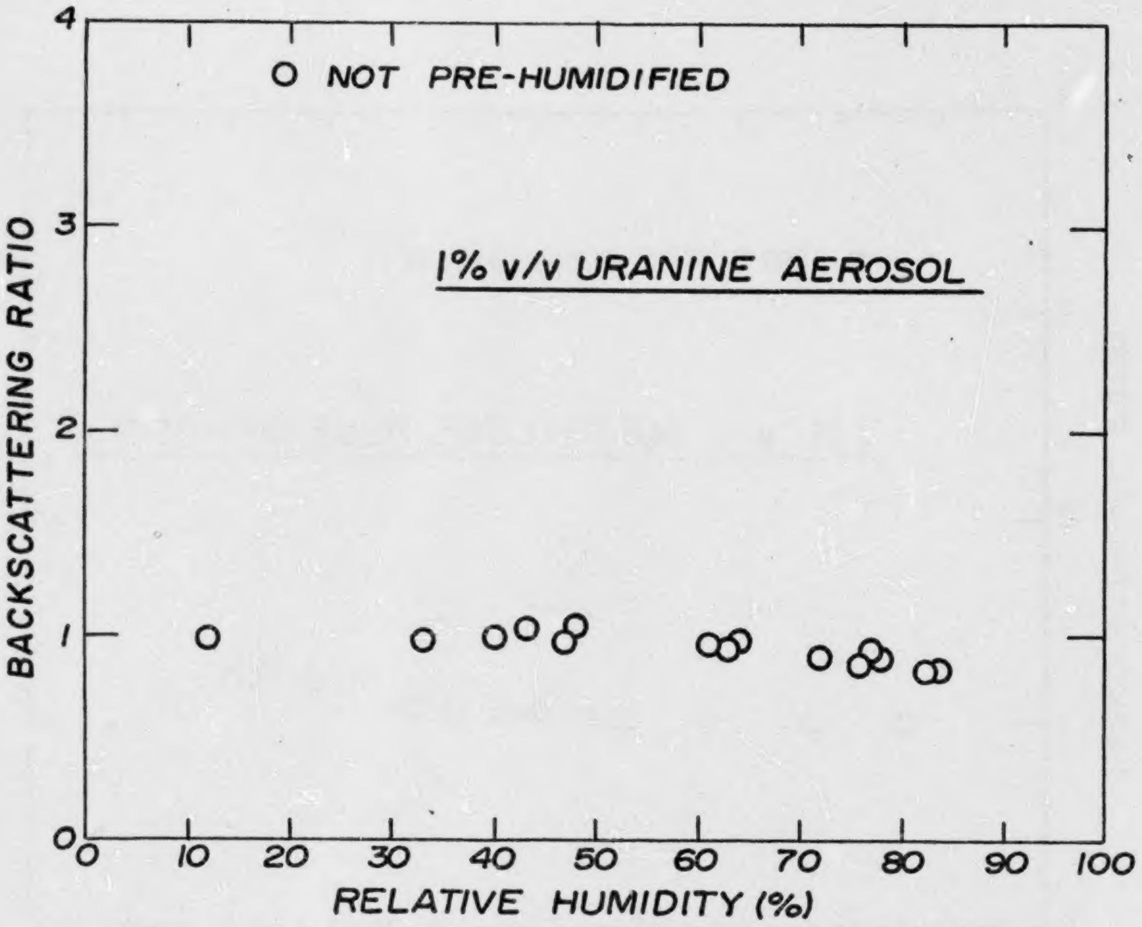

Figure 1.11. Backscattering vs. Relative Humidity for 1% v/v Uranine Aerosol

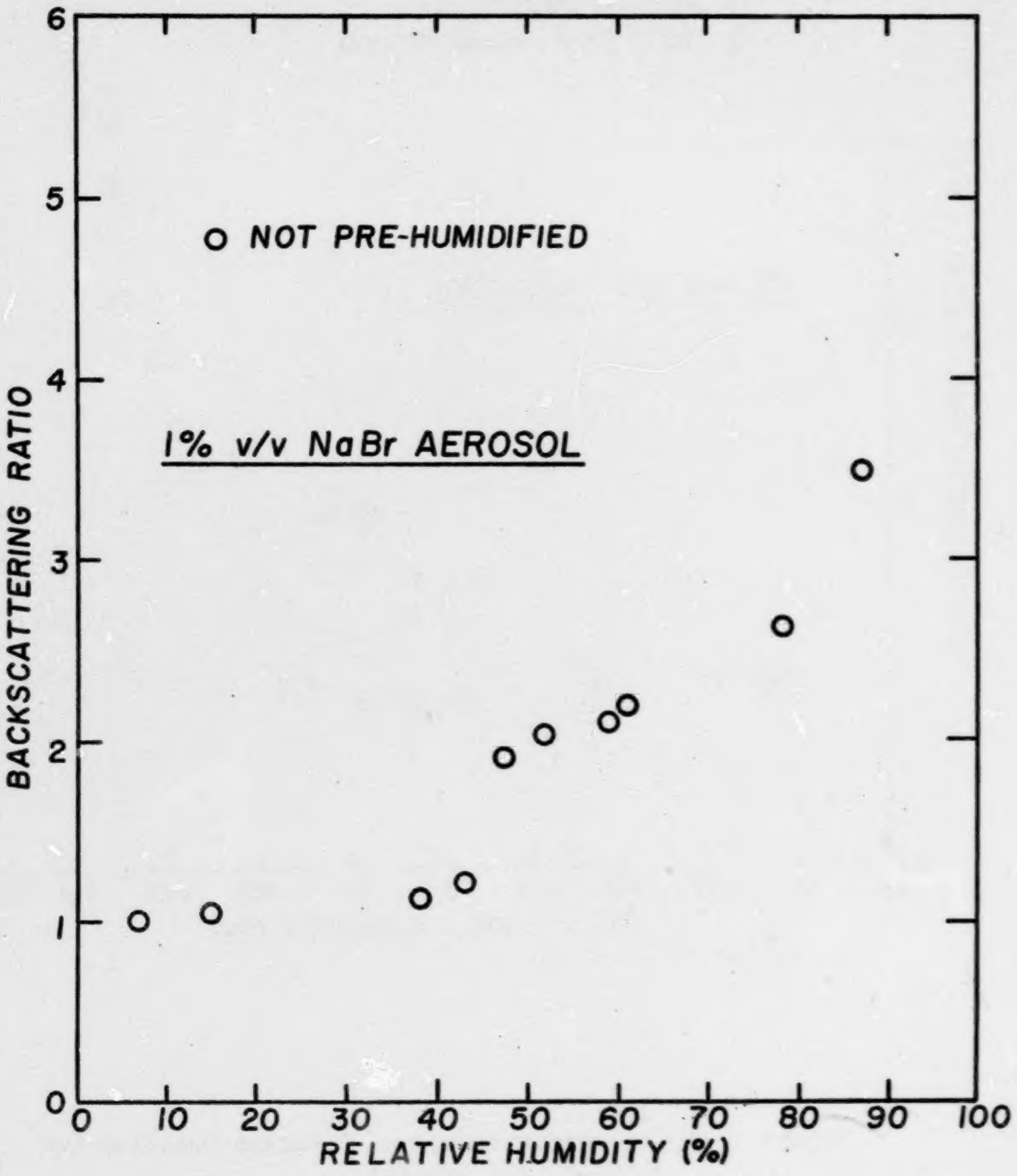

Figure 1.12. Backscattering vs. Relative Humidity for 1% v/v NaBr Aerosol

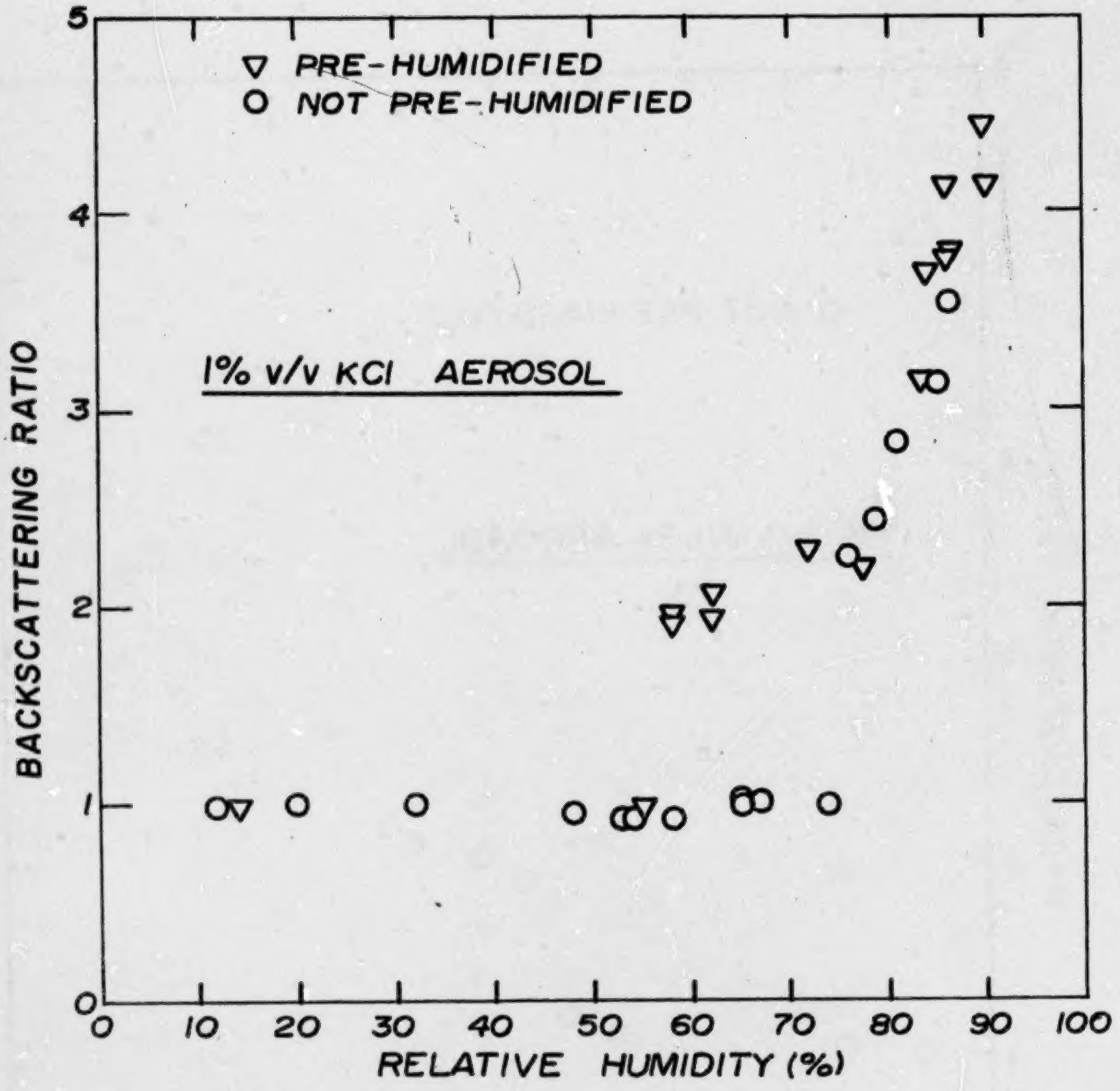

Figure 1.13. Backscattering vs. Relative Humidity for 1% v/v KCl Aerosol

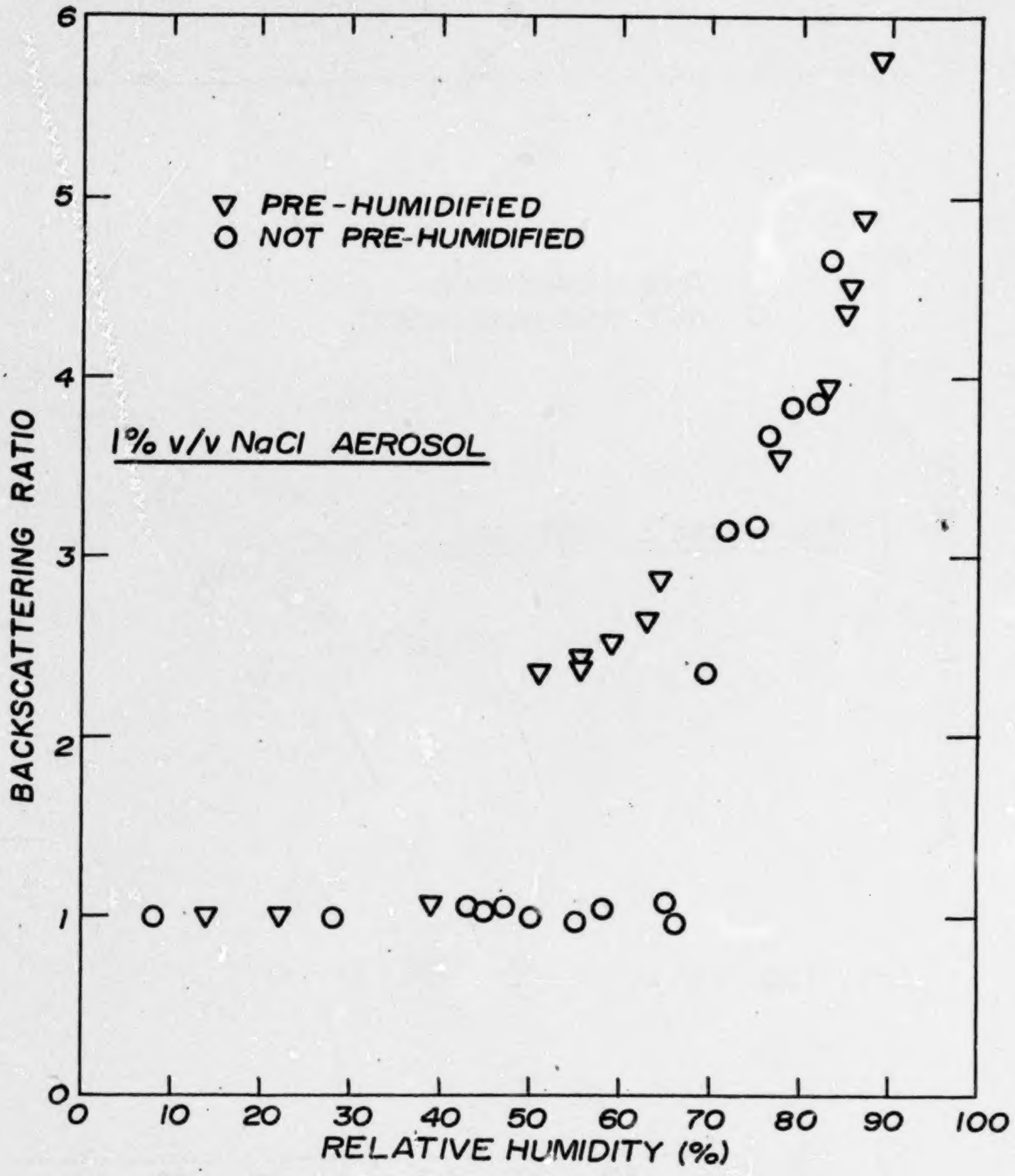

Figure 1.14. Backscattering vs. Relative Humidity for 1% v/v NaCl Aerosol

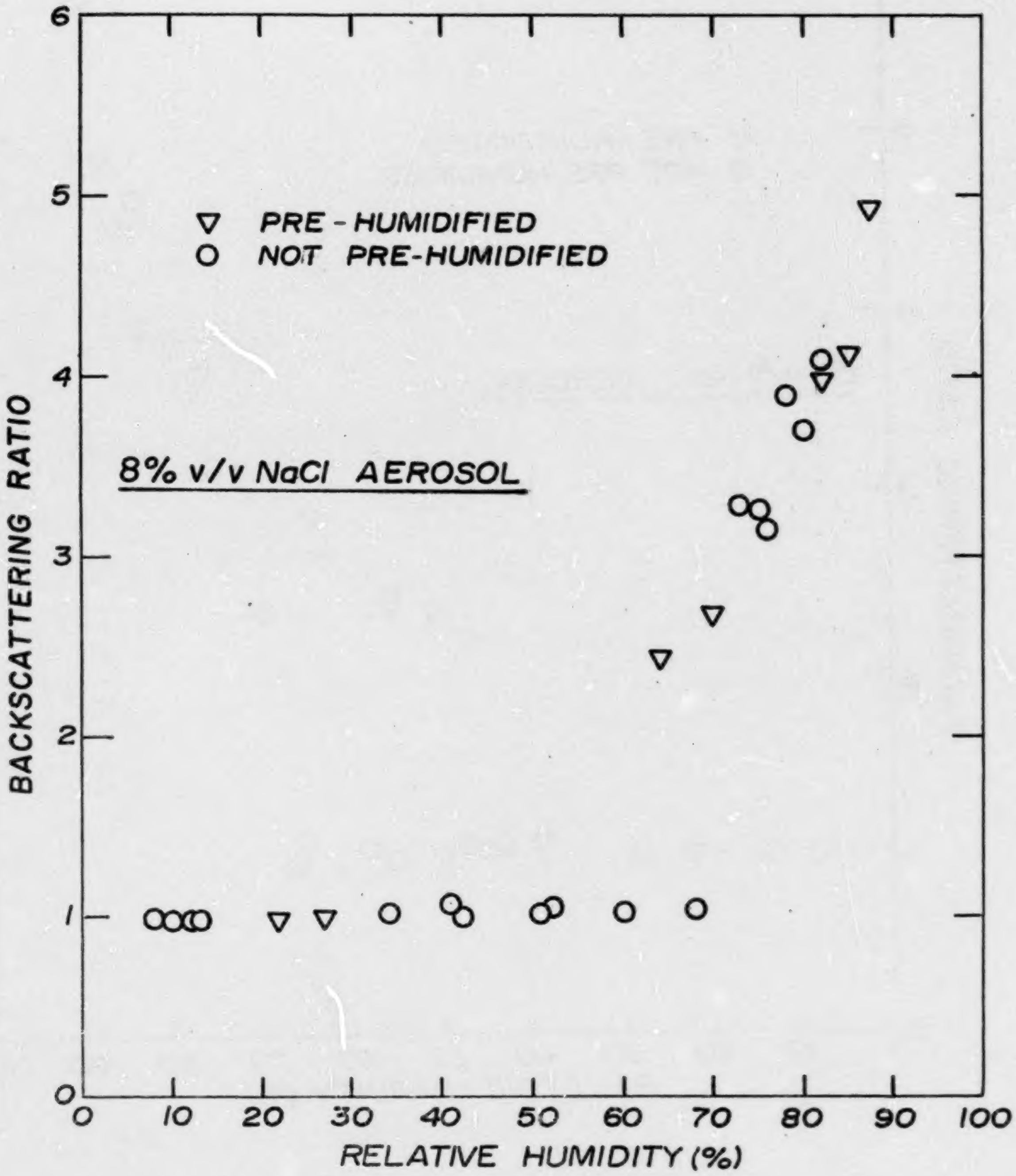

Figure 1.15. Backscattering vs. Relative Humidity for 8% v/v NaCl Aerosol

## Section 2. Depolarization of Laser Light By Laboratory Aerosols

### I. Introduction

The primary focus of the work in this section was to investigate the effect several aerosols have on the polarization of the light which they scatter. The scattering chamber was modified so that a rotatable polarizer could be mounted in front of the receiving light pipe. The purpose of this procedure was to study the received scattered light as a function of angle between the receiver polarization direction and the direction of polarization of the light incident on the particles. The received scattered light was measured as a function of four different angles between incident polarization direction and receiver polarization direction (0°, 30°, 60°, 90°), and for aerosols of five different chemical compositions (NaCl, NaBr, KCl, polystyrene latex, dioctyl phthalate). For two of these aerosols (NaCl, NaBr) the scattering was measured not only as a function of polarization angle, but also as a function of humidity. The control test baseline in all instances was the measurement of the scattering received when the chamber was filled with filtered air.

### II. Experimental System

In order to bring the effective scattering angle closer to 180° than it was with the Model 1 scattering chamber without decreasing the sensitivity of the instrumentation, the geometry of the Model 1 scattering chamber (Figure 1.4) was modified somewhat:

1. The 0.32 cm (1/8 inch) light pipe was replaced with one which is 0.64 cm (1/4 inch) in diameter.

2. The light pipe was moved as close to the laser inlet hole as construction permitted.
3. A black felt baffle was placed 13 cm from the back (light horn) end of the chamber. This prevented some or all of the light pipe from receiving light scattered from the intersection of the laser beam with the light horn. The beam almost touched the baffle edge.

To study the depolarizing characteristics of the aerosols used, another modification was made:

4. A polarizing filter was placed on a mount so that it could serve as an analyzer, allowing the light pipe to receive only the component of light intensity polarized along a given direction. The polarizer rotates; the light pipe is stationary.

Because some air leaked in around the mounting of the polarizer, another change had to be made:

5. A glass cover slide was put over the rectangular window through which scattered light must pass to reach the light pipe.

A sketch of the polarization modification constitutes Figure 2.1. Figure 2.2 is a cross-sectional side view of the chamber.

After the first two modifications listed above were made (the replacement of the light pipe and the change in its position), the beam profile was measured with the method described above. This involved moving a diffuse reflector along the beam axis and recording the scattering as a function of position, thus of angle.

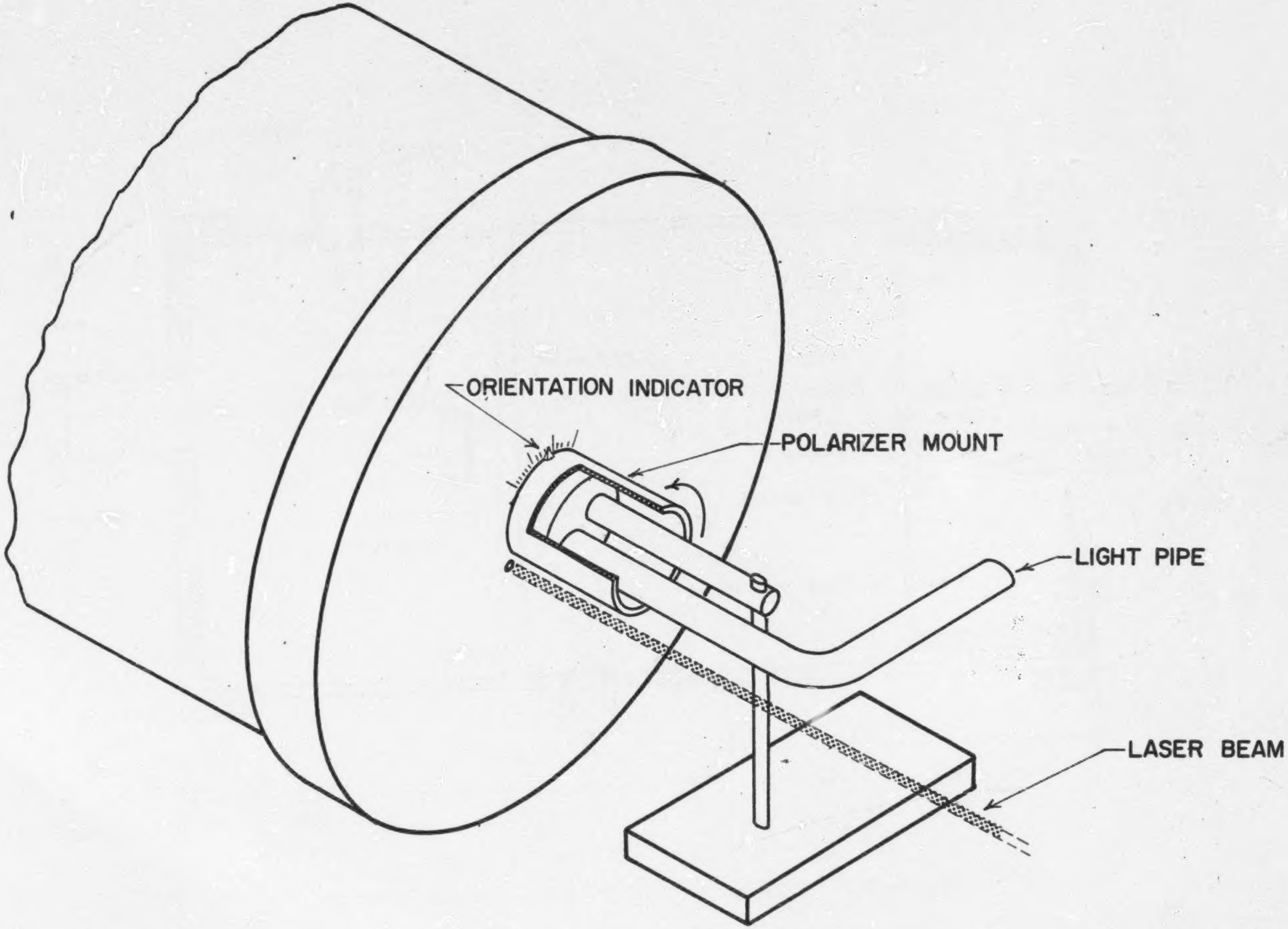
ORIENTATION INDICATOR
POLARIZER MOUNT
LIGHT PIPE
LASER BEAM

Figure 2.1. Polarization Modification

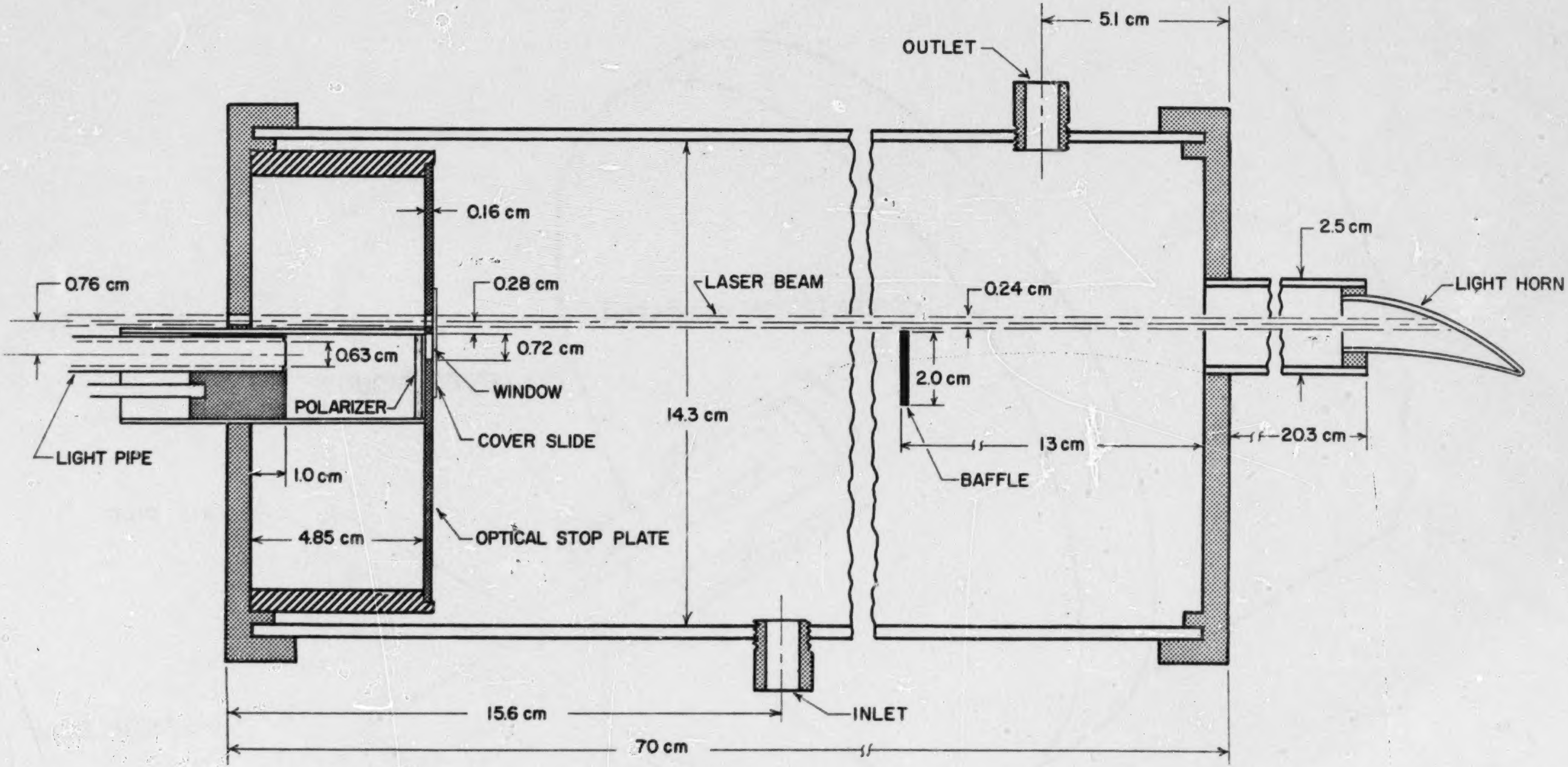
5.1 cm
OUTLET
0.16 cm
2.5 cm
0.76 cm
0.28 cm
LASER BEAM
0.24 cm
LIGHT HORN
0.63 cm
0.72 cm
2.0 cm
WINDOW
POLARIZER
14.3 cm
COVER SLIDE
20.3 cm
13 cm
LIGHT PIPE
1.0 cm
BAFFLE
4.85 cm
OPTICAL STOP PLATE
15.6 cm
INLET
70 cm

Figure 2.2. Scattering Chamber, Model 2,with Polarizer.

Results are shown in Table 2.1. The beam was measured at positions starting from the optical stop plate and going as far from the optical stop plate as the geometry of the test equipment allowed. The farthest distance perpendicular from the light pipe face plane was 64 cm. The light horn was 20 cm from the back plate of the scattering chamber, or 90 cm from the front plate. Hence, the beam profile measurements did not include the last 25 cm (approximately) of the beam length. The position (median) along the beam which divides the total scattering received into halves (half the light came from more distant scatterers and half from those nearer) is 14 cm from the plane of the light pipe face. The separation between the laser beam axis and the light pipe axis is 0.76 cm (19/64 inch). The median effective scattering angle corresponds to $\theta = \tan^{-1}$ (14/0.76) or $\theta = 177°$. Adding to the beam profile an overestimate for the contribution of the last 25 cm by assuming a net scattering of $0.1 \times 10^{-6}$ amp throughout, shifts the position of the median to 16 cm; this corresponds to 177.3°. Thus the median effective scattering angle is estimated to be 177°.

It was necessary to determine the fraction of the incident light transmitted when the polarization direction of the analyzer was perpendicular to the laser polarization. (The polarizer was a Klinger Cat. No. 063410 Polarizing Filter.) It was also necessary to determine this fraction when the analyzer polarization was parallel to the laser polarization. To determine these fractions, the polarizer was mounted on the front of the laser and the light from this combination was made to fall onto a black felt target placed inside the scattering chamber. The polarizer was rotated to get

Table 2.1. Optical Response as a Function of Scatterer Distance from Plane of Light Pipe Face.

| Perpendicular Distance from Light Pipe Face Plane (cm) | Scattering Angle (Degrees) | Net Scattering ($10^{-6}$ Amp) |
|---|---|---|
| 4.0 | 169.8 | 0.005 |
| 5.0 | | 0.020 |
| 6.0 | 173.8 | 0.44 |
| 6.4 | | 1.26 |
| 6.8 | | 1.86 |
| 7.2 | | 2.26 |
| 7.6 | | 2.41 |
| 8.0 | 174.6 | 2.46 |
| 8.4 | | 2.46 |
| 8.8 | | 2.41 |
| 9.0 | | 2.36 |
| 10.0 | 175.6 | 2.11 |
| 11.0 | | 1.86 |
| 13.0 | 176.6 | 1.56 |
| 15.0 | 177.1 | 1.37 |
| 17.0 | 177.4 | 0.87 |
| 21.0 | | 0.63 |
| 25.0 | 178.2 | 0.45 |
| 26.0 | | 0.43 |
| 34.0 | | 0.265 |
| 42.0 | | 0.175 |
| 50.0 | 179.1 | 0.145 |
| 60.0 | | 0.105 |
| 64.0 | 179.3 | 0.085 |

maximum and minimum readings and the photomultiplier dark current was measured. The averages of three such measurements were:

Polarizer polarization parallel to laser polarization:

$64 \times 10^{-7}$ A.

Polarizer polarization perpendicular to laser polarization:

$0.23 \times 10^{-7}$ A.

Photomultiplier dark current: $0.14 \times 10^{-7}$ A.

The net scattering without the polarizer on the laser was $105 \times 10^{-7}$ amp.

These readings indicate that the amount of light which is transmitted when the polarization directions are perpendicular compared to that which gets throught when they are parallel is (0.23 - 0.14) / (64 - 0.14) or 0.0014. For the present work this 0.14% transmission "leakage" is negligible. Once these tests were finished, the polarizer was mounted as in Figures 2.1 and 2.2.

The system for generating the aerosols is shown in Figure 1.1 and the rest of the flow path for the aerosols is shown in Figure 1.3. After being generated from a solution or suspension by a Collison atomizer, the aerosols were mixed with clean, dry air in a mixing chamber, ducted to a point where they were sampled in a holding chamber, mixed with clean air of controlled humidity, had their humidities measured in the RH chamber, were illuminated with a He-Ne laser and had their scattering measured. The only exception to this general description was the aerosol generated from a polystyrene latex (PSL) suspension. It did not undergo a second dilution by being mixed with air of controlled humidity.

## III. Procedure

When the polarization tests were to be made, the electronic equipment (laser, photomultiplier power supply, electrometer) would be allowed to warm up. The photomultiplier dark current would usually behave erratically at first and then settle down to a value less than $0.2 \times 10^{-7}$ A in about an hour, after which time tests would begin. An aerosol was then generated and passed through the entire apparatus flow path; when its concentration had stabilized, as shown by a stabilization in the scattering readings, the polarization measurements would begin. Almost all the aerosols used in the polarization study here were generated from a three-holed Collison atomizer at a pressure of 30 lb/in$^2$ (2 atm) above atmospheric and diluted with a $62 \times 10^3$cm$^3$/min flow of clean, dry air. The exceptions were: the polystyrene latex aerosol was generated from a six-hole Collison atomizer and diluted with $18 \times 10^3$cm$^3$/min clean, dry air and the dioctyl phthalate (DOP) aerosol was generated from a one-holed Collison atomizer at a pressure of 20 lb/in$^2$, and diluted with about $50 \times 10^3$cm$^3$/min of clean, dry air. All the aerosols except the polystyrene latex beads (PSL) aerosol passed through the same flow path used before (through a mixing chamber, holding chamber, mixing T where humidified or dried filtered air would be mixed with them, RH chamber, and then to the scattering chamber); as shown in Figure 1.3. The PSL aerosol followed a very similar path except that it was not mixed with humidified or dried filtered air after it left the mixing chamber. The PSL aerosol was nebulized from a 600 cm$^3$ volume of distilled, filtered, de-ionized water to which had been added 20 drops of Dow 0.500 micron Polystyrene Latex Emulsion (10% solids).

Dilution air was reduced to 18 x $10^3 cm^3$/min in the mixing chamber. None of the aerosols were pre-humidified by using the prehumidifier. Instead the humidities above 80% RH were obtained by heating slightly the filter holder which is upstream from the RH chamber. This evaporated moisture condensed on the filter causing an increase in the moisture content of the dilution air.

The chamber was checked for light leaks and made light-tight. The dark current was measured (the laser was off) and found to be, as it should, independent of the polarizer orientation.

After the aerosol had entered the scattering chamber, the polarization measurements were taken by turning the polarizer to four different angles: parallel to the laser polarization (0°), perpendicular (90°), and oblique (30°, 60°). The amount of scattering received (measured as current from the electrometer connected to the photomultiplier) was recorded for each of the four different angles, and this was repeated four times, giving a total of sixteen measurements for the aerosol. The dark current was measured. The humidity was recorded. The control experiment was to take the same readings after putting an absolute filter (Gelman Type E glass fiber filter) in-line between the RH chamber and the scattering chamber, so that the readings were being made on the carrier gas from which the aerosol was filtered. The control readings were subtracted from the total scattering readings to give the net scattering received; these data are presented in Table 2.2. The readings from the filtered air were a bit higher at high humidity than they were at low humidity (see Table 2.2), possibly because of some contamination on the window through which the light pipe "saw"

Table 2.2. Net Scattering Received as a Function of the Angle of the Receiver Polarization.

| Aerosol | Relative Humidity (percent) | Net Scattering Received ($10^{-7}$ A) | | | | | | Polarization Ratios | | |
|---|---|---|---|---|---|---|---|---|---|---|
| | | 0° | | 30° | 60° | 90° | | | | |
| | | Range | Average | Average | Average | Average | Range | 30°/0° | 60°/0° | 90°/0° |
| 1% v/v NaCl | 12 | 0.5 | 1.99 | 1.84 | 1.04 | 0.45 | 0.06 | 0.925 | 0.523 | 0.226 |
| 1% v/v NaCl | 76 | 0.4 | 4.20 | 3.34 | 1.44 | 0.37 | 0.01 | 0.795 | 0.343 | 0.088 |
| 8% v/v NaCl | 12 | 1.0 | 16.4 | 14.7 | 8.4 | 4.07 | 0.15 | 0.896 | 0.512 | 0.248 |
| 8% v/v NaCl | 77 | 1.0 | 42.9 | 34.6 | 13.6 | 4.49 | 0.30 | 0.807 | 0.317 | 0.105 |
| 8% v/v NaCl | 92 | 3.0 | 45.0 | 35.2 | 15.2 | 5.61 | 0.20 | 0.782 | 0.338 | 0.125 |
| 8% v/v NaCl | 12 | 0.6 | 10.9 | 10.0 | 5.62 | 2.71 | 0.15 | 0.917 | 0.516 | 0.249 |
| 8% v/v NaCl | 84 | 2.0 | 43.0 | 36.2 | 14.5 | 2.57 | 0.10 | 0.842 | 0.337 | 0.060 |
| 8% v/v KCl | 12 | 0.4 | 14.25 | 12.88 | 6.89 | 2.03 | <0.1 | 0.904 | 0.484 | 0.142 |
| 8% v/v KCl | 12 | 0.02 | 9.05 | 8.32 | 4.54 | 1.91 | 0.07 | 0.919 | 0.502 | 0.211 |
| Polystyrene | 46 | 0.2 | 1.95 | 1.64 | 0.79 | 0.10 | 0.02 | 0.840 | 0.405 | 0.051 |
| Latex Beads[c] | 46 | 0.3 | 2.11 | 1.81 | 0.83 | 0.14 | 0.01 | 0.856 | 0.393 | 0.066 |
| Dioctyl Phthalate[b] | 12 | 4. | 83. | 70.6 | 31.6 | 3.0 | 0.1 | 0.850 | 0.381 | 0.036 |
| Filtered Air[d] | 76 | 0.03 | 1.02 | 0.82 | 0.36 | 0.13 | <0.01 | 0.804 | 0.353 | 0.127 |
| Filtered Air[d] | 12 | 0.01 | 0.59 | 0.48 | 0.23 | 0.10 | <0.01 | 0.814 | 0.390 | 0.170 |
| 8% v/v NaBr | 12 | 0.4 | 7.3 | 6.4 | 3.2 | 1.01 | 0.03 | 0.876 | 0.438 | 0.137 |
| 8% v/v NaBr[a] | 12 | 0.2 | 7.3 | 6.2 | 3.1 | 0.94 | 0.03 | 0.850 | 0.425 | 0.129 |
| 8% v/v NaBr | 12 | 1.1 | 23.0 | 20.4 | 10.4 | 3.39 | 0.35 | 0.887 | 0.452 | 0.147 |
| 8% v/v NaBr | 12 | 0.6 | 31.2 | 27.8 | 15.4 | 5.43 | 0.20 | 0.891 | 0.493 | 0.174 |
| 8% v/v NaBr | 76 | 2.0 | 97.0 | 75.8 | 32.1 | 11.3 | 0.30 | 0.781 | 0.330 | 0.116 |
| 8% v/v NaBr | 76 | 4.0 | 67.1 | 53.2 | 23.2 | 6.52 | 0.30 | 0.792 | 0.346 | 0.097 |
| 8% v/v NaBr | 82 | 1.7 | 22.1 | 17.6 | 7.2 | 1.61 | 0.25 | 0.796 | 0.326 | 0.073 |
| 8% v/v NaBr | 82 | 0.9 | 23.0 | 18.5 | 7.6 | 1.71 | 0.10 | 0.805 | 0.330 | 0.074 |

a Baffle in scattering chamber removed.

b One-holed Collison atomizer at 20 lb/in$^2$

c Diameter = $0.50 \times 10^{-4}$ cm.

d This includes scattering from chamber walls, etc., and is the "background" which is subtracted to get "net" scattering.

the aerosols . Such contamination presumably would be from the salts used and would thus be hygroscopic. Except for the use of an altered flow path (as noted above) the procedure for the PSL aerosols was the same.

The laser output power changed during the tests, over a period of several months, so that valid comparisons from the data may only be drawn from the polarization ratios, not from the absolute scattering intensity data.

## IV. Results

The results of the polarization measurements are contained in Table 2.2. The first column indicates what aerosol was used. The percentages associated with the NaCl, KCl, and NaBr aerosols in this column are the volume percentages of the salts in the aqueous solutions from which they were nebulized.

The polystyrene latex beads were from Dow Chemical Company (Midland, Mich.)and were sized by Dow as being 0.500 microns in diameter with a standard deviation of 0.0027 microns. The readings for filtered air are the readings from the photomultiplier tube (RCA 7265 at 2000 volts) when filtered air was illuminated by the laser beam minus the readings of dark current for the photomultiplier tube (determined by blocking the laser light from reaching the scattering chamber) and the readings reflect the amount of light scattered by the chamber walls, etc. The net scattering received values are the readings obtained with the specified aerosol minus those readings obtained when the aerosol was passed through an absolute filter upstream from the scattering chamber. The relative humidity was measured while the aerosol was in the RH chamber. The RH chamber temperature was less than 0.2°C different from the temperature at the outlet end of the scattering chamber. The angles listed are the angles between the direction of polarization of the analyzer polarizer in front of the light pipe and the incident laser light polarization. The ranges are the differences between the largest and smallest of the four readings at each angle indicated; the ranges are intended to give a measure of the reproducibility of the readings. The averages are taken of the four readings at the given angle. The polarization ratios are the ratios of the net scattering received with the analyzing polarizer at the given angle to the net scattering received with the analyzer polarization parallel to the direction of incident polarization.

Comparison of the depolarization ratios (the 90°/0° ratios) is facilitated by Table 2.3 which lists these ratios and contains the measurement ranges as percentages. This table also gives the square roots of the sums of the squares of the range percentages and the products of these square roots with the corresponding depolarization ratios as an indication of the amount of the depolarization ratio uncertainty related to problems of reproducibility.

From the information in Tables 2.2 and 2.3 it is noted:

1. The salt aerosols, when dry, depolarized about one-fifth of the incident polarized light intensity.
2. When humidified, the salt aerosols depolarized less light than they did when they were dry. (The values for humidity other than 12% RH for the NaCl and NaBr aerosols are above the critical humidities at which these salts change phase, as determined earlier in this work and by others; see Appendix 3.)

Table 2.3. Ratios of the 90° Polarization Components to the 0° Polarization Components of the Net Scattering Received.

| Aerosol | Relative Humidity (per cent) | 90°/0° Polarization Ratio | % Range of 0° Readings | % Range of 90° Readings | Square Root of sum of squares of 0° and 90° % Ranges | Column 3 times Column 6 |
|---|---|---|---|---|---|---|
| 1% v/v NaCl | 12 | 0.23 | 25 | 13 | 28 | 0.06 |
| 1% v/v NaCl | 76 | 0.09 | 10 | 3 | 10 | 0.01 |
| 8% v/v NaCl | 12 | 0.25 | 6 | 4 | 7 | 0.02 |
| 8% v/v NaCl | 12 | 0.25 | 6 | 6 | 8 | 0.02 |
| 8% v/v NaCl | 77 | 0.11 | 2 | 7 | 7 | 0.008 |
| 8% v/v NaCl | 84 | 0.06 | 5 | 4 | 6 | 0.004 |
| 8% v/v NaCl | 92 | 0.12 | 7 | 4 | 8 | 0.01 |
| 8% v/v KCl | 12 | 0.14 | 3 | 5 | 6 | 0.008 |
| 8% v/v KCl | 12 | 0.21 | 0 | 4 | 4 | 0.008 |
| Polystyrene | 46 | 0.05 | 10 | 20 | 22 | 0.01 |
| Latex Beads[c] | 46 | 0.07 | 14 | 7 | 16 | 0.01 |
| Dioctyl Phthalate | 12 | 0.04 | 5 | 3 | 6 | 0.002 |
| Filtered Air[d] | 12 | 0.17 | 2 | <10 | <10 | <0.02 |
| Filtered Air[d] | 76 | 0.13 | 3 | <10 | <10 | <0.01 |
| 8% v/v NaBr | 12 | 0.14 | 5 | 3 | 6 | 0.008 |
| 8% v/v NaBr | 12 | 0.13 | 3 | 3 | 4 | 0.005 |
| 8% v/v NaBr | 12 | 0.15 | 4 | 10 | 11 | 0.02 |
| 8% v/v NaBr | 12 | 0.17 | 2 | 4 | 4 | 0.007 |
| 8% v/v NaBr | 76 | 0.12 | 2 | 3 | 4 | 0.005 |
| 8% v/v NaBr | 76 | 0.10 | 6 | 5 | 8 | 0.008 |
| 8% v/v NaBr | 82 | 0.07 | 7 | 15 | 17 | 0.012 |
| 8% v/v NaBr | 82 | 0.07 | 4 | 6 | 7 | 0.005 |

[a] No baffle in scattering chamber.

[b] One-holed Collison atomizer at 20 $\text{lb/in}^2$

[c] Diameter = $0.50 \times 10^{-4}$ cm.

[d] This includes cattering from chamber walls, etc., and is the "background" which is subtracted to get "net" scattering.

3. There were no measurable differences between the depolarization made by the 1% v/v NaCl aerosol and the depolarization made by the 8% v/v NaCl aerosol, either at 12% relative humidity or at 76% relative humidity.
4. Removing the baffle (see Figure 2.2) did not significantly alter the scattering recorded from the 8% v/v NaBr aerosol at 12% RH and made an average difference of 5% for the scattering from the same aerosol at 82% RH.
5. The dry NaCl aerosols depolarized light more effectively than did the dry 8% v/v NaBr aerosol, but when humidified into droplets these aerosols depolarized the light to about the same degree.
6. The random error in the measurement of the depolarization by the 8% v/v KCl seems insufficient to explain the discrepancy between the two (12% RH) figures listed. The depolarization by 8% v/v NaCl measured at 84% RH seems anomalous.
7. In all cases the polarization ratios were greater than those predicted by the law of Malus (cosine squared dependence of the intensity on the angle between the polarization directions) for no depolarization by the targets; if the Malus law had held, the ratios in the last three columns (30°/0°, 60°/0°, 90°/0°) of Table 2.2 would be 0.75, 0.25, 0.00.
8. The nearly spherical aerosols (PSL, DOP, salts at humidities above their change of phase humidities) gave depolarization measurements which were non-zero within the estimated random error.

Since it was possible that some of the light scattered by the particles struck the inside of the chamber and scattered again in appreciable amounts into the light pipe, a test was run to estimate the magnitude of this secondary scattering from the scattering chamber walls. A long, thin strip (64 cm long, 0.64 cm wide, 0.16 cm thick) of balsa wood was painted flat black and positioned so that it ran from the space between the light pipe and the laser inlet hole along a line essentially parallel to the laser beam to the back plate of the scattering chamber. At the back it was placed so that it touched the circumference of the light horn holder at the light pipe side of the laser beam. The obstacle thus blocked the light pipe from the rays of light scattered directly back from the particles, but it did not keep the light pipe from being exposed to scattering from almost as much of the chamber walls as it would have been exposed to had the obstacle not been there. Readings were taken on filtered air before and after they were taken at 8% v/v NaBr. The range and average of four such readings at each condition are presented in Table 2.4, along with measurements taken the same day of 8% v/v NaBr scattering without the obstacle, from which data secondary scattering may be estimated.

The secondary scattering from the chamber for 8% v/v NaBr was (0.10/7.3) = 1.4% and (0.02/0.92) = 2% for scattering analyzed with the analyzer polarizer parallel and perpendicular to the laser beam polarization at 12% RH. The corresponding values at 82% RH were 1.2% and 3%; all are negligible for this work.

## V. Discussion

The greater ability of aerosol particles to depolarize light could be a means of distinguishing between backscattering from gas

Table 2.4. Results of Secondary Scattering Tests

| | | | Scattering ($10^{-7}$) | | | |
|---|---|---|---|---|---|---|
| | | | 0° | | 90° | |
| Aerosol | Relative Humidity (% RH) | Obstacle | Range | Average | Average | Range |
| Filtered Air | 12 | yes | 0.08 | 3.03 | 0.42 | 0.025 |
| 8% v/v NaBr | 12 | yes | 0.05 | 3.05 | 0.43 | 0.02 |
| Filtered Air | 12 | yes | 0.03 | 2.86 | 0.40 | 0.01 |
| | Average Net Scattering: | | | 0.10 | 0.02 | |
| Filtered Air | 12 | no | 0.01 | 4.62 | 0.90 | 0.01 |
| 8% v/v NaBr | 12 | no | 0.02 | 11.9 | 1.82 | 0.03 |
| | Average Net Scattering: | | | 7.3 | 0.92 | |
| Filtered Air | 82 | yes | 0.08 | 4.75 | 0.68 | 0.01 |
| 8% v/v NaBr | 82 | yes | 0.08 | 4.95 | 0.72 | 0.01 |
| Filtered Air | 82 | yes | 0.06 | 4.62 | 0.66 | 0.01 |
| | Average Net Scattering: | | | 0.27 | 0.05 | |
| Filtered Air | 82 | no | 0.07 | 7.24 | 1.11 | 0.03 |
| 8% v/v NaBr | 82 | no | 1.7 | 29.4 | 2.72 | 0.15 |
| | Average Net Scattering: | | | 22.1 | 1.61 | |

molecules and from aerosol particles (Clemesha, et al. 1967; Cohen, et al. 1969). Homogeneous spheres made of molecules which do not depolarize light would not depolarize light, but irregular particles and radially inhomogeneous spheres would depolarize light.

This work measured the depolarization by colorless, cubic crystals (NaCl, NaBr, KCl) with a variety of non-absorptive refractive indices (1.54, 1.64, 1.49). The two sizes of NaCl particles used had mass mean diameters of 0.4 microns and 0.2 microns and gave depolarizations of 0.25 ± 0.02 and 0.23 ± 0.06. The NaBr and KCl are assumed to have had mass mean diameters of 0.4 microns and gave depolarizations ( 90°/ 0°) of 0.15 ± 0.02 and 0.18 ±0.04 respectively. Significantly, this means a considerable fraction of the light was depolarized by the aerosol particles. In contrast, clean air has given measured depolarization of 0.015 (Cohen et al., 1969). Polluted air has given depolarizations up to 0.7 (Cohen et al., 1969).

The full Mie scattering equations have not been solved for generally irregular particles and have been solved for only a few non-spherical cases. Rayleigh scattering ( $\alpha = \pi D_{.} / \lambda < 0.03$) has been studied more fully, however, and we include a Rayleigh-scattering depolarization calculation which may indicate the order of magnitude of depolarization to be expected for particles that are approximately spherical.

Kerker (1969) gives the following exact analysis of the problem of depolarization by scattering by a collection of randomly oriented ellipsoids in the Rayleigh scattering approximation. This approximation requires that the particle dimensions be much smaller than the wavelength of the light, a condition met by only a fraction of the particles used in this work. The depolarization ratio $\rho_v$ is defined as the ratio of the horizontally polarized component (90°) of scattered light intensity to the vertically polarized light intensity component (0°) scattered for incident light having vertical polarization. The scattering plane is taken as horizontal.

$$\rho_v = I_2/I_1 = (\overline{f_x^2}\cos^2\theta + \overline{f_z^2}\sin^2\theta)/\overline{f_y^2}$$

Here, $\overline{f_x^2}$ is the average of the square of the scattered electrical field horizontal component at right angles to the direction (z) of the incident radiation. At 180° backscattering this expression becomes ($\sin^2\theta \rightarrow 0$) after mathematical manipulation

$$\rho_v = (L' - L'')^2/[3(L')^2 + 4(L'L'') + 8(L'')^2],$$

for a non-absorbing particle. L' and L" are related to the polarizabilities $\alpha'$ and $\alpha''$ by

$$\alpha' = (3V/4\pi)L' = V(m^2 - 1)/[4\pi + (m^2-1)\, P'_e]$$

$$\alpha'' = (3V/4\pi)L'' = V(m^2 - 1)/[4\pi + (m^2-1)\, P''_e]$$

where V is the particle volume and m is the refractive index. For the case of oblate (flattened) spheroids the depolarization factor $P'_e$ is given on the figure axis (length B) by

$$P'_e = \frac{4\pi}{e_s^2}\left[1 - \left(\frac{1-e_s^2}{e_s^2}\right)^{1/2} \sin^{-1} e_s\right]$$

and by

$$P''_e = (4\pi - P'_e)/2$$

on the two equal axes (diameters), A = C>B.

The eccentricity is $e_s$,

$$e_s = (A^2 - B^2)^{1/2}/A.$$

As a sample calculation for $\rho_v$, it was supposed that a salt particle (m = 1.5) was somewhat irregular and could be approximated by an oblate spheroid with A = C = 5, B = 4; that is, approximated by an oblate spheroid whose figure axis was 80% of its diameter. Then

$$e_s = (A^2 - B^2)^{1/2}/A = 0.6$$

$$P'_e = 5.0$$

$$P''_e = 3.8$$

Thus,

$$L' = (4\pi/3)\ (m^2-1)/[4\pi + (m^2-1)\ P'_e] = 0.278,$$

and

$$L'' = 0.302\ .$$

Therefore,

$$\rho_v \doteq 4 \times 10^{-4}\ ,$$

or the $I_2$ component (90°) would be 0.04% of the $I_1$ component (0°).

The depolarizations measured for the dry salt particles were two orders of magnitude greater than this estimate. One possible reason for the discrepancy is that a significant fraction of the particles was larger than the Rayleigh scattering regime, although the similarity in the dry depolarizations of the 8% v/v NaCl aerosol and the 1% v/v NaCl aerosol, which was smaller, weakens the case for an explanation based on aerosol particle size. Another possible reason is that the depolarization from angular (roughly cubic) crystals is poorly approximated by that from somewhat oblate spheroids, which are curved rather than angular. The limiting cases for backscattering depolarization from randomly oriented oblate spheroids (circular disks) is 0.125 and from randomly oriented prolate spheroids (circular cylinders) is 0.333, according to Kerker (1969).

Even the spherical particles (salt solutions, polystyrene, dioctyl phthalate) depolarized the laser light. Why was non-zero depolarization measured for the spherical particles?

Several possibilities present themselves:

1. The molecules which comprise the spheres individually depolarize the light.
2. There are small-scale (greater than a molecule, much smaller than the particle) inhomogeneities such as layers in the polystyrene or concentration fluctuations in the salt solution.
3. The particles are not quite spherical.
4. The depolarization figures are due to a systematic error.

Because the control test should have eliminated most systematic errors and the test of secondary scattering from the chamber walls eliminated secondary scattering as a significant problem and no other interference is apparent, the non-zero depolarizations for spherical particles are evidently due to experimental error.

The information in this research should be of use to those doing work in Light Detection and Ranging (LIDAR) measurements of atmospheric aerosols, using the backscattering of pulsed ruby laser light to measure concentration profiles of suspended particulates. Such work had been described in papers by Barret and Ben-Dov (1967); Clemesha et al. (1967); Johnson (1969); Reagan (1968), who pointed out humidity as a possible interference; and many others in a growing number of papers on the topic.

Since particle behavior depends strongly on size, there is always the problem of the degree to which a laboratory aerosol approximates the natural aerosols. One cannot exactly reproduce the ambient aerosols in the laboratory. They may only be approximated by using particles size distributions similar in essential characteristics. The particle size distributions of the aerosols used in this work are given above.

Another characteristic one would want to match between atmospheric and test aerosols is that of refractive index. Hanel's (1968) measurements ascribed to the atmospheric aerosol a real part of the refractive index of 1.57 at 40% RH, with values of real refractive index ranging from 1.7 to 1.33 as the relative humidity went from 0% RH to 100% RH. As noted above, NaCl has a refractive index of 1.54. Water has a refractive index of 1.33. As relative humidity increases, the refractive index of the salt droplets will approach that of water. Thus, NaCl would seem well suited with regard to index of refraction to model some atmospheric aerosols. There remains the question of the degree to which the change-of-phase characteristics of NaCl successfully model the relative humidity dependence of the atmospheric scatterers for aerosols of other than maritime origin.

The applicability of the NaCl data must not be overstated in the case of continental aerosols. The work of Meszaros (1968) shows that the water soluble fraction of these aerosols have a much greater mass fraction of sulfate and ammonium particles than chloride particles, and that the mass fraction of water soluble materials in the particles over Budapest in the summer was 20% for particles with radii smaller than 0.14 microns and 8% for particles with larger radii. Thus water soluble particles are a fraction of the atmospheric aerosol, and chlorides a fraction of water solubles.

## VI. Conclusions

Laboratory aerosols were illuminated by vertically polarized light from a He-Ne laser; the backscattered light contained a horizontally polarized component of intensity as well as a vertically polarized component of intensity. The ratio of the horizontally polarized component to the vertically polarized component is the depolarization ratio, and this ratio was 0.04 for dioctyl phthalate oil droplets, about 0.1 for droplets and aqueous salt solutions, and as high as 0.25 for dry NaCl particles. These depolarizations are greater than the 0.015 characteristic of air and could be used to distinguish particulate scattering from scattering by the air. Humidity can influence the degree to which hygroscopic particles depolarize polarized light most obviously by controlling the phase, liquid or solid, of the aerosol particle. The data from this work do not demonstrate whether or not changes in relative humidity during which the particle remains a droplet change the depolarization ratio. The data indicate that the depolarized light from droplets may be a significant fraction (5-10%) of the scattered light received by LIDAR probes using polarized laser light and that scattering from irregular particles should have even greater depolarization. Depolarization measurements of particles large enough to be in the Mie scattering range showed a difference between spherical and non-spherical particles. Such measurements could be useful in determining the shape asymmetry of aerosol particles.

## Section 3. Field Experiment

### I. Introduction

A one week study with two days of sampling was undertaken the week of May 10th. The purpose of the field test was to study qualitatively the relationship between lidar backscatter measurements and relative humidity. The site selected for the field test was the General Electric Space Center at King of Prussia, Pennsylvania. King of Prussia is located about ten miles West North West of Philadelphia. This site was selected to provide for safe operation of the lidar probe relative to the general public.

### II. Equipment

A Dodge van equipped with a 5000 watt generator supplied the sample station with power. The G.E. lidar was located near a building from which power for its operation was acquired. The overall range from the lidar to a grassy embankment used as a stop was approximately 130 meters. Four standard General Metals high volume samplers were operated with glass fiber filters (Gelman, Type E). A Sinclair-Phoenix Aerosol Photometer (Model No. JM-3000-AL) and the laser backscatter device used in the earlier experiments were set up inside the van.

Three methods were used to record temperature and relative humidity. The Hygrodynamics Electric Hygrometer-Indicator (Model 15-3001) used in the earlier experiments was operated in conjunction with the laser device, a continuous recording hygrothermograph (Belfort Instrument Company) was placed outside the van, and periodic readings were taken with a sling psychrometer.

## III. Sampling Plan and Instrument Description

A sampling probe for the instruments inside the van extended approximately one meter out in front of the unit and two meters from the ground. Figure 3.1 illustrates the layout of the range and the location of the field sampling equipment. The four high volume ("hi-vol") samplers were started consecutively at two hour intervals beginning at approximately 0700 in order that an estimate could be made of changing concentrations. The G. E. LIDAR probe was activated at random intervals at the rate of three to four shots per hour, weather permitting. Figure 3.2 shows the arrangement of the laser backscatter device inside the van.

The weather on Tuesday, the 11th of May, was sunny and warm with light and variable winds in the morning and a light westerly wind in the afternoon. Wednesday was cloudy with intermittent light rain over the entire day. Winds were moderate out of the west with occasional gusts.

A calibration curve for the flowrate of each high volume sampler was made in the laboratory prior to the field experiment. The glass fiber filters were put in the dessicator and dryed for 24 hours before obtaining the initial weight and the same procedure was followed prior to the final weighing. The Sinclair-Phoenix aerosol photometer measures the total forward scattering of the particulate matter and has its own internal calibtation. Filtered air was used as the zero point for the Model 2 laser device and the scattering above this point was that attributable to the particles in the air.

The G. E. LIDAR probe was operated by Dr. G. W. Bethke and Dr. C. S. Cook of the Space Sciences Laboratory of the General Electric Company, Philadelphia, Pa. Their report on the operation of the probe

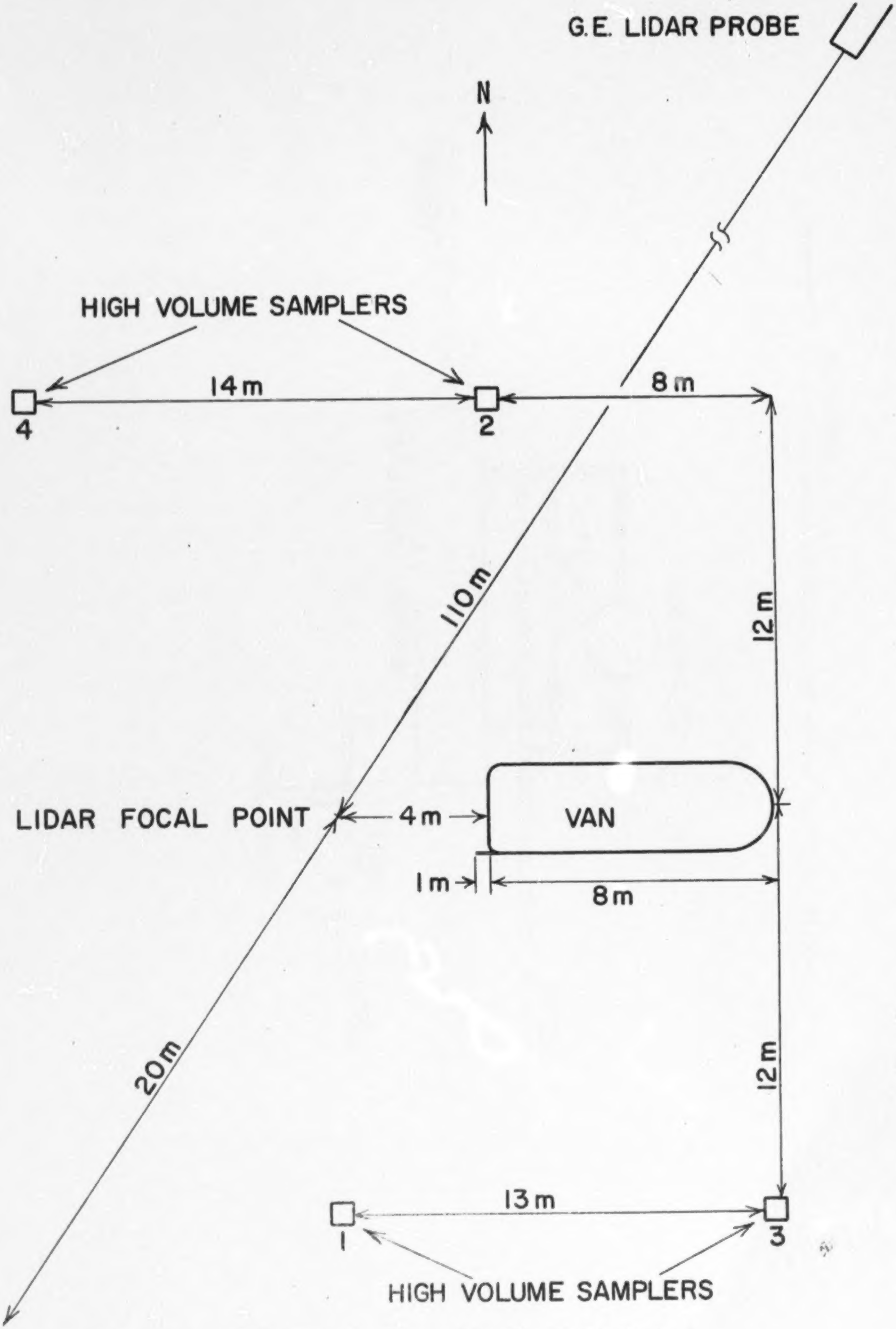
G.E. LIDAR PROBE
N
HIGH VOLUME SAMPLERS
14 m
8 m
4
2
110 m
12 m
LIDAR FOCAL POINT
4 m
VAN
1 m
8 m
20 m
12 m
13 m
1
3
HIGH VOLUME SAMPLERS

Figure 3.1. Equipment Configuration for Field Test.

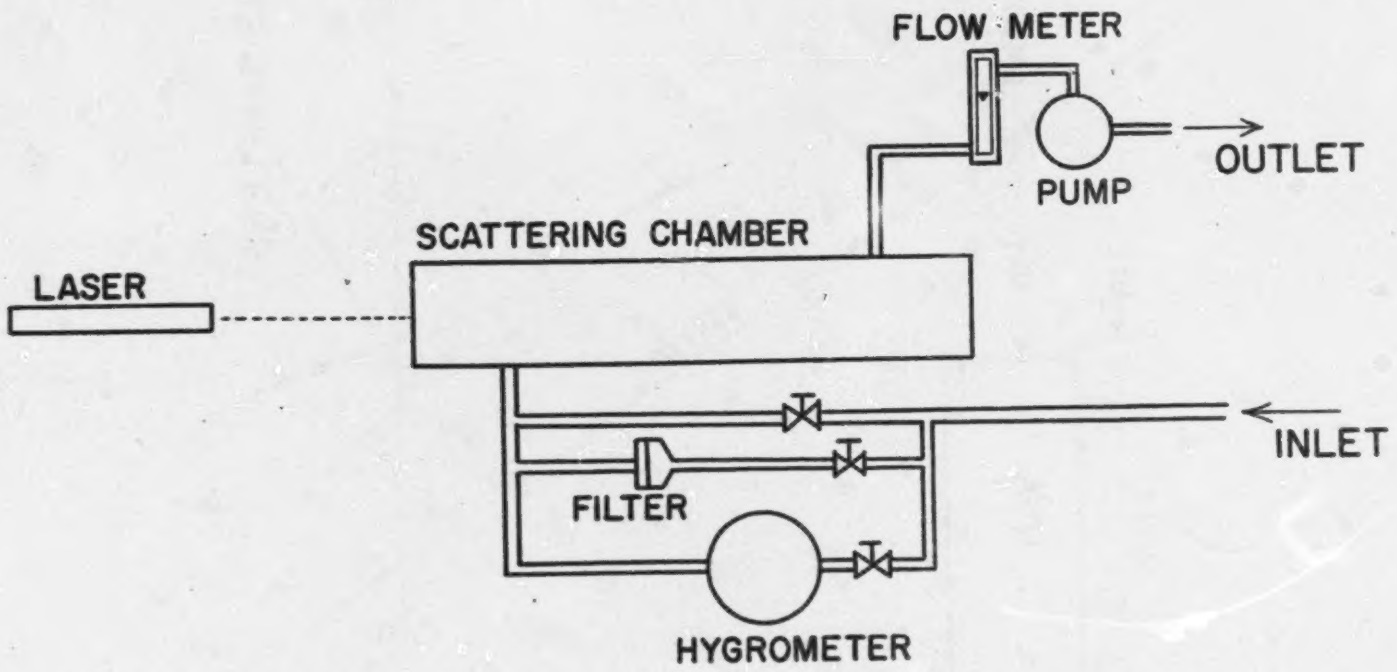
FLOW METER
OUTLET
PUMP
SCATTERING CHAMBER
LASER
INLET
FILTER
HYGROMETER

Figure 3.2. Laboratory Laser Backscattering Device (Model 2, without polarizing filter).

and analysis of results is presented in its entirety as Appendix 5 in the form of a final report. Figures 3.6 and 3.7 contain information based on Figure A.1 of Appendix 5.

## IV. Results and Analysis

Table 3.1 summarizes the high volume sampler results. On Tuesday sampler number 4 operated four hours and the loading was too light to give significant results. A wind gust upset samplers two and four on the afternoon of May 12th thus these results were not considered to be valid.

The hi-vol data from samplers two and three for May 11th indicate that from 0900 to 1700 the particulate loading was about 58 micrograms per cubic meter ($\mu gm/m^3$). For sampler number one to record 65 $\mu gm/m^3$ for the period 0700 to 1700 the loading would have to be of the order of 95 $\mu gm/m^3$ from 0700 to 0900.

Figures 3.3 and 3.4 are plots of the relative humidity and the light scattering data from the van instruments as a function of time of day.

Of major interest is the relation of the backscatter from the G.E. LIDAR probe to relative humidity and particulate loading. Figure 3.5 is a graph of relative humidity versus the backscattering signal received plotted as a function of the total mass backscattering section for particulates, $m \cdot \sigma_M(180°)$ [See Appendix 5] for May 11th. The similarity of the relationship shown in Figure 3.5 to that obtained for laboratory aerosols can be noted by comparing this figure to Figures 1.12 through 1.15, which show increasing backscatter with increasing humidity. A similar graph to Figure 3.5 is not given for May 12th since there was little change in humidity for that day. See Figure 3.7 for a qualitative comparison of backscattering and relative humidity for May 12th.

TABLE 3.1

High Volume Sampler Results

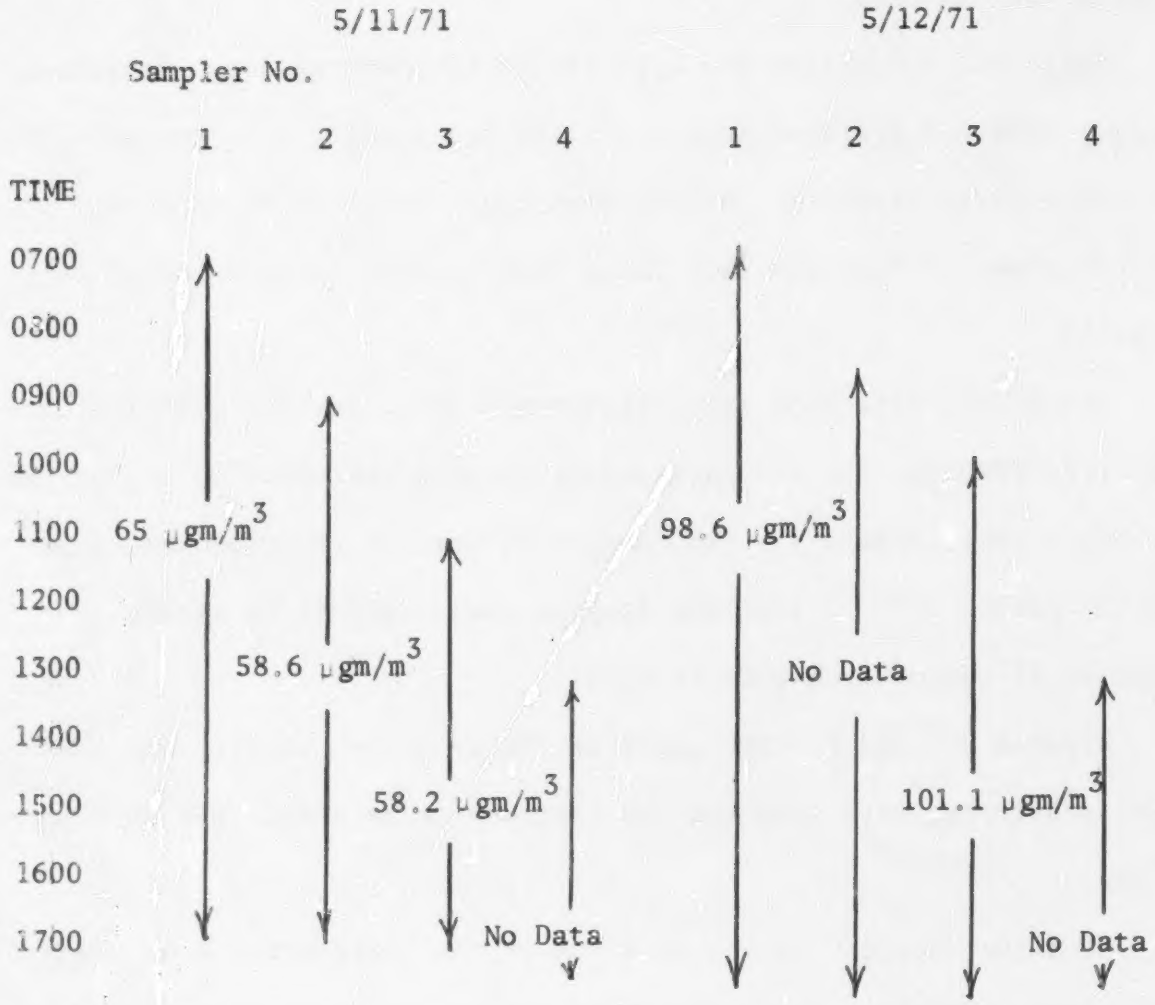

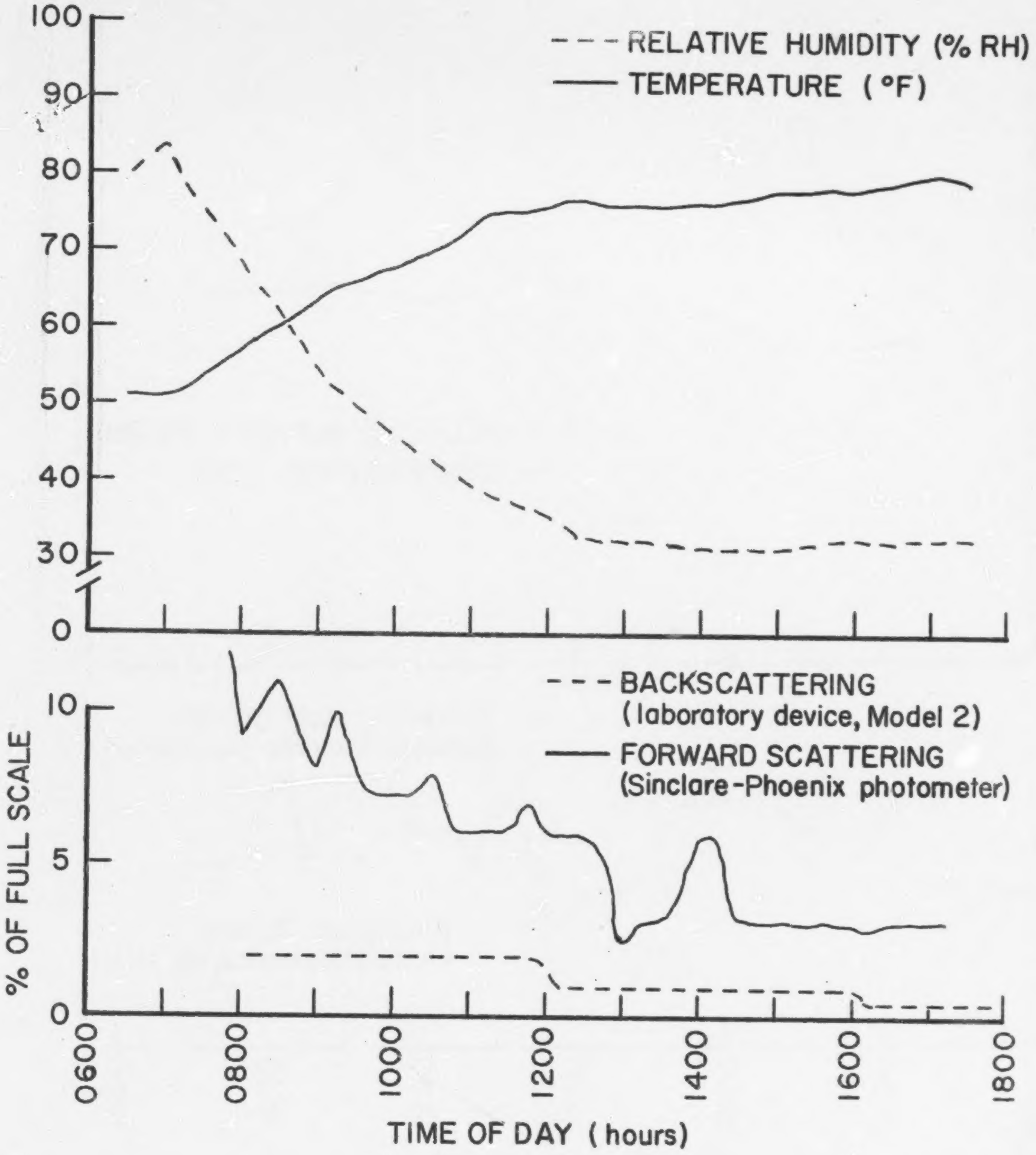

Figure 3.3. Temperature, Humidity, and Light Scattering on May 11, 1971.

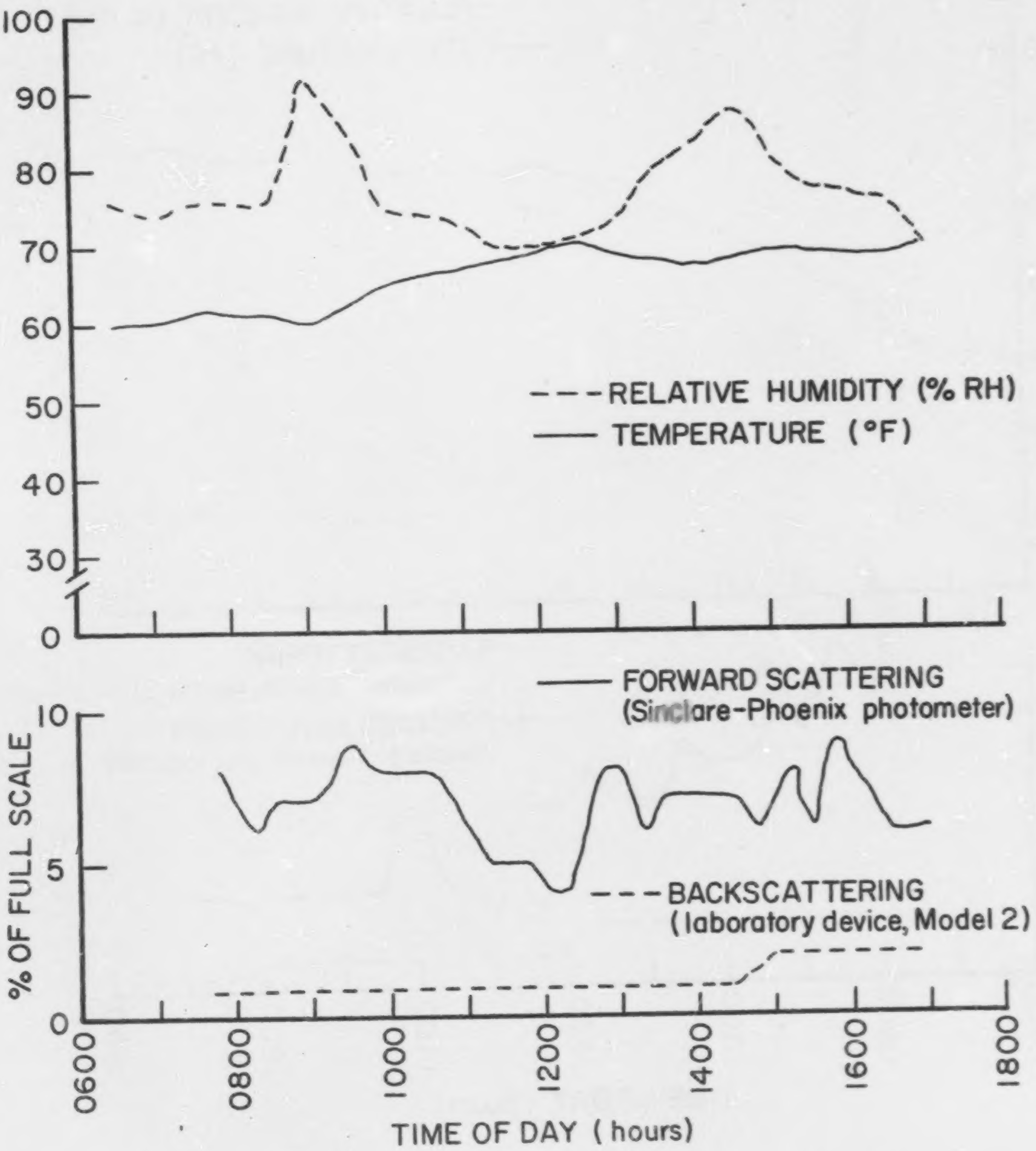

Figure 3.4. Temperature, Humidity and Light Scattering on May 12, 1971.

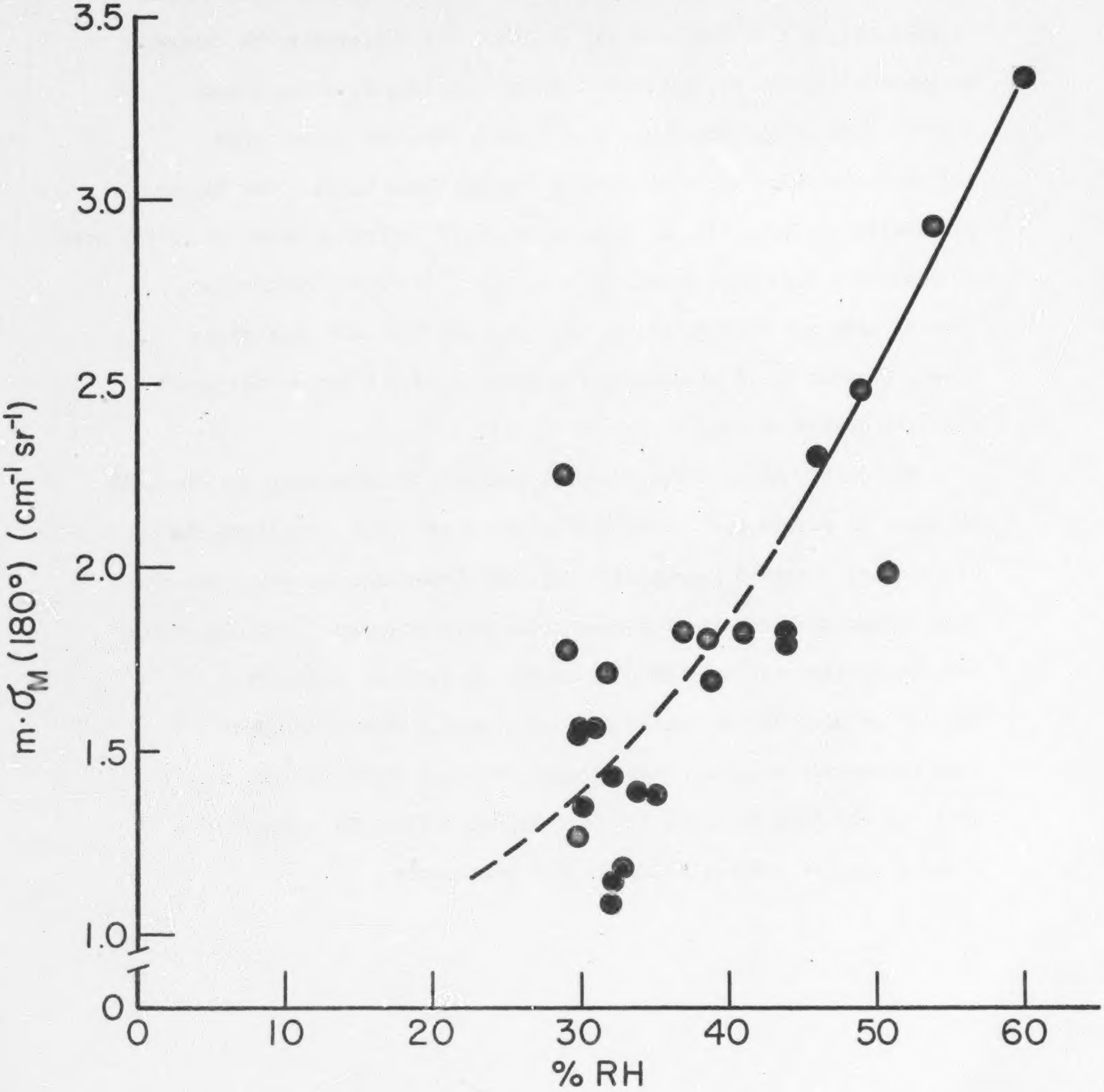

Figure 3.5. Product of aerosol mass concentration times aerosol backscatter cross section versus relative humidity for May 11, 1971.

Figure 3.6 shows both backscattering and relative humidity as a function of time of day for May 11th. The two spikes noted in the backscatter, one at 0900 and one at 1500, are believed to be caused by periods of high particulate loading resulting from increased traffic flow on the adjacent Pennsylvania Turnpike interchange and the Schuylkill River Expressway during these hours. The higher particulate loading for the 0900 hour can be inferred from the hi-vol data of Table 3.1 (see discussion on page 105). Increased particulate loading does not show in the hi-vol data for the 1500 hour since hi-vol sampler No. 4 produced no measurable result due to the short sampling period of four hours.

The backscatter versus relative humidity relationship for May 12th is shown in Figure 3.7. Considering the gusty wind conditions the backscatter remained essentially uniform throughout the day. For the same period the humidity remained relatively constant. The dependence between backscatter and humidity is not as obvious in Figure 3.7 but the results do not negate the relationship shown in Figure 3.6. Some laboratory aerosols show changes in light scattering at a relative humidity of about 50% (see Figure 1.12-1.15). Figure 3.6 shows a similar change, although less pronounced.

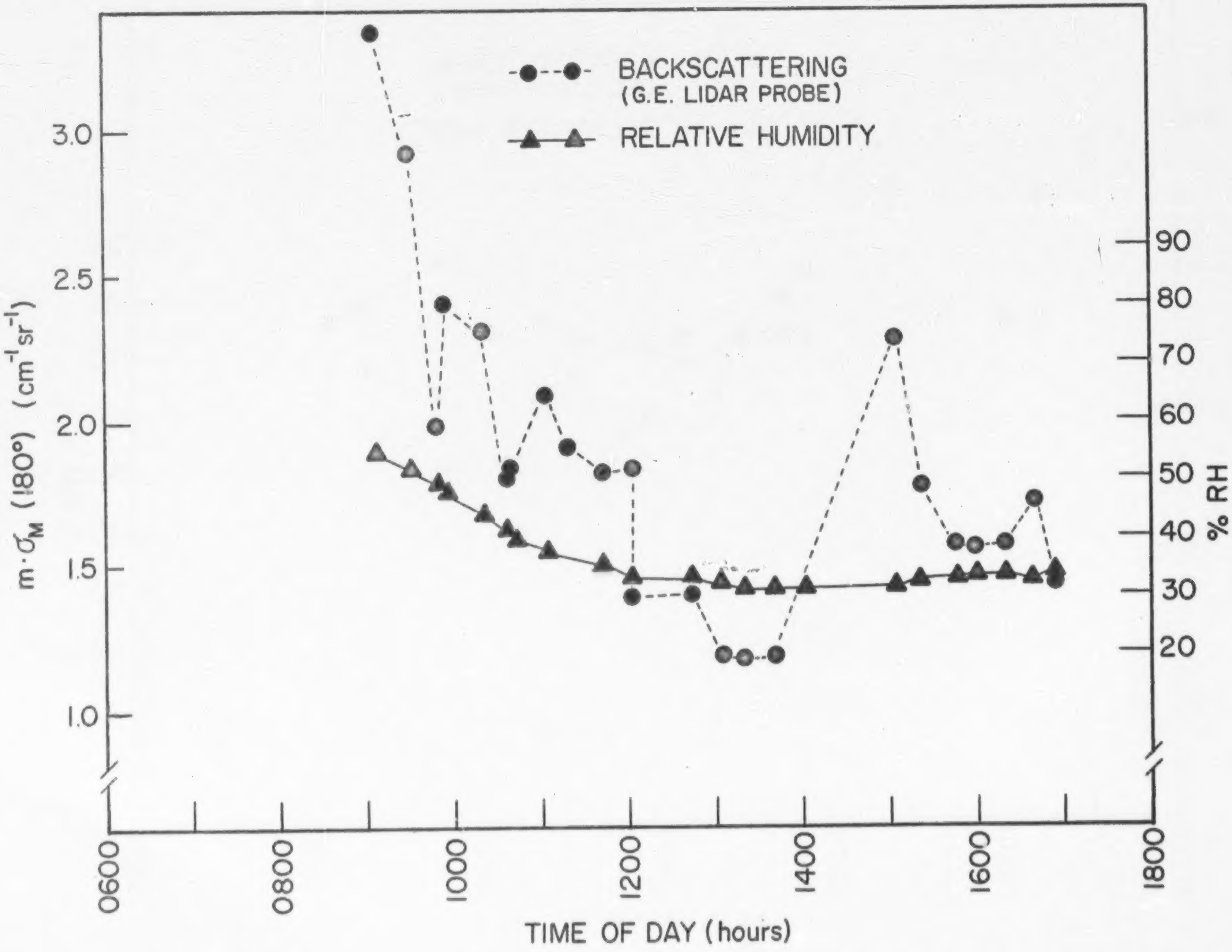

Figure 3.6. Backscatter and Relative Humidity versus Time of Day, May 11, 1971.

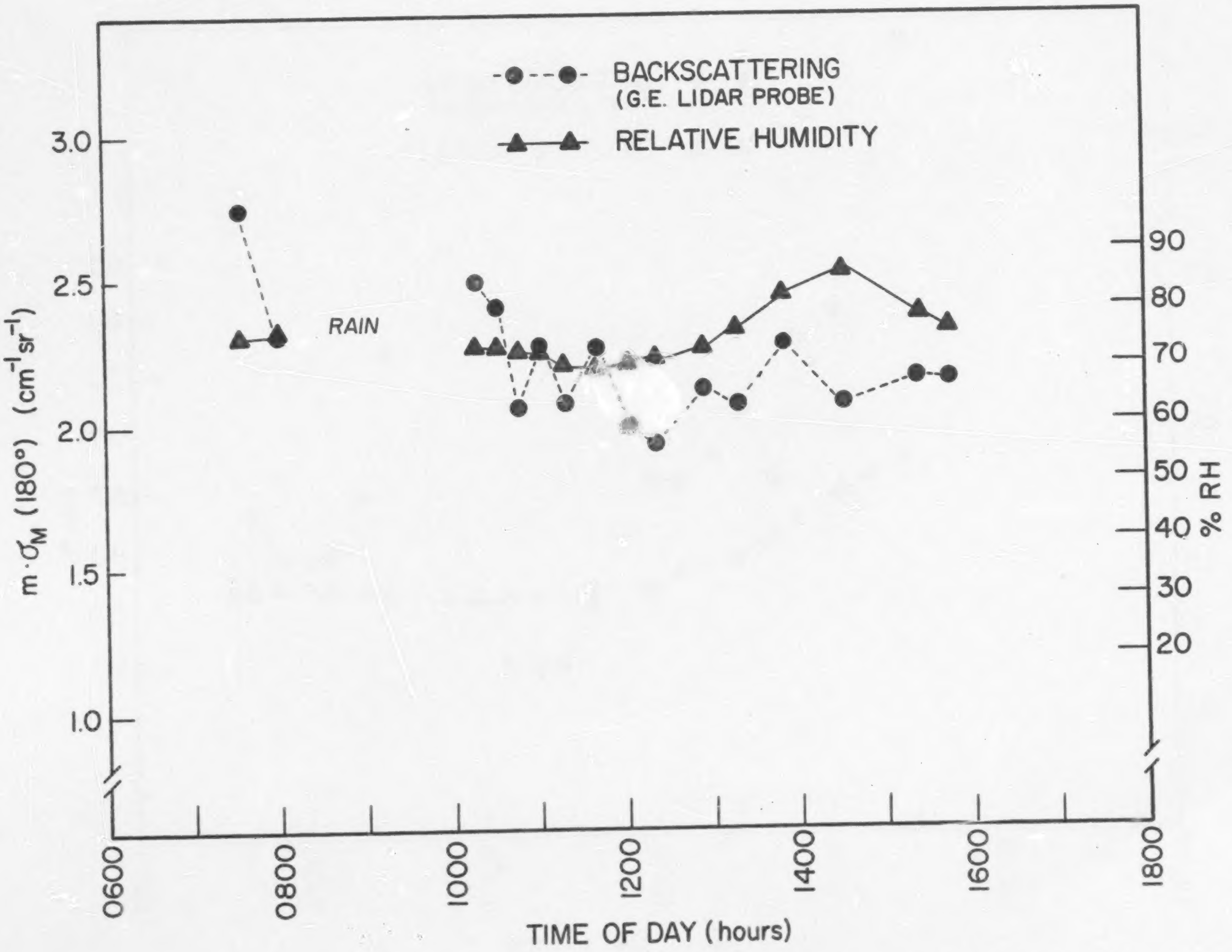

Figure 3.7. Backscatter and Relative Humidity versus Time of Day, May 12, 1971.

Light scattering data were collected using the forward scattering Sinclair-Phoenix and Model 2 of the laboratory laser backscattering device. Figures 3.3 and 3.4 indicate the same general relationship between forward scattering and humidity was found as existed for the atmospheric lidar probe. Unfortunately, the signal from the Model 2 laboratory laser (see Figures 3.3 and 3.4) was so weak that meaningful results could not be obtained. The weak signal is believed to be the result of the much lower number concentration of particles experienced in the atmosphere as compared to laboratory aerosols.

## V. Conclusions

The limited number of measurements made in this field study were meant only to study qualitatively the atmospheric relative humidity and lidar backscatter relationship. It has been found that this relationship follows the trends shown by quantitative laboratory measurements. Lidar measurements of atmospheric particulates seem to be affected by relative humidity as well as by particulate concentration but additional data are needed to confirm this supposition. A clear definition of this humidity backscatter relationship needs to be established before lidar techniques will adequately be able to assess size or concentration properties of atmospheric particulates.

BLANK PAGE

## REFERENCES

Aden, A. L. and M. Kerker (1951), J. Appl. Phys., 22, 1242.

Barret, E. C. and O. Ben-Dov (1967), J. Appl. Met., 6, 500.

Born, M. and E. Wolf (1965), Principles of Optics, Pergamon Press, Oxford.

Charlson, R. J. and H. Horvath, and R. F. Pueschel (1967), Atm. Environment 1, 469.

Clemesha, B. R. and G. S. Kent, and R. W. H. Wright (1967), J. Appl. Met., 6, 386.

Cohen, A., J. Neuman, W. Low (1969), J. Appl. Met., 8, 952.

Cooper, Douglas W. and R. Lee Byers (1970), J. Air Poll. Control Assn., 20, 43.

Dave, J. V. (1969), Appl. Optics, 8. 155.

Davies, C. N. (1964), Recent Advances in Aerosol Research, The MacMillan Company, London.

Davies, C. N. (1966), editor, Aerosol Science, Academic Press, Inc., New York.

Dobbins, R. A., and G. S. Jizmagian (1966), J. Opt. Soc. Am., 56, 1345.

Dobbins, R. A. and J. G. Stephen (1966), J. Opt. Soc. Am., 56, 1345.

Eiden, R. (1966), Appl. Optics, 5, 569.

Fuchs, N. A. (1964), The Mechanics of Aerosols, The MacMillan Company, New York.

Green, H. L. and W. R. Lane (1964), Particulate Clouds: Dusts, Smokes, and Mists, D. Van Nostrand Company, Inc., Princeton, New Jersey.

PRECEDING PAGE BLANK

Hanel, G. (1968), Tellus, 21, 377-379.

Herdan, G. (1960), Small Particle Statistics, Academic Press, London.

Holliday, D. and R. Resnick (1966), Physics, John Wiley and Sons, New York.

Huffman, Paul J., and William R. Thursby, Jr. (1969), J. Atm. Sci., 26, 1073.

Jackson, J. D. (1962), Classical Electrodynamics, John Wiley and Sons, New York.

Johnson, W. B. (1969), J. Air Poll. Control Assn., 19, 176.

Junge, C. (1966), Air Chemistry and Radioactivity, Academic Press, London.

Kerker, M. (1968), Ind. and Eng. Chem., 60, No. 10, 37.

Kerker, M., J. P. Kratohvil, and E. Matijevic (1962), J. Opt. Soc. Am., 52, 551.

Lange, N. A. (1952), editor, Handbook of Chemistry, Handbook Publishers, Inc., Sandusky, Ohio.

Lapple, C. E. (1968), Chem. Eng., 149.

Ligda, M. G. H. (1965), Discovery, 26, 30.

Lundgren, D. A. and D. W. Cooper (1969), J. Air Poll. Control Assn., 19, 243.

MacKinnon, David J. (1969), J. Atm. Sci., 26, 500.

Maron, S. H., M. E. Elder and P. E. Pierce (1963), J. Coll. Sci. 18, 733.

Meszaros, E. (1968), Tellus, 20, 443.

Mie, G. (1908), Ann. der Physik, 25, 377.

Neiburger, M. and M. G. Wurtele (1949), Chem. Rev., 44, 321.

Noll, K. E., P. K. Mueller, and Miles Imada (1968), Atm. Env., 2, 465.

Orr, C., F. K. Hurd, and W. T. Corbett (1958), J. Coll. Sci., 13, 472.

Phillips, D. T., P. J. Wyatt, and R. M. Berkman (1970), J. Coll. and Interf. Sci., 34, 159.

Pueschel, R. F. and K. E. Noll (1966), "Comparison of Observed and Calculated Visibilities Based on Measured Size Distributions", Paper presented at the 1966 annual meeting of the Pacific Northwest International Section of A.P.C.A., Seattle, Washington.

Pueschel, R. F., R. J. Charlson, and N. C. Ahlquist (1969), J. Appl. Met., 8, 995.

Pueschel, R. F. and A. T. Rossano (1966), "Light Extinction by Mixed Aerosol Systems", Paper presented at 1966 Air Pollution Control Association Annual Meeting, San Francisco, California.

Reagan, J. A. (1968), Laser Focus, 4, 26.

Sehmel, G. A. (1967), Amer. Ind. Hyg. Assoc. J., 28, 491.

Seltzer, D. E. (1969), Appl. Optics, 8, 905.

Twomey, S. (1954), J. Meteo., 11, 334.

Whitby, K. T. and C. M. Peterson (1965), I. & E. C. Fund., 4, 66.

## APPENDIX 1

### Correction Factor Relative Humidity vs. Temperature

The relative humidity of the air at a certain temperature is the ratio of the amount of water vapor in the air to the amount the air would have when saturated at that temperature. This is the amount of water vapor the air would have when in equilbrium with an infinite plane surface of pure water. Air having a certain amount of water vapor would have different relative humidities at different temperatures.

The saturated vapor pressure over water in millibars is the following:

| Temperature (°C) | Saturation Vapor Pressure (millibars) |
|---|---|
| 20 | 23.373 |
| 21 | 24.861 |
| 22 | 26.430 |
| 23 | 28.086 |
| 24 | 29.831 |
| 25 | 31.671 |
| 26 | 33.608 |
| 27 | 35.649 |
| 28 | 37.796 |
| 29 | 40.055 |
| 30 | 42.430 |

PRECEDING PAGE BLANK.

Most of the present tests were made at about 23°C,where an increase of 1°C gives a change of (28.086 - 29.831) / (28.086) or - 6.2%. A decrease of 1°C gives (28.086 - 26.430) / (28.086) or + 5.9%. Thus 80% R.H. at 23°C would be [80 - (0.62) (80)] = 75% at 24°C.

The temperature of the mixture of aerosol and dilution air was taken both in the R.H. measuring chamber and at the inlet to the scattering chamber. The temperature difference was usually less than 0.5°C, and the correction was applied. [The inlet temperature was usually the same temperature as the room within a few tenths of a centigrade degree.]

# APPENDIX 2

## Pressure Correction for Humidity

The humidity sensors were calibrated for atmospheric pressure rather than for 10" $H_2O$ less than atmospheric, which was the R.H. chamber pressure. To estimate the effect of this pressure difference, the actual humidity was calculated for atmospheric pressure for three examples (10% R.H., 50% R.H., 90% R.H.) at $\Delta P$ = 10" $H_2O$ from a formula given by Platt and Griffiths, (Environ. Measurement and Interpretation, Reinhold Publ. Corp. New York, 1964).

$R_x = (90 + 0.1 R_{30}) - 3x (1 - 0.01 R_{30})$

or

$R_{30} = (R_x + 3x - 90) / (0.1 + 0.03x)$

$R_x$ = humidity at x inches Hg pressure

$R_{30}$ = humidity at 30 inches Hg pressure

$x = 30 - (10'' H_2O\ x) (1'' Hg/13.6'' H_2O) = 30 - .74 = 29.26$

$R_{30} = (R_x - 2.21) / (0.1 + 0.90 - .022)$

$= (R_x - 2.21) / (.98)$

Thus

$R_x = 10\%$ $R_{30} = 8.0\%$

$R_x = 50\%$ $R_{30} = 48.8\%$

$R_x = 90\%$ $R_{30} = 89.6\%$

PRECEDING PAGE BLANK.

The differences are small, although they may be important for some purposes. Corrections have not been made for them.

## APPENDIX 3

## Relative Humidities at Which Some Salts Change Phase

Different salts change phase from solid to liquid at different relative humidities as listed below. This table is taken from Twomey's (1954) experimental work and does not include the effect of particle size on transition humidity.

| Salt | Transition Point (20°C) |
|---|---|
| NaCl | 75-77 |
| KCl | 86 |
| NaBr | 57 |
| $Na_2SO_4$ | 91 |
| $NH_4Cl$ | 80.5 |
| $(NH_4)_2SO_4$ | 80 |
| $K_2CO_3$ | 45 |

PRECEDING PAGE BLANK

## APPENDIX 4

### Estimate of Weighing Errors

The mass concentrations of the aerosols were determined by the weight gain of glass fiber filters. To estimate weighing errors, one weighing was made per day for ten days of both a 2" diameter glass fiber filter (Gelman Type E) and of a 47 mm membrane filter (Millipore 0.45μ) both of which were kept in a dessicator between weighings.

| Glass Fiber | Membrane |
|---|---|
| 0.1552 gm | 0.0907 |
| 0.1552 | 0.0907 |
| 0.1554 | 0.0906 |
| 0.1554 | 0.0904 |
| 0.1553 | 0.0907 |
| 0.1555 | 0.0907 |
| 0.1554 | 0.0904 |
| 0.1555 | 0.0905 |
| 0.1554 | 0.0903 |
| 0.1555 | 0.0905 |

Mean: 0.15538 Mean: 0.9055

Standard deviation: .00012 Standard deviation: 0.00015

Thus, the weighing error is about ± 0.15 mgm.

PRECEDING PAGE BLANK

# APPENDIX 5

# ATMOSPHERIC LIDAR MEASUREMENTS

## "LIDAR MEASUREMENTS"

## FINAL REPORT

May 24, 1971

Prepared by: G. W. BETHKE and C. S. COOK

General Electric Company
Space Sciences Laboratory
P. O. Box 8555
Philadelphia, Pa. 19101

Prepared for: Center for Air Environment Studies
The Pennsylvania State University
University Park, Pennsylvania 16802

PRECEDING PAGE BLANK

SYMBOLS:

| | |
|---|---|
| $A$ | Clear acceptance area of lidar receiving objective ($cm^2$) |
| $c$ | Velocity of light in air ($2.9979 \times 10^{10}$ cm/sec) |
| $C$ | Total capacitance of photomultiplier tube output lead to oscilloscope plus oscilloscope input capacitance |
| $E$ | Total energy per laser pulse (joules) |
| $E_o$ | Total optical efficiency of lidar system (unitless) |
| $m$ | Particulate (aerosol) mass concentration in air, (μgm/cc of air) |
| $n$ | Number concentration of air molecules or of scatterers ($cm^{-3}$) |
| $n_o$ | n for air at 0° C and 1 atm pressure ($2.6871 \times 10^{19}$/cc) |
| $P$ | Atmospheric pressure near lidar (inches of mercury) |
| $P_o$ | One atmosphere (29.921 inches Hg.) |
| $r$ | Range from lidar receiving objective (cm) |
| $R$ | Lidar detector (photomultiplier tube) load resistance (ohms) |
| $R_a$ | Clear acceptance radius of lidar receiving objective |
| $S$ | Lidar photomultiplier tube sensitivity at anode (amps/watt) |
| $t$ | Average time since the laser beam was produced (sec) |
| $T$ | Air temperature near lidar (degrees Rankine) |
| $T_o$ | Freezing point of water (491.7°R) |
| $V$ | Voltage drop across lidar detector load resistor (volts) |
| $V_c$ | Integrated photomultiplier tube output voltage obtained from calibration run |
| $\rho$ | Total reflectance of diffuse white target |
| $\sigma_M(180°)$ | Mass normalized backscattering cross section for particulates in air ($cm^2 \ \mu gm^{-1} \ sr^{-1}$) |
| $\sigma_R(180°)$ | Rayleigh backscattering cross section per molecule for air ($1.9925 \times 10^{-28}$ $cm^2 \ sr^{-1}$ for $\lambda = 6943Å$) |
| $\tau$ | Absorbing filter transmittance at 6943Å |

## INTRODUCTION

As part of a program to investigate the effect of relative humidity on aerosol scattering, a series of ground level lidar (LIght Detection And Ranging) backscattering measurements were made of ambient atmospheric aerosols which were also being sampled by other techniques. These measurements were made on May 11, 1971 and May 12, 1971 at General Electric Company's Valley Forge Space Center which is located in King of Prussia, Pennsylvania. King of Prussia is an an outer suburban light industrial-residential area WNW of Philadelphia. The first day was sunny and warm with the relative humidity dropping from 60% to 29% during the lidar measurements. The second day was mostly cloudy, developed gusty SW winds and frequent light showers, and had humidity ranging from 64% to 79% during the lidar measurements.

## EXPERIMENTAL SET-UP

The lidar system was focused, aligned, and aimed at a point 366.5 feet away and about seven feet above the ground, this point being inside an open cluster of four high volume samplers. About 100 feet beyond this measurement point, the laser beam was terminated by a grassy bank. The high volume samplers as well as a Sinclair-Phoenix Photometer and point-sampling laser light scattering device were operated by personnel from the Pennsylvania State University Center for Air Environment Studies.

The truck-mounted lidar system used for these measurements consists of a ruby laser beamed through a transmitter telescope which is mounted alongside a scattered light receiving system. The Q-switched ruby laser emits a short pulse ( ∿30 nanoseconds wide) of ∿0.5 joules at 6943Å wavelength. A laser-mounted photodiode monitors the exact energy of each laser pulse. After passing through the Galilean collimating telescope, the laser light pulses have a divergence less than 1 milliradian. The adjacent parallel-mounted receiving system consists of a 6 inch diameter refractive telescope with 4 milliradian diameter field stop, a small collimating lens, a thermally controlled narrow band pass interference filter, and a photomultiplier tube detector with S-20 spectral response. A double beam oscilloscope plus camera is used to simultaneously display and record both the photomultiplier tube output and the photodiode laser monitor output.

## ANALYSIS AND RESULTS

### Lidar Range Equation

As already indicated the lidar backscatter data is displayed as an oscilloscope voltage (V) which decreases with increasing time (t) as the laser light beam propagates away from the lidar system. The "range equation" which permits the extraction of particulate mass concentration in air (m) from the lidar data was developed elsewhere (Bethke, et al. 1970), with a somewhat restricted result being,

$$V = c\ R\ (SE_o)\ \frac{EA}{2\ r^2}\ [n(r) \cdot \sigma_R(180°) + m(r) \cdot \sigma_M(180°)], \qquad (1)$$

where

$$n = n_o\ (T_o/T)\ (p/p_o) \qquad (2)$$

Also, since the light received from range r must first travel out, be scattered, and then return to the lidar system, we have,

$$r = c\ t/2 \qquad (3)$$

The symbols for the above and all other equations are defined at the front of this appended report.

This form of the range equation includes the effects of both particulate (Mie) backscattering and molecular (Rayleigh) backscattering. Due to the short range used for these measurements (366.5 feet), neither atmospheric extinction effects nor change-of-altitude effects are included in equations (1) and (2). Reference 1 gives the complete form of these equations which includes all of the mentioned effects.

All parameters of equations (1) through (3) are well known constants or are readily obtained from the lidar system, except for S, $E_o$, and the particulate backscatter cross section $\sigma_M(180°)$. The terms S and $E_o$ are both lidar system efficiency parameters which can be considered as one parameter, $(SE_o)$, that varies with photomultiplier tube power supply voltage. The parameter $(SE_o)$ is further discussed and its experimental evaluation described later. The term $\sigma_M(180°)$ is the mass normalized particulate backscatter cross section.

If equation (1) is solved for the product $m(r) \cdot \sigma_M(180°)$ at a specific range r, we have,

$$m \cdot \sigma_M(180°) = \frac{2\,r^2\,V}{c\ RA\ (SE_o)\ E} - n \cdot \sigma_R(180°) \qquad (4)$$

We thus see that the lidar data leads us to the product of aerosol mass concentration and aerosol backscatter cross section, $m \cdot \sigma_M(180°)$. By combining this result with mass densities obtained by other means such as high volume samplers, we can extract $\sigma_M(180°)$ from the lidar results.

## Lidar System Calibration

At the single photomultiplier tube voltage used for all lidar shots, the lidar system sensitivity, $(SE_o)$ in equations (1)and (4), was determined by the following method: During the first day of measurements (5/11/71), the lidar system was fired at a diffuse white target placed 366.5 feet away, this target consisting of a 2 ft. x 2 ft. Masonite board undercoated with flat white spray paint and then overcoated with 3M "Nextel" Velvet White Coating (a spray paint). The backscattering diffuse reflectance ($\rho$) from this surface when placed perpendicular to the lidar axis has been determined to be about 0.90 at the laser wavelength.

Since the return signal from such an effective scatterer would grossly overilluminate the photomultiplier tube (PMT) and perhaps even damage it, a Schott absorbing glass neutral density filter was placed near the PMT between the narrow band interference filter and the receiving telescope small collimating lens. The transmittance of this filter has been measured by Infrared Industries as a function of wavelength. At 6943Å, the filter used for these calibration measurements has a transmittance ($\tau$) of 0.0116 (optical density = 1.934). Also, the 6 inch diameter objective lens of the receiving system was masked down to 3/16 inch clear aperture further reducing the light intensity at the PMT. These signal attenuating procedures kept use of the PMT well into its linear response region for pulsed signals.

Since the backscattered return from such a flat target lasts about 30 nanoseconds (the laser pulse period) the combined PMT plus recording system response of also about 30 nanoseconds was not sufficient to permit sufficiently accurate presentation of the backscatter signal. Thus, the PMT output signal ($V_c$) was integrated through use of the PMT output coaxial cable capacitance plus other stray capacitances (C). A 9.3 K ohm load was used as the bleed resistor.

When this PMT integrated output is divided by the laser output energy, the resulting normalized signal yields ($SE_o$) via equation (5).

$$\begin{aligned}(SE_o) &= C\,V_c/[E\,\rho\,\tau\,\sin^2\,(R_a/r)] \\ &= C\,V_c\,\pi\,r^2/(E\,\rho\,\tau\,A)\end{aligned} \tag{5}$$

Here, A and $R_a$ are the clear acceptance area and radius of the receiving objective, respectively.

Using the values C = 334 pf (measured with a capacitance bridge), $\rho = 0.90$, $\tau = 0.0116$, r = 4398 inches, and $R_a$ = 3/32 inch, the lidar system $SE_o$ was determined as described while using several laser energies (E) through the range 0.25 to 0.75 joules. Although we would not normally expect $SE_o$ to be a function of E, the reduced results show $SE_o$ to linearly increase from 71 amps/watt at E = 0.25 joule to 93 amps/watt at E = 0.75 joule. Such a variation of $SE_o$ would normally be caused by a nonlinear PMT or an incorrectly calibrated laser monitor. However, the PMT linearity had previously been checked in detail, and the PMT was used well within its linear range for all of these measurements. Also, the laser monitor had previously been calibrated against a calorimeter type laser energy monitor. Although the reason is not known for this apparent variation in $SE_o$ as a function of E, the lidar runs were reduced using the $SE_o$ value appropriate for the laser energy of each shot. This procedure is equivalent to the ($SE_o$) E method discussed in the next paragraph.

Since equation (5) can be slightly rearranged to solve for ($SE_o$) E which is also to be found in equation (4), we see that the lidar calibration does not actually depend upon an absolute calibration of the laser energy monitor. Thus, in the absence of a laser energy monitor calibration, the lidar system is still correctly calibrated by determining $(SE_o)$ E at several laser outputs, and plotting $(SE_o)$ E versus monitor output voltage (as a reference).

## RESULTS

The results from these measurements are tabulated in Tables A.1 and A.2 for May 11, 1971 and May 12, 1971, respectively. Tables A.1 and A.2 list for each lidar shot the time of day, relative humidity, $p/p_o$, $T_o/T$, and $m \cdot \sigma_M(180°)$. The relative humidity and $T_o/T$ values are interpolated and calculated from data supplied by Mr. J. Davis of Pennsylvania State University. The $p/p_o$ values are calculated for the correct altitude and time from hourly data supplied by the Philadelphia Inquirer Newspaper Weather Bureau. The $m \cdot \sigma_M(180°)$ values are calculated from equation (4) using R = 93.1 ohms, A = 181.5 $cm^2$, r = 366.5 feet = $1.119 \times 10^4$ cm, and $SE_o$ as described in the previous section. In Figure A.1 $m \cdot \sigma_M(180°)$ is plotted versus time of day for both 5/11/71 and 5/12/71.

All of the data and reduced results are considered equally valid except for $m \cdot \sigma_M(180°)$ from the 8:27 AM shot on 5/12/71. An accuracy analysis of the lidar measurements shows 20 possible sources of errors which could combine such that the $m \cdot \sigma_M(180°)$ values of Tables A.1 and A.2 generally have maximum possible relative (precision) errors of ±25% and maximum possible absolute errors of ±70%. Of course, individual errors will tend to offset each other such that actual total errors will be considerably less than these maximum possible values.

The 8:27 AM result from 5/12/71 is more than ten times smaller than all other results from that day. In this case, the maximum possible relative and absolute errors are ±0.16 x $10^{-8}$ and ± 0.46 x $10^{-8}$ $cm^{-1}$ $sr^{-1}$, respectively. We do not know why this one $m \cdot \sigma_M(180°)$ result is so low compared with the others, but the difference is sufficiently large that the data point should be discarded. When making this lidar shot, we possibly used the wrong oscilloscope sensitivity or PMT voltage without realizing it.

Although there were frequent scattered light rain showers or sprays during the afternoon of May 12, 1971, there was no noticeable rain or spray in the air during the actual times of lidar shots. Even a slight rain or spray in the air would strongly scatter light and invalidate the results.

Given the high volume sampler mass concentration results (from J. Davis, Pennsylvania State University) of about 60 - 100 $\mu gm/m^3$ for 5/11/71 and 5/12/71, particulate backscatter cross sections can be calculated from the $m \cdot \sigma_M(180°)$ values determined here and listed in Tables A.1 and A.2. These particulate backscatter cross sections (2-5 x $10^{-4}$ $cm^2$ $sr^{-1}$ $\mu gm^{-1}$) are in approximate agreement with the equivalent cross sections calculated[1] by Mie theory using the Junge size distribution function parameter, $\nu$, = 3.0 ($d^{-4}$ size distribution), index of refraction 1.5 and average mass density of 2.0 $gm/cm^3$. These values are generally used in describing continental aerosols.

## REFERENCES

1. Bethke, G., C. Cook, and F. Mezger, "Laser Air Pollution Probe," General Electric Company, TIS No. 70SD6, April 1970.

Table A.1. Atmospheric and Lidar Data for May 11, 1971

These measurements were made at General Electric Company's Valley Forge Space Center, King of Prussia, Pa.

| Time of day | Rel. hum.* | $(p/p_o)$ | $(T_o/T)$* | $m \cdot \sigma_M(180°)$ $(cm^{-1} sr^{-1})$ | Comments |
|---|---|---|---|---|---|
| 9:05 | 60% | 1.0003 | 0.943 | $3.32 \times 10^{-8}$ | Fair Weather |
| 9:24 | 54% | " | 0.938 | 2.92 " | |
| 9:40 | 51% | " | 0.935 | 1.98 " | |
| 9:56 | 49% | " | 0.932 | 2.39 " | |
| 10:18 | 46% | " | 0.930 | 2.30 " | |
| 10:37 | 44% | " | 0.929 | 1.78 " | |
| 10:40 | " | " | " | 1.82 " | |
| 11:03 | 41% | " | 0.927 | 2.07 " | |
| 11:20 | 39% | 1.0002 | 0.926 | 1.89 " | |
| 11:42 | 38% | 1.0001 | 0.924 | 1.80 " | |
| 12:02 | 37% | 1.0000 | 0.921 | 1.82 " | |
| 12:25 | 35% | 0.9995 | " | 1.38 " | |
| 12:42 | 34% | 0.9991 | 0.920 | 1.38 " | |
| 13:05 | 33% | 0.9987 | 0.918 | 1.18 " | |
| 13:19 | 32% | " | 0.916 | 1.16 " | |
| 13:42 | " | " | 0.912 | 1.17 " | |
| 14:01 | 30% | " | 0.911 | 1.35 " | |
| " | " | " | " | 1.26 " | |
| Lidar calibration runs during 14:02 - 15:00 hours. | | | | | |
| 15:04 | 29% | 0.9980 | 0.909 | $2.26 \times 10^{-8}$ | |
| 15:22 | " | 0.9978 | 0.910 | 1.77 " | |
| 15:45 | 30% | 0.9974 | " | 1.56 " | |
| 15:59 | " | 0.9973 | 0.911 | 1.54 " | |
| 16:20 | 31% | 0.9972 | 0.912 | 1.56 " | |
| 16:40 | 32% | 0.9971 | 0.913 | 1.71 " | |
| 16:55 | " | 0.9970 | " | 1.43 " | |

* These results are based on data supplied by J. Davis, Penn State Univ.

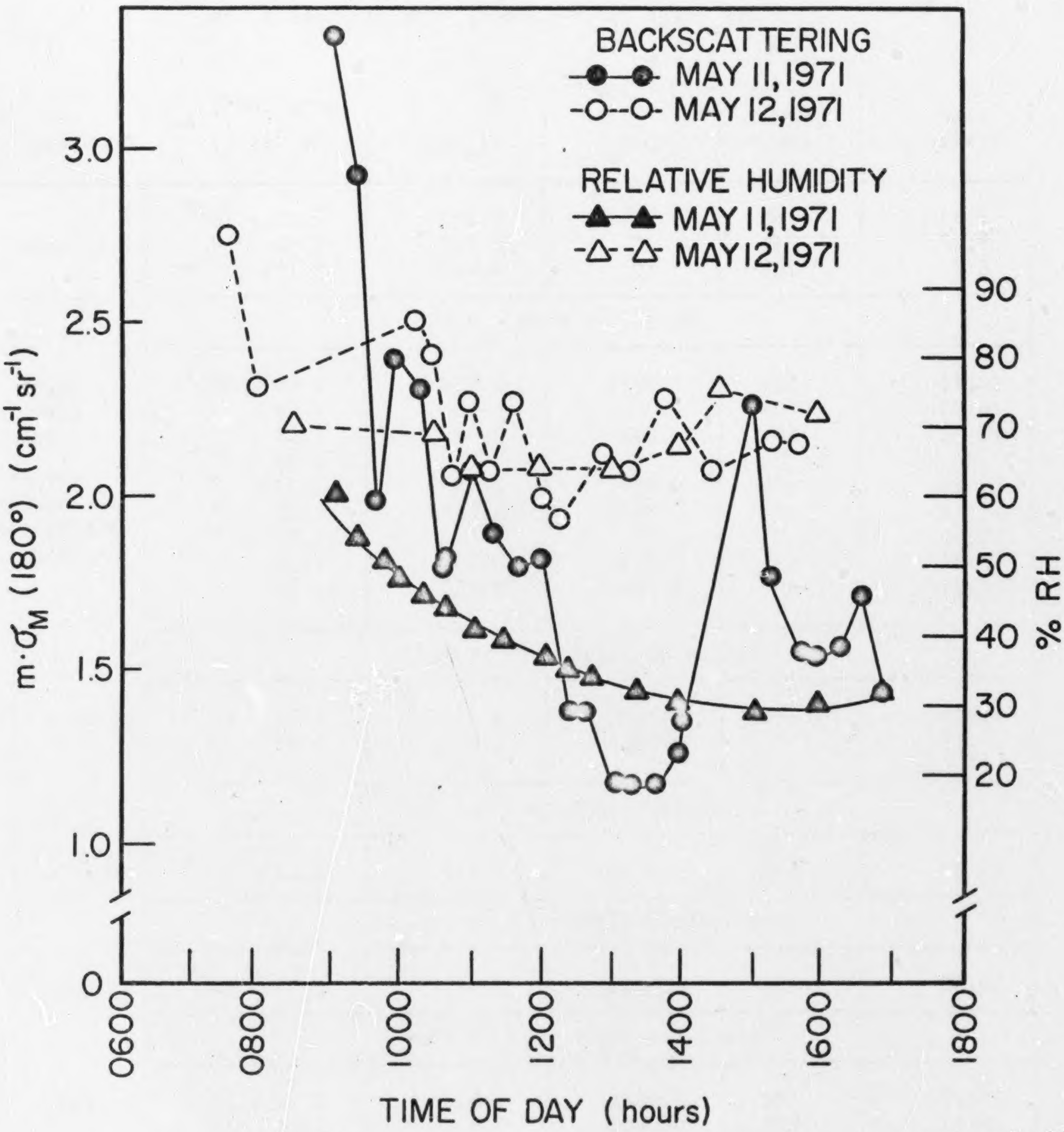

Figure A.1. Product of aerosol mass concentration times aerosol backscatter cross section versus time of day for May 11, 1971 and May 12, 1971.

Table A.2. Atmospheric and Lidar Data for May 12, 1971

These measurements were made at General Electric Company's Valley Forge Space Center, King of Prussia, Pa.

| Time of day | Rel. hum.* | $(p/p_o)$ | $(T_o/T)$* | $m \cdot \sigma_M(180°)$ $(cm^{-1} sr^{-1})$ | Comments |
|---|---|---|---|---|---|
| 7:34 | 78% | 0.9936 | 0.943 | $2.75 \times 10^{-8}$ | no wind |
| 8:00 | 74% | " | 0.942 | 2.31 " | |
| 8:27 | 70% | " | 0.941 | 0.160 " ** | |
| Rain from 8:30 - 9:30 | | | | | |
| 10:15 | 72% | 0.9932 | 0.938 | $2.50 \times 10^{-8}$ | light gusty wind |
| 10:30 | 69% | " | 0.936 | 2.40 " | |
| 10:46 | 66% | 0.9931 | 0.935 | 2.17 " | |
| " | " | " | " | 2.06 " | |
| 11:00 | 64% | 0.9930 | 0.933 | 2.27 " | Increasingly strong gusty wind |
| 11:18 | " | 0.9928 | 0.932 | 2.06 " | |
| 11:40 | " | " | " | 2.27 " | |
| 12:03 | " | 0.9926 | 0.931 | 1.99 " | |
| 12:21 | " | 0.9925 | 0.930 | 1.93 " | |
| Scattered light rain showers | | | | | |
| 12:55 | 64% | 0.9923 | 0.928 | $2.12 \times 10^{-8}$ | no rain |
| 13:18 | " | 0.9922 | 0.927 | 2.07 " | " " |
| Scattered light rain showers | | | | | |
| 13:50 | 67% | 0.9920 | 0.930 | $2.28 \times 10^{-8}$ | no rain |
| Scattered light rain showers | | | | | |
| 14:30 | 76% | 0.9915 | 0.933 | $2.07 \times 10^{-8}$ | no rain |
| Scattered light rain showers | | | | | |
| 15:22 | 74% | 0.9908 | 0.931 | $2.16 \times 10^{-8}$ | no rain |
| 15:45 | 72% | 0.9905 | 0.930 | 2.14 " | " " |

* These results are based on data supplied by J. Davis, Penn State Univ.

** See discussion in text.

completed at least one year in their studies for an associate degree in engineering technology. Also initiated under this program is a Pennsylvania survey of vegetation damage. Agricultural extension personnel and county agents were trained to recognize air pollution damage to crops and are now reporting damage seen in their daily work to the Center for analysis.

A two year course leading to the Associate Degree in Air Pollution Technology is given at the Berks Campus of the Pennsylvania State University. The graduate of this program is trained to be responsible for the calibration, installation, and operation of air sampling and monitoring equipment. He may also be expected to investigate complaints, conduct plant inspections, make source evaluations, and formulate recommendations based on his findings.

Address requests for more information concerning the training programs to the Director, Center for Air Environment Studies, 226 Chemical Engineering II, The Pennsylvania State University, University Park, Pennsylvania 16802.

## Publications Available

AIR POLLUTION TITLES, a current awareness publication service, is available on a January-December subscription basis. This publication is a quick guide to current literature and has some capacity as a retrospective searching tool. APT uses a computer-produced, Keyword-in-Context (KWIC) format to provide a survey of current air pollution and related literature. During the year over 1,000 journals are scanned for pertinent citations.

Subscriptions to APT at $15/year, cover issues per year as follows: No. 1, January-February; No. 2, March-April; No. 3, May-June; No. 4, July-August; No. 5, September-October; No. 6, cumulative issue for the year, including November-December citations. The 1971 subscription of APT is now available. Cumulative issues for 1967, 1968, 1969 and 1970 are available; the cost is $10 each.

INDEX TO AIR POLLUTION RESEARCH was published in July of 1966, 1967, and 1968. Each Index included government sponsored research in the air pollution field and the results of a survey of air pollution research projects conducted by the industrial, sustaining, and corporate members of the Air Pollution Control Association and the American Industrial Hygiene Association, and research supported by other industries and non-profit organizations.

The Index utilizes the Keyword-in-Context (KWIC) format for rapid scanning of project titles. In addition, this publication provides a complete bibliography including mailing addresses where additional information about the project may be obtained. Beginning with the 1967 edition, a section containing citations of papers resulting from the research in progress was included. Copies of the 1966 and 1967 editions are available at $1.25 each. The 1968 edition costs $2.

NOTE: The National Air Pollution Control Administration of the United States Public Health Service selected the Center for Air Environment Studies to prepare A Guide to Air Pollution Research which paralleled and replaced the 1969 Index. By contract agreement, the National Administration is managing the distribution of all copies.

HANDBOOK OF EFFECTS ASSESSMENT VEGETATION DAMAGE was published in 1969 as part of the survey of vegetation damage. It describes in detail the many sources of pollution and the effect of pollutants on vegetation; color pictures showing characteristics of plant damage symptoms are included. The cost is $6.

Requests for additional information and orders should be addressed to:
Information Services, Center for Air Environment Studies, 226 Chemical Engineering II, University Park, Pennsylvania 16802.